LYN REGULATES DRUG RESISTANCE MECHANISMS IN CHRONIC MYELOGENOUS
LEUKEMIA (CML)

Denis O. Okumu

A dissertation submitted to the faculty of the University of North Carolina at Chapel Hill in
partial fulfillment of the requirements for the degree of Doctor of Philosophy in the Department
of Pharmacology in the School of Medicine.

Chapel Hill
2018

Approved by:

Lee M. Graves

Gary L. Johnson

Jen Jen Yeh

Yanping Zhang

Antonio Baines

ABSTRACT

Denis O. Okumu: Lyn Regulates Drug Resistance Mechanisms in Chronic Myelogenous
Leukemia (CML)
(Under the direction of Lee Graves)

Acquired resistance to anti-cancer therapy presents a critical challenge to effective clinical

management of chronic myelogenous leukemia (CML). Drug-resistant CML cells devise diverse

molecular adaptations to evade therapy. Examples of such adaptations include: target (Bcr-Abl)

mutations that eliminate drug binding, target amplification, up-regulation of drug exporter

proteins, and activation of alternative kinase(s). The CML cell (MYL-R) model described in this

dissertation is a classic example of how CML cells can activate alternative kinase(s) to promote

cell survival. Herein, I discuss two molecular adaptations regulated by Lyn in MYL-R cells.

In the first project, I showed that increased Lyn expression and activity in MYL-R cells up-

regulated the expression and stability of BIRC6, a member of the inhibitor of apoptosis proteins

(IAP) family known to bind and inactivate active caspases. BIRC6's role in promoting imatinib

resistance was confirmed by the 15-fold increase in imatinib sensitivity upon BIRC6 shRNA

knockdown. Pharmacological or genetic inhibition of Lyn reduced BIRC6 expression and

stability. Further, BIRC6 stability was increased via Lyn-dependent phosphorylation of serine

residues in a region that overlapped with caspase cleavage motifs. Pharmacological inhibition of

Lyn resulted in caspase-mediated degradation of BIRC6.

In the second project, I am investigating Lyn's role in regulating creatine uptake by MYL-R

cells. Our lab previously showed that total intracellular creatine pool was 5-fold higher in MYL-

R than MYL cells. Our unpublished data show that the increased intracellular creatine comes from uptake from the cell culture media and not *de novo* synthesis. I, therefore, investigated the role of creatine in MYL-R cells by incubating the cells in normal growth media into which competitive inhibitors of creatine uptake were added. Our data show that reduction in total intracellular creatine pool lowered cell viability. Others previously showed that the Na^+/K^+-ATPase pump activity was critical for creatine uptake. Our data show that Lyn inhibition or shRNA knockdown reduced Na^+/K^+-ATPase activity and total intracellular creatine pool, suggesting a tripartite signaling cascade that supports MYL-R cell survival.

Taken together, these studies enrich our understanding of the diverse therapy-survival mechanisms utilized by CML cells, and provide insights into novel targets for effective cure of CML.

To my late parents, Margaret Osore Okumu and Henry Okumu Ochieng', thank you for always believing in my abilities to excel in anything I choose to do. To my mother, for the courage and love you always showed us even as you fought against cancer long after our father's death. Your tribulations and resilience inspired me to seek a deeper understanding of why cancer can be so devastating and hard to treat.

ACKNOWLEDGEMENTS

The work described in this dissertation is the product of tremendous support and encouragement I have received from diverse groups of people in the course of my long academic career. I want to start by thanking my mentor, Dr. Lee Graves for accepting me into his lab, and for his never-ending support in the course of my graduate studies. Lee's enthusiasm for science, his ability to bring in multiple research projects, and his readiness to always engage with students about their research have helped me develop into an independent scientist, able to concurrently run multiple projects. My sincere thanks go to the very distinguished members of my dissertation committee, Dr. Gary Johnson, Dr. Jen Jen Yeh, Dr. Yanping Zhang, and Dr. Antonio Baines, for their invaluable guidance and insightful criticisms of my research work. Thanks for the many recommendation letters you have penned in support of my applications for further training and jobs.

During the latter part of my graduate school, I have been blessed to have Dr. Michael Patrick East, a postdoctoral fellow, as a colleague in the Graves lab. Mike, like Lee, has always been available to talk with me about my research in ways that have helped me develop as a scientist. Mike, thanks for the several weeks that you never got tired of me bothering you with my CRISPR-Cas9 and Gateway cloning experiments. Thanks, also, for your help with bioinformatics stuff. You and Lee have been wonderful resources and have a huge impact on the work discussed in this document. Your gentle demeanor and commitment to people around you are invaluable attributes for which all of us in the Graves lab are grateful. You have been a great and reliable friend! I wish you all the best in life. I would also like to thank the rest of the

Finally, my very heartfelt thanks go to my friends and my family for their never-ending love and support during this long and difficult journey. To my wife, Eunice, you have always been my rock in life. You and the kids (Maggie and Harley) have been a great source of encouragement to me. You know how hard it has been with childcare, schools, kids activities, and the like…thanks for most of the time picking up most of these responsibilities so that I could stay in the lab late or work on weekends and public holidays. To my siblings, Alice, Lucy, Elizabeth, Celestine, and Calvin, our many long-distance phone conversations have served to assure me of your love and well wishes. Successful completion of this work has been made possible by the constant reminder that it is not all about me, the individual, but the community that I represent.

THANK YOU ALL!

TABLE OF CONTENTS

LIST OF TABLES

LIST OF FIGURES

LIST OF ABBREVIATIONS AND SYMBOLS

α	Alpha
Allo-HSCT	Allogeneic hematopoietic stem cell transplantation
AML	Acute myelogenous leukemia
Ara-C	Cytarabine
ATP	Adenosine triphosphate
β	Beta
B-ALL	B-cell acute lymphocytic leukemia
Bcl-2	B-cell lymphoma 2
B-CLL	B-cell chronic lymphocytic leukemia
Bcr-Abl	Breakpoint cluster region – Abelson
BCR	B-cell receptor
BIR	Baculovirus IAP repeat
BIRC6	Baculoviral IAP repeat containing 6
Cbl	Casitas B-lineage lymphoma protein
CCr	Cyclocreatine
CDK9	Cyclin-dependent kinase 9
Chk	C-terminal Src kinase-homologous kinase
CK2	Casein kinase 2
CKB	Creatine kinase, brain-type
CLL	Chronic lymphocytic leukemia
CML	Chronic myelogenous leukemia
Cr	Creatine

Csk	C-terminal Src kinase
Ctk	Csk-like tyrosine kinase
dFBS	Dialyzed fetal bovine serum
EEF1D	Elongation factor 1-delta
FAK	Focal adhesion kinase
FLT3-ITD	Fms-like tyrosine kinase 3-internal tandem duplication
GLUT1	Glucose transporter 1
GM-CSF	Granulocyte-macrophage colony-stimulating factor
3-GPA	3-Guanidinopropionic acid
^{1}H NMR	Proton nuclear magnetic resonance
IAP	Inhibitor of apoptosis protein
JNK	c-Jun N-terminal kinase
κ	Kappa
Lyn	Lyn tyrosine kinase
Mcl-1	Myeloid cell leukemia-1
MIB/MS	Multiplexed inhibitor bead/mass spectrometry
miRNA	microRNA
Na^{+}/K^{+}-ATPase	Sodium/potassium-adenosine triphosphatase
NEK9	Never in mitosis A related kinase 9
NF-κB	Nuclear factor kappa-light-chain-enhancer of activated B cells
NRTK	Non-receptor tyrosine kinase
PCr	Phosphocreatine
PDGF	Platelet-derived growth factor

P-glycoprotein	Permeability glycoprotein
Ph	Philadelphia chromosome
PI3K	Phosphoinositide 3-kinase
PKA	Protein kinase A
PKCβ	Protein kinase C beta
pY	Phosphotyrosine
RbCl	Rubidium chloride
RIPK2	Receptor-interacting serine/threonine-protein kinase 2
SFK	Src-family kinase
shRNA	Short (or small) hairpin ribonucleic acid
siRNA	Small (or short) interfering ribonucleic acid
SLC6A8	Solute carrier family 6 member 8 (Creatine transporter)
STAT5	Signal transducer and activator of transcription 5
TiO$_2$	Titanium dioxide
XIAP	X-linked inhibitor of apoptosis protein
Z-VAD-FMK	Carbobenzoxy-valyl-alanyl-aspartyl-[O-methyl]- fluoromethylketone

CHAPTER 1: INTRODUCTION

1.1 Chronic Myelogenous Leukemia (CML) overview

Chronic myelogenous leukemia (CML), also called chronic granulocytic leukemia, is a slow and progressive malignancy of myeloid origin, occurring during or after middle age ($\geq$55 years), and rarely occurs in children (< 10% of cases) (1-3). CML accounts for ~15% of all leukemia cases, and approximately 9,000 cases will be diagnosed in 2018, with an estimated ~1000 deaths (4,5). CML is characterized by an accumulation of granulocytes (or leukemia cells), immature and less differentiated cells that fail to differentiate into mature, functional white blood cells (**Figure 1.1**). CML's hallmark cytogenetic diagnosis is the presence of Philadelphia (Ph) chromosome, a mutation resulting from balanced reciprocal translocations between portions of chromosomes 9 (Abl gene) and 22 (Bcr gene), t(9;22)(q34;q11.2). The result is a chimeric and constitutively active Bcr-Abl kinase that promotes growth and proliferation, and is the initiating oncogene in CML (1,4,6,7). Failure to initiate therapy in the early stages of CML will lead to accelerated buildup of granulocytes in the blood and bone marrow resulting in less room for healthy white blood cells, red blood cells, and platelets to develop. When this happens, infection, anemia, or easy bleeding may occur, sometimes resulting in death (3,4,6).

Before the advent of targeted therapy in 2000, CML treatment was limited to non-selective chemotherapeutic agents including busulfan, hydroxyurea, cytarabine, and interferon-alpha (IFN-α) (4,8). The modest efficacies shown by these compounds in

terms of altering the course of disease and the associated toxicities left allogeneic

hematopoietic stem cell transplantation (allo-HSCT) as the only alternative cure for

CML. Allo-HSCT, however, is beset with risks of morbidity and mortality due to

advanced age at time of CML diagnosis, and lack of suitable donors. This fueled the

need for more research to develop novel drugs with better efficacies and minimal adverse

effects, culminating in the approval of the first kinase inhibitor, imatinib, in 2001 (4,8).

Imatinib is a first generation Bcr-Abl inhibitor and constitutes first-line therapy for Ph+

CML. Although initially successful, high incidences of disease relapse and drug

resistance have been recorded in CML patients treated with imatinib (4,7,9,10). With the

emergence of therapy-limiting Bcr-Abl mutations that eliminate imatinib binding, and

activation of alternative kinase (Lyn) signaling pathways that promote drug resistance,

recent research advances have yielded more effective targeted therapies including second

generation (dasatinib and bosutinib) and third-generation (ponatinib) inhibitors that target

both Bcr-Abl and Lyn (Src-family kinases, SFKs), with ponatinib being able to also

circumvent Bcr-Abl mutations (4,8,11).

1.2 Lyn modulates various signaling cascades in human cells

1.2.1 Lyn kinase

Lyn kinase (Lyn) is a member of the Src-Family Kinases (SFK), the largest group of

non-receptor tyrosine kinases (NRTKs) involved in regulation of various normal cellular

processes including growth, differentiation, proliferation, apoptosis, migration, immune

responses, adhesion and metabolism (12-16). Three main subfamilies exist within the

SFK with Lyn being a member of the Lyn-related family comprising of Lck/Yes-related

novel tyrosine kinase (Lyn), hematopoietic cell kinase (Hck), lymphocyte-specific

protein tyrosine kinase (Lck), and B lymphocyte kinase (Blk) (15). SFK proteins are defined by the presence of an N-terminal region (SH4) unique to each member, followed by three homologous domains: Src Homology 3 (SH3) for protein-protein interactions, Src Homology 2 (SH2) for binding to phosphorylated tyrosines on other proteins, and Src Homology 1 (SH1, the kinase domain) (14,15). The SH4 domain is critical for plasma membrane targeting and binding, and encodes a myristoylation site in addition to containing either one or two palmitoylation sites as in Lyn and Fyn respectively (14,17,18). The C-terminal region of SFKs contains an auto-inhibitory phosphorylation site whose phosphorylation by, for example, C-terminal Src Kinase (Csk) or Csk-like protein tyrosine kinase (Ctk) or C-terminal Src kinase-homologous kinase (Chk) is critical for regulating the normal cellular activities of these kinases (15,19-21).

Lyn has two major splice variants that differ by the excision of 21 amino acids (residues 23 – 43) in the SH4 domain resulting in two protein isoforms, Lyn A (p56) and Lyn B (p53) (22-24) (**Figure 1.2**). Even though p56Lyn is taken to be the canonical isoform, research is ongoing to understand if any significant functional differences exist between the two isoforms. Data from recent studies suggest the two isoforms may have different biological functions as manifested by the dual nature of Lyn's signaling in which it is able to both activate and inhibit signaling in diverse systems (14). The SH4 domain is critical for Lyn localization, and given that the splice site is proximal to regions in the SH4 domain that undergo lipid post-translational modification (PTM), excision of the 21 amino acids may suggest isoform-specific localization (17,25). Other studies demonstrated that Lyn localization to intracellular membranous structures like the Golgi membranes was mediated by certain regions within the kinase and SH4 domains, and that

3

deletion of the kinase domain prevented trafficking of Lyn from the Golgi apparatus to the plasma membrane. Closed-conformation induced by phosphorylation at tyrosine 508 (Y508) was observed to have a similar effect (26,27). Moreover, inhibition of Lyn's kinase activity increases its accumulation in the nucleus (28).

Like Src kinase, Lyn can be switched from an inactive to an active conformation in a phosphorylation-dependent manner or via protein interactions. As shown in Figure 1.2, there are two major, conserved phosphorylation sites on Lyn: Tyr397 (Tyr416 in Src) in the kinase domain and Tyr508 (Tyr 527 in Src) in the C-terminal tail of the protein. Phosphorylation of Tyr508 (Y508) by Csk or Ctk or Chk inactivates the protein through interaction of the phosphorylated tyrosine with the SH2 domain thereby folding up the kinase into an inactive conformation (26,29) (**Figure 1.2**). Dephosphorylation of Y508 opens up Lyn to trans-autophosphorylation on Tyr397 (Y397) leading to an open, active conformation. Dephosphorylation of Y508 may be achieved via one or more of the following: protein tyrosine phosphatases (for example, SHP-1 phosphorylase), reduced Csk activity, displacement of protein-protein interactions, and mutational activation (due to mutation or deletion of Y508). Lyn kinase activity is derived from dephosphorylation of this residue that leads to displacement of pY397 from the binding pocket thereby enabling substrate access (29). Data from domain deletion studies showed that loss of SH2 and SH3 decreased Lyn activity. Similar deletions did not affect Src activity; pointing to variability in the manner Src and Lyn are auto-regulated, and also provides evidence that despite their homology, SH3 domains of various Src family members have critical functional differences (30). Protein interactions may directly activate SFK proteins or activate them by moving them to sites of action. For example, platelet-

derived growth factor (PDGF) and focal adhesion kinase (FAK) activate Src by directly interacting with their SH2 domains (29).

1.2.2 Lyn in Health

Lyn is expressed in all blood cells except T-lymphocytes, and has been shown to act both as an inhibitor and activator of signaling (31). Normally, Lyn, like other SFKs, is mostly inactive in cells and is activated only when required (29). Although previous studies had identified Lyn to be exclusively expressed in hematopoietic cells especially those of myeloid origin and B-cell lymphocytes (32), recent data show that Lyn is expressed in a lot other tissues where it modulates signaling (14). Lyn is an activator of the B-cell receptor (BCR) complex and physically interacts with the erythropoietin receptor (EpoR) to induce tyrosine phosphorylation on the receptor thereby transducing growth signals that promote B-cell development (33) and erythrocyte differentiation (12,34). Thus, Lyn is a transducer of signals from growth factor receptors like BCR, GM-CSF receptor, Epo-receptor and c-kit to support development and proliferation of various cells. Additionally, Lyn functions in several mature blood cells where it regulates cell growth, differentiation, adhesion, movement and the cytoskeleton (14). Like Src, Lyn's subcellular localization affects its function. For example, whereas at the plasma membrane Lyn transduces signals from a variety of growth factor receptors to affect cell growth and proliferation, it phosphorylates certain nuclear proteins that are involved in chromatin remodeling and cell cycle regulation (29,35,36). Accordingly, Lyn modulates critical signaling cascades necessary for the development and proliferation of hematopoietic and other cells.

1.2.3 Lyn in Cancer

Like Src, alternating phosphorylation and dephosphorylation events in the cell tightly regulate the activity of Lyn. However, the fine balance between these two events may sometimes be disrupted, altering Lyn activity with dire consequences (15,29). Like Src, enhanced Lyn activity resulting from de-regulation and overexpression has been documented to have an oncogenic role in various human cancers where the enhanced activity often correlates with adverse disease outcomes. Increased Lyn activity has been shown to promote solid tumor growth, proliferation, metastasis and tumor cell survival (14,15). For example, hard-to-treat human solid tumors expressing hyperactive Lyn include, among others: colon carcinoma, prostate, Ewing's sarcoma, colorectal, cervical, lung adenocarcinoma, glioblastoma and breast cancers (37-47). Moreover, targeting Lyn in cancer has been shown to reduce epithelial-mesenchymal transition (EMT) thereby abolishing metastasis (48). Accordingly, several studies show that Lyn is one of the most consistently activated tyrosine kinases in solid tumors where it plays a significant role in tumor development and drug resistance.

Being mainly a hematopoietic kinase, however, Lyn has been shown to play an important role in sustaining hematologic tumors. Data from studies involving several types of leukemia and lymphoma, especially acute myeloid leukemia (AML), chronic myeloid leukemia (CML), chronic lymphocytic leukemia (CLL), B-cell acute lymphocytic leukemia (B-ALL), B-cell chronic lymphocytic leukemia (B-CLL), B-Non Hodgkin's lymphoma, and myelo-proliferative disorders, strongly suggest Lyn as an important regulator of several signaling pathways modulating these diseases (14). Hence,

understanding what Lyn does has broader implications for therapy of both solid and liquid tumors.

1.2.4 Lyn kinase in myeloid leukemia

The duality of Lyn signaling has been documented in various cell types including hematopoietic progenitors, mature myeloid cells (neutrophils, macrophages, and dendritic cells), platelets and erythrocytes. Lyn knockout mice studies suggest that Lyn inhibits myeloid progenitor responses to colony stimulating factors (CSFs) leading to abnormal myeloid cell development characterized by rapid myeloproliferation and accumulation of large numbers of myeloblasts (31). On the contrary, numerous studies show that many hematologic malignancies including myeloid leukemias depend on increased expression and activity of Lyn for survival and proliferation (14). For example, increased Lyn activity has been documented as playing an important role in AML cell lines and primary AML progenitor cells (14,49,50) as shown by the loss in proliferation and induction of apoptosis upon treatment of the cells with PP2, a SFK inhibitor, or by siRNA knockdown of Lyn (50). Constitutively active FLT3-ITD, a mutated kinase expressed in ~30% of AML cases, provides docking sites upon which Lyn binds with high affinity and gets phosphorylated to mediate downstream activation of STAT5 leading to enhanced growth and proliferation of AML cells (14,51). Inhibition of Lyn activity (using genetic and small molecule inhibitors) in FLT3-ITD-driven AML suppressed cell growth and resulted in loss of Lyn activity and STAT5 phosphorylation. Tumor formation and tumor size were similarly suppressed when mice transplanted with FLT3-ITD cells were treated with PP2. These observations underscore the important role Lyn plays in maintaining AML cells (51).

Various studies have demonstrated that Bcr-Abl fusion protein is the initiating molecule for CML (14). However, Lyn has been shown to bind and undergo reciprocal phosphorylation with Bcr-Abl thereby modulating the ability of Bcr-Abl to transform cells. Lyn phosphorylation of Bcr-Abl leads to recruitment of the adaptor Gab2, a key activator of the PI3K pathway essential for Bcr-Abl induced leukemogenesis (14). In pivotal studies involving selection of K562 or MYL cells for imatinib resistance, the resultant cell line (K562R or MYL-R) was found to have increased Lyn expression and activity without associated Bcr-Abl mutations (14,52). Moreover, the cells regained their imatinib sensitivity upon down-regulation of Lyn. Similarly, elevated Lyn levels were observed in primary CML cells from patients who had acquired imatinib resistance in the course of therapy (14). Thus, there exists a critical role for Lyn in the progression and maintenance of myeloid leukemias.

1.2.5 Lyn regulates Bcr-Abl-independent drug resistance mechanisms in CML

Imatinib resistance in CML cells is mediated by the up-regulation of Lyn protein and Lyn kinase activity as demonstrated by various studies using diverse CML cell systems. Increased proliferation and survival of Lyn-overexpressing CML cells are mediated by diverse mechanisms (11,52-57). Studies comparing primary cells taken from CML patients before and after failure of imatinib therapy, suggest that increased Lyn expression and/or activation leading to acquired imatinib resistance occurs in the course of therapy and during disease progression (14,53). Of particular significance is the observation that drug resistance in these cells occurs almost exclusively in the absence of detectable Bcr-Abl kinase mutations known to abolish drug binding. Thus, Lyn mediates drug resistance in CML cells in a Bcr-Abl-independent manner (52,53,58,59). In the

8

same CML cell systems, targeting Lyn with small molecule inhibitors or knockdown of Lyn suppressed both proliferation and pro-survival signaling, and sensitized the cells to imatinib (52,55). Of clinical significance is the observation that administration of dual Lyn (or SFK) and Bcr-Abl inhibitors like ponatinib and dasatinib to CML patients that are non-responsive to imatinib causes disease remission (4,60).

The underlying mechanisms by which Lyn regulates drug resistance in CML are not fully understood. It is, however, known that Lyn modulates diverse signaling mechanisms that regulate drug resistance in CML. For example, studies using K562R, LAMA-R, and MYL-R cells, three imatinib-resistant CML cell lines with elevated Lyn expression and/or activity revealed changes in both expression and activation of various proteins known to enhance cell proliferation and mediate cell survival (11,52-57). Notably, the loss in imatinib sensitivity was not mediated by expression of multidrug resistance genes (53) like P-glycoprotein, a drug-efflux protein that has been linked to resistance in certain CML cells (61). MYL-R, LAMA-R, and K562R cells, however, showed some variability in terms of down-regulated or up-regulated genes, further suggesting that Lyn's regulation of diverse signaling mechanisms that drive imatinib resistance in CML may be cell-specific.

Whereas immunoblot analyses of lysates from K562R and LAMA-R cells showed that Bcr-Abl protein and its phosphorylated form were reduced compared to that in their imatinib-sensitive counterparts, there was no significant difference in expression of these proteins between MYL-R cells and their imatinib-sensitive counterparts, MYL cells (52-54). As opposed to reduced STAT5 expression and phosphorylation in K562R and LAMA-R cells compared to their imatinib-sensitive counterparts, STAT5 expression and

phosphorylation were significantly increased in MYL-R cells compared to MYL cells (52-54). Previous studies had associated increased Bcl-2 expression and drug resistance with increased Lyn (or SFK) activity (54). However, in contrast to LAMA-R and K562R that showed elevated levels of Bcl-2, MYL-R cells did not show increased Bcl-2 expression compared to MYL cells (52,54), further suggesting that the mechanism of imatinib resistance in MYL-R cells may be different from that of LAMA-R and K562R cells. PP2, but not imatinib, treatment of LAMA-R cells reduced Bcl-2 expression (54). Bim, one of the pro-apoptotic proteins in the Bcl-2 family whose suppression has been linked to imatinib-resistance was found to be elevated in MYL-R compared to MYL cells (52), further pointing to the unique nature in which Lyn regulates imatinib-resistance in this system. Later studies using proteomics approach in MYL and MYL-R cells linked increased Lyn activity to up-regulation of various cell signaling pathways (Ras/MEK/ERK; PI3K/AKT; NF-κB) as well as up-regulation of certain genes involved in increased transcriptional activation (PKCβ), cell proliferation (NEK9), migration (FAK), and immune response (JNK, RIPK2) (57).

Micro-RNA (miRNA) expression analyses of K562/K562R and MYL/MYL-R cells revealed substantial reduction in expression of certain miRNAs in K562R and MYL-R cells compared to K562 and MYL cells in a Lyn-dependent manner (56), pointing to yet another mechanism by which Lyn regulates drug resistance in CML. Of note, there was between ~11 to ~25-fold reduction in miR181 family (a – d) expression that correlated with increased expression of myeloid cell leukemia-1 (Mcl-1) protein in K562R and MYL-R cells compared to their imatinib-sensitive counterparts (56). Mcl-1 is an anti-apoptotic protein of the Bcl-2 family whose expression is increased in MYL-R cells and

cells of other drug-resistant leukemias with increased Lyn activity. Lyn's dual role in regulating expressions of miR181 and Mcl-1 was evident from the observation that dasatinib treatment of MYL-R cells or siRNA knockdown of Lyn in MYL-R cells increased miR181 expression and decreased Mcl-1 expression (56). Furthermore, overexpression of Lyn was shown to decrease miR181 expression and increased Mcl-1 expression. Thus, Lyn drives drug resistance in CML by suppressing expression of certain miRNAs known to target and degrade Mcl-1.

Earlier studies investigated Lyn's role in modulating Bcr-Abl oncogenesis. In CML cells from patients who did not respond to imatinib therapy despite expressing Bcr-Abl without detectable kinase domain mutations, Lyn was observed to couple with and directly phosphorylate Bcr-Abl on Tyr177 (59), a docking site for growth factor receptor-bound protein 2 (GRB2). Once at this site, GRB2 recruited the adaptor protein GRB2-associated binder 2 (Gab2) which was then persistently phosphorylated and activated by Lyn. Gab2 is a key activator of the PI3K pathway essential for Bcr-Abl-mediated oncogenesis characterized by increased differentiation, cell-cycle progression, proliferation, and enhanced cell survival (14,62). Thus, through phosphorylation of transformation-regulatory sites on Bcr-Abl and activation of Gab2, hyperactive Lyn in CML mediates phospho-regulatory control of Bcr-Abl signaling in a manner that supports imatinib resistance (59).

Lyn also supports cancer cell survival by negatively regulating both tyrosine phosphorylation and protein expression of c-Cbl, an E3 ubiquitin ligase known to ubiquitinate activated protein tyrosine kinases (PTKs) (63) resulting in reduced cell signaling. RNAi-mediated silencing of Bcr-Abl or Lyn demonstrated that silencing Bcr-

Abl reduced c-Cbl tyrosine phosphorylation in both imatinib-sensitive and imatinib-resistant K562 cells, but did not affect c-Cbl protein. Conversely, Lyn silencing increased both c-Cbl protein and c-Cbl tyrosine phosphorylation levels. C-Cbl silencing, on the other hand, had no impact on Lyn expression in K562R cells (59). Findings from these studies show that Lyn, rarely a primary causative agent in leukemia, regulates drug resistance in these CML systems by intimately integrating itself into and altering the transforming signaling cascades initiated by Bcr-Abl (14,59).

In earlier studies, Dai et al had demonstrated that transfection of Lyn into K562 cells resulted into increased, Lyn activity-dependent expression of XIAP, a member of the inhibitor of apoptosis proteins (IAP) family known to bind and inactivate active caspases leading to drug resistance in cancer (54,64). More recently, our lab has undertaken proteomics based studies in an effort to better understand the underlying mechanisms and interrogate key downstream substrates of Lyn implicated in drug resistance in CML (11,57). In addition to the up-regulation of certain signaling pathways and genes implicated in drug resistance (57), global phosphorylation analyses revealed that increased Lyn expression and activity in MYL-R cells contributed to increased expression and stability of certain IAPs (11). Of particular significance was the finding that substantial amounts of a multiply serine-phosphorylated peptide (**Figure 1.3**) unique to BIRC6, an IAP, were found in extracts of MYL-R, but not MYL cells (11). Western blot and RT-PCR analyses revealed that BIRC6 protein and mRNA levels were increased in MYL-R compared to MYL and K562 cells. Knockdown of BIRC6 in MYL- R cells using anti-BIRC6 shRNA made the cells significantly ($p < 0.05$) more sensitive to imatinib and gemcitabine, a cytotoxic nucleoside analog used in cancer chemotherapy.

The shifts in sensitivity (to the left of the dose-response curves) were ~15-fold and ~13-fold for imatinib and gemcitabine respectively (11). Similarly, BIRC6 shRNA knockdown-MYL-R cells showed significant ($p < 0.05$) increase in caspase activation when exposed to imatinib (1 μM, 24 hrs.) compared to MYL-R cells bearing empty vector. Even though the BIRC6 peptide was phosphorylated on serine residues, pharmacological targeting of Lyn resulted in lower counts of the peptide (11) suggesting Lyn's involvement in the observed phosphorylation events. Earlier studies had shown that Lyn up-regulated the expression and activity of CK2 (65), a ubiquitously expressed serine/threonine kinase whose consensus sequence often overlaps with caspase cleavage motifs thus regulating global caspase signaling (66). The multiply phosphorylated serine residues on the BIRC6 peptide were proximal to acidic residues, a consensus sequence that very closely approximates to that for CK2, S-X-X-E/D/pS/pY (**Figure 1.3**). Further, pharmacological and genetic targeting of Lyn in MYL-R cells reduced BIRC6 expression and stability, and resulted in increased caspase activation (11). Accordingly, increased expression and stability of IAPs via phosphorylation of regions overlapping with caspase cleavage motifs are some other mechanisms by which Lyn promotes drug resistance in CML.

Transduction of MYL-R cells with anti-Lyn shRNA resulted in loss of mitochondrial membrane potential, release of cytochrome c and increased caspase activation (11). Studies in other systems had shown that Lyn accumulated in the mitochondrial inter-membrane space in an active form where it phosphorylated a multi-protein complex leading to the preservation of mitochondrial integrity (67). Thus, though such studies have not been undertaken in MYL-R cells, my data from shRNA knockdown of Lyn

suggest that Lyn probably promotes cell survival by regulating phosphorylation events that lead to enhanced stability of the mitochondria.

^{1}H NMR analysis of metabolic profiles of MYL and MYL-R cells revealed substantial differences between the two cell lines in a manner consistent with increased Lyn activity and imatinib-resistance in MYL-R cells (68). Of particular significance was the finding that the total intracellular creatine pool (creatine + phosphocreatine) was ~5-fold higher in MYL-R compared to MYL cells (68). In the cell, creatine kinase converts creatine into phosphocreatine, a high-energy phosphate donor that regulates ATP homeostasis in the cell (**Figure 1.4**). Additionally, studies in other systems have shown that phosphocreatine promotes cell survival by regulating mitochondrial oxidative phosphorylation (69). Similarly, Lyn has been shown to promote autophagy as a survival mechanism for cancer cells under conditions of nutrient deprivation (41). Our unpublished data show that Lyn's regulation of increased creatine uptake in MYL-R cells is accomplished via Lyn phosphorylation and activation of the Na$^+$/K$^+$-ATPase leading to establishment of an energy gradient that facilitates coupled uptake of Na$^+$ and creatine. Further, pharmacological or genetic inhibition of Lyn resulted in reduced total intracellular creatine pool in MYL-R cells. Finally, incubation of MYL-R cells with creatine uptake inhibitors resulted in reduced cell viability suggesting that creatine promotes MYL-R cell survival through diverse mechanisms.

Lyn signaling plays an important role in promoting acquired resistance to therapy in myeloid cell cancer through various mechanisms including kinome reprogramming, up-regulation of survival genes, and changes in metabolism of CML cells. Thus, Lyn has proven to be an important target in the development of novel therapies for malignancies

of myeloid origin. However, to develop more effective therapies, much still remains to

be done to gain deeper understanding of what Lyn does to modulate the various adaptive

responses to CML therapy.
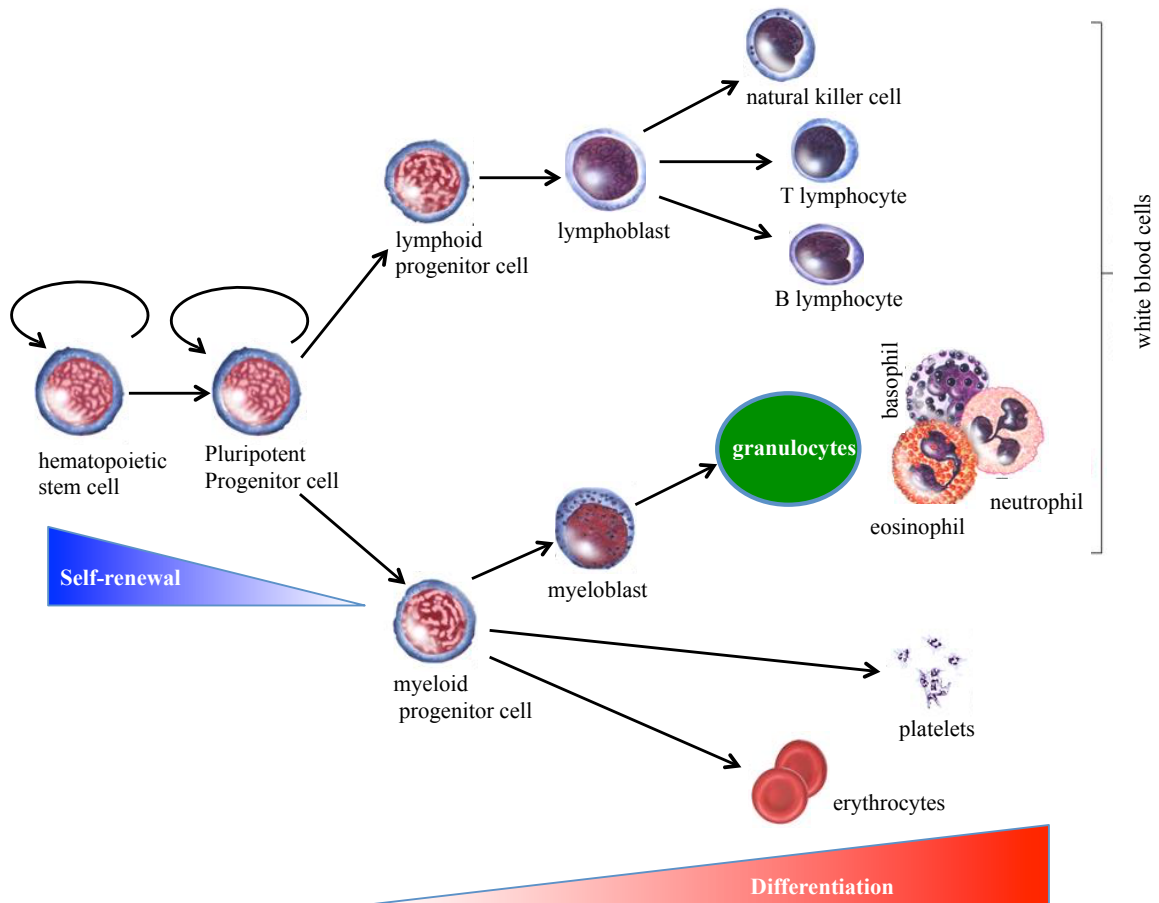
Figure 1.1. Illustration of the process of normal human blood cell development.

Increased accumulation of granulocytes (leukemia cells) from the myeloid lineage leads to the development of CML. (Figure modified from: http://www.cancer.gov/types/leukemia/patient/cml-treatment-pdq)
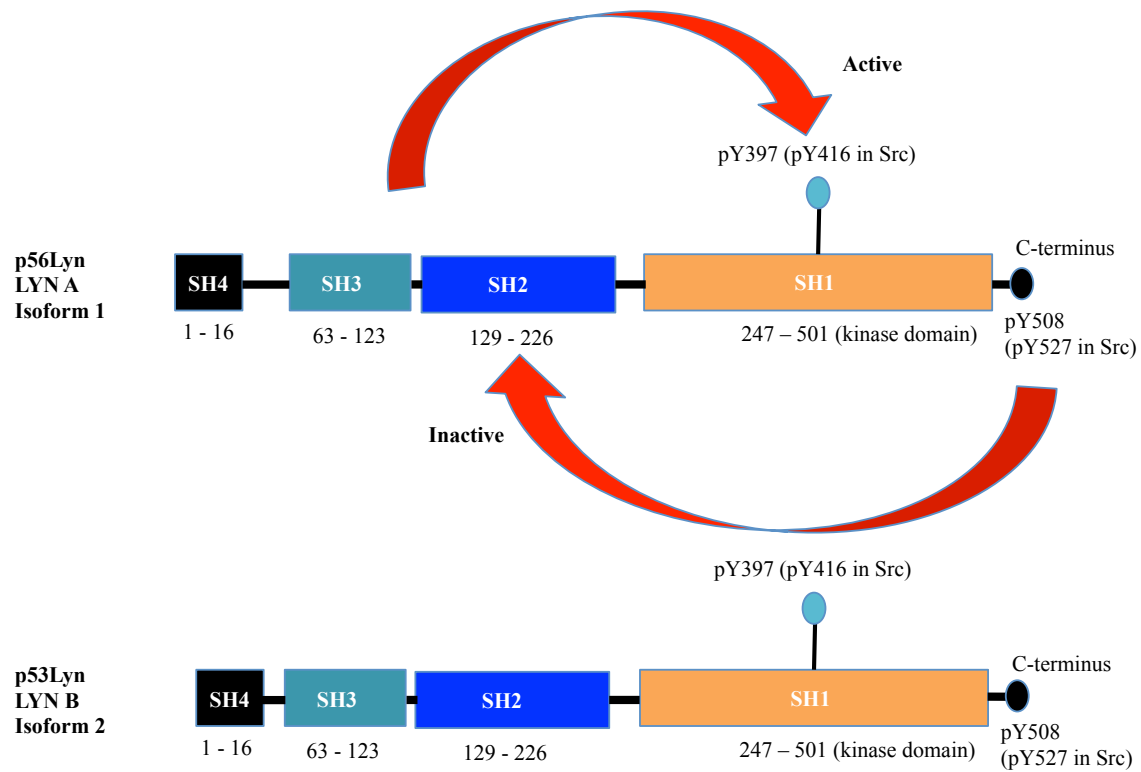
Figure 1.2. Lyn domain structure.

Schematic representation of the various Lyn functional domains and motifs, Src Homology 4 (SH4), Src Homology 3 (SH3), Src Homology 2 (SH2), and Src Homology 1 (SH1, kinase domain). Critical pY motifs that are either deactivating (pY508 or pY527 in Src) or activating (pY397 or pY416 in Src).
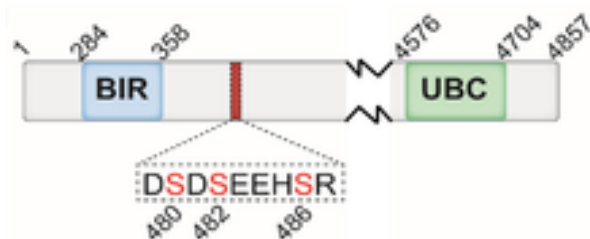
Figure 1.3. Sequence and position of the BIRC6 phosphopeptide.

BIRC6 is phosphorylated on multiple serine residues flanked by acidic residues proximal to the BIR domain.
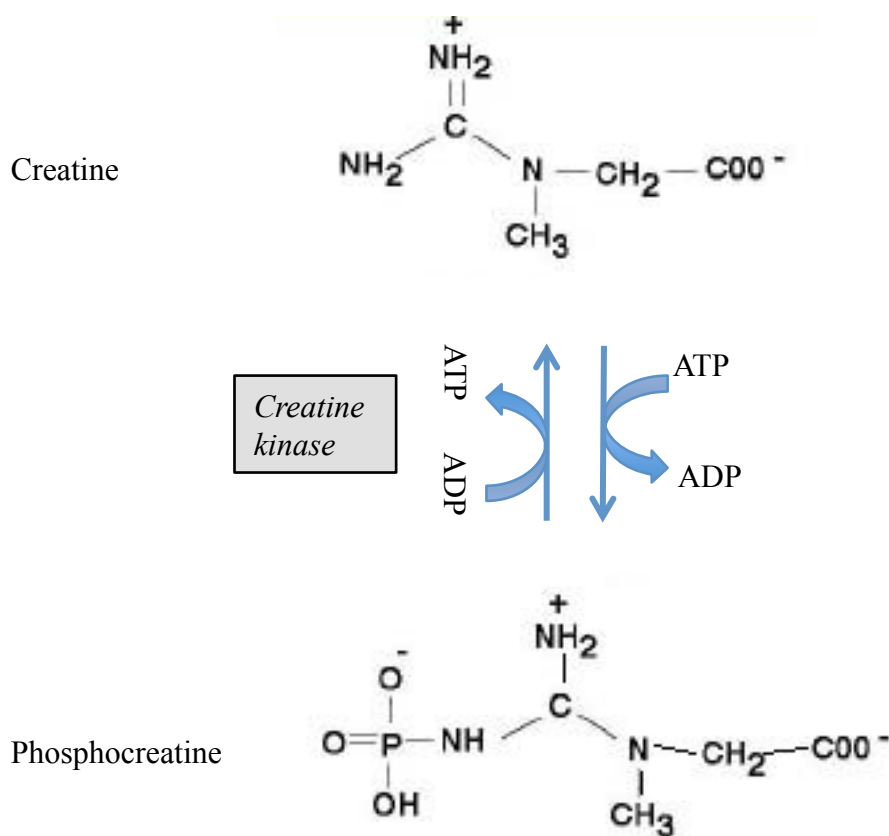
Figure 1.4. Creatine is converted into phosphocreatine by creatine kinase.

In the presence of ATP, creatine kinase phosphorylates creatine to produce phosphocreatine in a reversible reaction in the cell. (Figure modified from: https://www1.udel.edu/chem/C465/senior/fall00/Performance1/ phosphocreatine.htm.html)

18

1.3   Dissertation overview

Acquired drug resistance presents significant challenges to effective treatment of malignancies of myeloid origin. Various mechanisms of drug resistance including increased expression of drug exporter proteins, amplification of target, target mutation, and kinome reprogramming develop due to chronic exposure of patients to drugs. In this dissertation, I discuss certain ways in which activation of alternative signaling cascades (modulated by Lyn) promote drug resistance in chronic myelogenous leukemia (CML) initiated by Bcr-Abl fusion protein.

The dissertation is partitioned into 4 chapters. Chapter 1, "Introduction", I review Lyn kinase signaling in drug resistant human cancers with specific focus on CML. I discuss how Lyn activity is increased in Bcr-Abl initiated CML, and how this alters global signaling cascades leading to emergence of drug resistance. In Chapter 2, "BIRC6 mediates imatinib resistance independently of Mcl-1", I used an imatinib-resistant CML cell model (MYL-R) to interrogate downstream effectors of drug resistance modulated by Lyn. I showed that increased Lyn activity up-regulated expression and stability of BIRC6, a member of the inhibitor of apoptosis proteins family. In Chapter 3, "Lyn regulates creatine uptake in an imatinib-resistant CML cell line", I investigate the role Lyn plays in the increased accumulation of creatine and phosphocreatine in MYL-R cells, and the implications for MYL-R cell survival. Finally, in Chapter 4, "Conclusions and Future Directions", I review the broad implications of these observations and suggest certain experiments that should be done to further characterize Lyn's role in CML, and to inform the development of new, more effective therapies for drug resistant CML.

CHAPTER 2: BIRC6 MEDIATES IMATINIB RESISTANCE INDEPENDENTLY OF Mcl-1[1]

2.1 Introduction

Chronic myelogenous leukemia (CML) is a malignancy of myeloid cells characterized by accumulation of mostly myeloid cells in the bone marrow and bloodstream (1,3). CML is a result of the fusion of the breakpoint cluster region (Bcr) and Abelson (Abl) genes due to reciprocal translocations between chromosomes 9 and 22, t(9;22), resulting in a chimeric, constitutively active Bcr-Abl tyrosine kinase(1,6-8,70-73). While successfully treated with the Bcr-Abl kinase inhibitor imatinib, high incidences of disease relapse and drug resistance have been recorded in CML patients (7,8,10,70,74).

Imatinib mesylate (IM, Gleevec®, STI571, CGP57148B), the first clinically available kinase inhibitor, is an ATP-competitive inhibitor of Bcr-Abl developed as a frontline treatment for CML (70,75,76). Some of the IM therapy-related (Bcr-Abl-dependent) mechanisms of resistance include Bcr-Abl amplification or expression of inhibitor-resistant Bcr-Abl with mutations in the kinase domain. For example, the T315I "gatekeeper mutation" diminishes the kinase's affinity for the drug. Additional evidence suggest that imatinib resistance is due to Bcr-Abl independent mechanisms like enhanced expression of drug exporters (like P-glycoprotein) or activation of alternative kinase

---

signaling cascades (52,57,72). These challenges have led to the development of second generation (dasatinib and bosutinib) and third generation (ponatinib) inhibitors that target both Bcr-Abl and Src family kinases (8,75,77). Alternatively, hematopoietic stem cell transplantation remains the only other feasible cure for refractory CML. Unfortunately, most patients cannot benefit from this approach due to advanced age at diagnosis or lack of a suitable stem cell donor (6,78).

Inhibitors of apoptosis proteins (IAPs) are a group of highly evolutionarily conserved anti-apoptotic proteins known to globally regulate caspases and immune signaling (79-84). Studies have shown that up-regulation of IAPs such as cellular inhibitor of apoptosis protein 2 (cIAP2), X-linked inhibitor of apoptosis protein (XIAP), survivin and others correlates with decreased apoptosis and increased drug resistance (81,85-89). Non-IAP anti-apoptotic proteins of the Bcl-2 family such as myeloid cell leukemia-1 protein (Mcl-1), are known to also mediate drug resistance in diverse cancers (52,56,90). Mcl-1 is a well-known marker of anti-apoptosis whose role in cancer drug resistance is well documented (91-94). It is localized to the outer mitochondrial membrane where it heterodimerizes with and neutralizes pro-apoptotic Bcl-2 proteins like Bak, Bim, Noxa, and PUMA resulting in suppression of cytochrome c release and prevention of apoptosis (52,56,57,91-94). We previously observed that Mcl-1 is increased in the imatinib-resistant CML cell line (MYL-R) characterized by overexpression and activity of the Src family kinase, Lyn (56,57,95,96). These results suggest that Mcl-1 may play a role in the Bcr-Abl-independent, Lyn-mediated imatinib resistance in these cells (52,56,57). This is consistent with several studies over the last decade that have focused on Mcl-1 as a key anti-apoptotic protein mediating drug resistance in various human cancers (90,93,94,97-

99). The development of effective Mcl-1 inhibitors, however, has met various challenges

with the few commercially available candidates having limited success in the clinic (98-

101).

   Baculoviral inhibitor of apoptosis repeat-containing protein 6 (BIRC6), also known as

Apollon or BRUCE, is a member of the BIR domain containing family of IAPs

(81,83,89,102). BIRC6 is localized to the trans-Golgi membrane and vesicular networks,

and possesses a single BIR domain of 75 amino acid residues arranged in tandem repeats

in the N-terminal region of the protein. This domain is the region that binds and inhibits

caspases, thereby preventing caspase activation required for apoptosis (81). BIRC6 has a

UBC domain at its C-terminus that allows it to function as a chimeric E2/E3 ubiquitin

ligase, one target being the pro-apoptotic protein, Diablo (81,103,104). This domain is

also a binding site for mitochondrial proteins like Diablo/Smac and HtrA2/Omi that

antagonize BIRC6's anti-apoptotic activity in cells.   It was shown that BIRC6 only

binds and inhibits caspases as a homodimer, and that caspases could cleave this dimer

and degrade BIRC6, thereby quenching its anti-apoptotic properties (81). Thus, the

reciprocal inhibition between BIRC6 and caspase activation is a potential mechanism by

which cells may coordinate survival and apoptotic processes (81,103,105,106).

   BIRC6 has been shown to be important in cell cycle progression and DNA damage

repair where it functions as a scaffold protein for assembly of the DNA damage repair

machinery (107-109). Furthermore, several *in vivo* studies show that total ablation of

BIRC6 causes growth retardation and, embryonic and perinatal lethality, underscoring the

protein's critical role in cell viability (103,110,111). Recent studies show that BIRC6 is

increased in a number of intractable human cancers, including *de novo* acute myeloid

leukemia, breast cancer, ovarian cancer, hepatic cancer, prostate cancer, colon cancer, neuroblastoma, and non-small-cell lung cancer where it may contribute to cancer cell survival and proliferation (80,82,84,105,112-115). Despite increased interest in BIRC6 and its role in cancer cell survival, its regulation and involvement in mediating drug resistance is not well understood.

In this study, I examined BIRC6 regulation in an imatinib-resistant cell line (MYL-R) and compared this to its imatinib-sensitive counterpart (MYL). MYL-R cells are independent of Bcr-Abl mutations, amplification or overexpression of multi-drug resistance proteins like P-glycoprotein (52,116). Our studies show that BIRC6 expression is increased in this cell line, and that BIRC6 knockdown is sufficient to restore imatinib sensitivity. Our data further show that Lyn activity is important for up-regulation of both Mcl-1 and BIRC6 in MYL-R cells, and suggest that BIRC6 plays a dominant role in mediating imatinib resistance in these cells. Lastly, our results suggest that Lyn-dependent BIRC6 phosphorylation may regulate BIRC6 stability by preventing degradation by caspases. In summary, these studies suggest BIRC6 may be a promising target for the treatment of some drug resistant human cancers.

2.2 Materials and Methods

2.2.1   Cells, Cell Culture and Reagents

MYL and MYL-R human CML cell lines were generous gifts from Dr. Hideo Tanaka (Department of Haematology and Oncology, Hiroshima University, Hiroshima, Japan) (52). K562 cells, another CML cell line, were bought from American Type Culture Collection (ATCC) (Manassas, VA). Cells were cultured in culture flasks suspended in RPMI 1640 medium (Gibco® by Life Technologies™, U.S.A.) supplemented with 10%

fetal bovine serum (Atlanta Biologicals; Norcross, GA), and 1% antibiotic/antimycotic (Invitrogen; Carlsbad, Ca). Cells were maintained at 37 $^{\circ}$C in a humidified 5% CO_2 atmosphere in concentrations of approximately $0.6x10^6$ cells mL^{-1}. Culture medium was replaced every 2 to 4 days. For most experiments described here, cells were harvested by low-speed centrifugation and washed with 1X PBS prior to lysis.

Reagents were obtained from the following sources: ponatinib and dasatinib were from LC Laboratories (Woburn, MA); Z-VAD-FMK, imatinib, dinaciclib, and flavopiridol were from Selleckchem (Houston, TX); and HY-16462 was from MedChem Express (Monmouth Junction, NJ). The primary human antibodies used include: BIRC6 (Abcam, Cambridge, MA and Cell Signaling Technology, CST, Danvers, MA), Cytochrome c (Abcam), CDK9, phospho-CDK9, phospho-Src (Y416), PARP/Cleaved PARP, phospho-c-Abl (CST), phospho-EEF1D, phospho-CK2beta, phospho-IF2B (Litchfield Lab, University of Western Ontario, Canada), Lyn, Mcl-1, c-Abl, alpha-Tubulin, Hsp60, Erk2, and β-actin (SCBT); with secondary antibodies, anti-mouse and anti-rabbit IgG-HRP conjugated (Promega {Madison, WI}). Phospho-EEF1D, phospho-CK2beta, and phospho-IF2B antibodies were diluted per supplier recommendations: 1:20,000, 1:10,000, and 1:10,000 respectively in 3% bovine serum albumin (BSA) in Tris-buffered saline supplemented with Tween-20, TBS-T (10 mM Tris-HCl pH 7.6, 150 mM NaCl, 0.05% Tween-20). All other primary antibodies were diluted following supplier recommendations: 1:1000 in 5% BSA/TBS-T. Secondary antibodies were diluted at 1:10,000 in 5% dry, non-fat milk in TBS-T.

2.2.2 Multiplexed Inhibitor Bead (MIB) Affinity Chromatography / MS Analysis

Kinases were isolated from MYL and MYL-R cell lysates as previously described (57,117). Briefly, cells were harvested by centrifugation and washed once with PBS. Cells were lysed in MIB Lysis Buffer [50 mM HEPES pH 7.5, 150 mM NaCl, 0.5% Triton X-100, 1 mM EDTA, 1 mM EGTA, 10 mM NaF, and 2.5 mM Na_3VO_4, supplemented with protease inhibitor cocktail (Roche) and phosphatase inhibitor cocktails 2 & 3 (Sigma-Aldrich)]. Lysates were sonicated, clarified by centrifugation, and filtered through a 0.2 μm syringe filter. The amount of starting material was 5 mg protein, and was diluted to 1.25 mg/mL with MIB lysis buffer. Diluted lysates were passed over a mixture of 117uL each of the following kinase inhibitors conjugated to ECH Sepharose beads: Purvalanol B, VI-16832, and PP58, layered from top to bottom respectively. The kinase inhibitor-bead conjugates were previously equilibrated in high salt buffer (50 mM HEPES pH 7.5, 1 M NaCl, 0.5% Triton X-100, 1 mM EDTA, and 1 mM EGTA). MIBs columns were sequentially washed with high salt buffer, low salt buffer (50 mM HEPES pH 7.5, 150 mM NaCl, 0.5% Triton X-100, 1 mM EDTA, and 1 mM EGTA), and SDS buffer (50 mM HEPES pH 7.5, 150 mM NaCl, 0.5% Triton X-100, 1 mM EDTA, 1 mM EGTA, and 0.1% SDS). Proteins were eluted by boiling samples in elution buffer (100 mM Tris-HCl pH 6.8, 0.5% SDS, and 1% B-mercaptoethanol) for 15 minutes twice. Dithiothreitol (DTT) was added to a final concentration of 5 mM and samples were incubated at 60°C for 25 minutes. Samples were then cooled to room temperature on ice and alkylated by adding iodoacetamide to a final concentration of 20 mM and incubating for 30 minutes in the dark at room temperature. Samples were then concentrated in 10K Amicon Ultra centrifugal

concentrators (Millipore) followed by methanol and chloroform precipitation of proteins. The final protein pellets were re-suspended in 50 mM HEPES pH 8.0 and incubated with trypsin at 37°C overnight. Residual detergent was removed by three sequential ethyl acetate extractions then desalted using Pierce C-18 spin columns (Thermo Scientific) according to the manufacturers protocol. Samples were run on the Q-Exactive HF mass spectrometer (see LC/MS/MS analysis). Kinases were quantified by label-free analysis of kinase peptides using the MAXQUANT software package with integrated search engine (ANDROMEDA). Peptides required a minimum length of six amino acids and protein identification required at least two unique peptides. The cutoff of global false discovery rate for peptides and proteins was set at 1% and only unique peptides were used for label free quantification.

2.2.3   Trypsin Digestion and Phosphopeptide Enrichment

For phosphoproteome analysis, 4 volumes of cold acetone were added to 1 mg of each lysate for protein precipitation. The samples were then reconstituted in 7 M urea, reduced, alkylated, and digested overnight with trypsin (Promega). Peptides were desalted using Sep-Pak C18 cartridges (Waters) according to manufacturer's protocol, then dried down and stored at -80°C until further use. Phosphopeptide enrichment was performed using the 200 μl TiO_2 Spin Columns from GL Sciences. Peptide samples were reconstituted with 80/20 ACN/lactic acid in 1% TFA, then loaded onto the TiO_2 spin column prewashed with 80% ACN, 1% TFA. Peptides were washed once with 80/20 ACN/lactic acid in 1% TFA and twice with 80% ACN, 1% TFA. Retained peptides were eluted twice with 20% ACN, 5% NH_4OH and acidified < pH 4 with formic acid. All

phosphopeptide eluates were desalted using C18 Spin Columns (Thermo Fisher) then dried down and stored at -80°C until further use.

2.2.4   LC/MS/MS Analysis

Each sample was analyzed by LC-MS/MS using an Easy nLC 1000 coupled to a QExactive HF equipped with an Easy Spray source (Thermo Scientific). First, samples were reconstituted in loading buffer (1% ACN, 0.1% formic acid), and then loaded onto a PepMap 100 C18 column (75 μm id × 25 cm, 2 μm particle size) (Thermo Scientific). Peptides were separated over a gradient consisting of 5–32% mobile phase B over 60 min at a 250 nl/min flow rate, where mobile phase A was 0.1% formic acid in water and mobile phase B consisted of 0.1% formic acid in ACN. The QExactive HF was operated in data-dependent mode where the 15 most intense precursors were selected for subsequent fragmentation. Resolution for the precursor scan (m/z 400–1600) was set to 120,000 with a target value of 3×10^6 ions. For MS/MS scans with HCD (normalized collision energy 27%), resolution was set to 15,000 with a target value of 2×10^4 ions. Peptide match was set to preferred, and precursors with unknown charge or a charge state of 1 and >7 were excluded.

2.2.5   Data Analysis

Raw data files were processed using MaxQuant software (version 1.5.3.17). Data were searched against a human UniProt database (downloaded Aug 2015) using the integrated Andromeda search engine. The following parameters were used to identify tryptic peptides for protein identification: up to two missed trypsin cleavage sites; carbamidomethylation (C) was set as a fixed modification; and oxidation (M), deamidation (NQ), and phosphorylation (STY) were set as variable modifications. A

27

false discovery rate (FDR) of 1% was used to filter all results, and match between runs was enabled. Bioinformatics analyses were performed with Perseus software (version 1.5.3.0). Phosphorylation sites with a localization probability of at least 0.70 were considered.

2.2.6 Immunoblot Analysis

Cells were harvested and lysed in a modified RIPA (RIPA, no SDS) buffer (150 mM NaCl, 9.1 mM Na_2HPO_4, 1.7 mM NaH_2PO_4, 1% NP-40, and 0.5% deoxycholic acid; adjusted to pH 7.4) and supplemented with 2 mM sodium orthovanadate, 10 mM NaF, 0.0125 μM calyculin A, and cOmplete Protease Inhibitor Cocktail (Roche Diagnostics, U.S.A.). The lysates were clarified by centrifugation and the protein concentrations were normalized using a Bradford assay (with reagents from BIO-RAD). Samples for gel electrophoresis were prepared by adding protein lysates to Laemmli sample buffer (final concentration: 0.25 M Tris pH 6.8, 10% glycerol, 5% β-mercaptoethanol, 0.001 μg/mL Bromophenol blue) and 30 μg of protein were loaded into each well of an SDS-polyacrylamide gel for protein separations. Proteins were transferred to polyvinylidene difluoride (PVDF) membranes (BIO-RAD) which were then blocked for 1 hr with 5% non-fat dry milk or 5 % BSA dissolved in Tris-buffered saline supplemented with Tween-20 (TBS-T). The membranes were then incubated in primary antibodies at 4° C overnight, washed 3 times with TBST, then incubated with anti-mouse / rabbit IgG-HRP conjugated secondary antibodies for 1 hr at room temperature. The membranes were rinsed 3 times with TBST then developed using Clarity ™ ECL Western Substrate (BIO-RAD), and imaged using a ChemiDoc ™ Touch Imaging System (BIO-RAD).

2.2.7 RNA Extraction and cDNA Synthesis

Total RNA was extracted and purified using RNeasy® Mini Kit (Qiagen, U.S.A.) according to the manufacturer's protocol. cDNA was synthesized from reverse transcription on 1.5 μg total RNA in a 50 μL reaction using High Capacity cDNA Reverse Transcription Kit (Applied Biosystems, U.S.A.) and iCycler (BIO-RAD, U.S.A.), according to the manufacturer's protocol.

2.2.8 Quantitative Real-time PCR (qRT-PCR)

The cDNA was analyzed by real-time qPCR using TaqMan[TM] Gene Expression Assays Kit and TaqMan[TM] 2X Universal PCR Master Mix (Applied Biosystems by Life Technologies) on an Applied Biosystems 7500 Fast Real-Time PCR System. All procedures followed company protocol.

2.2.9 Cell Viability Assay

Cell viability was determined by seeding triplicate populations of MYL-R or MYL or BIRC6 knockdown MYL-R cells on a 96-well plate at 5×10^3 cells/well in 100 μL culture medium supplemented with various concentrations of kinase inhibitors. Cells were incubated at 37 ºC / 5% CO_2 for 72 hours. 20 μL of Resazurin[TM] (SIGMA) MTS assay reagent was added to each well, and the plate returned to the incubator for ~ 2 hrs. Cells were transferred into opaque, black 96-well assay plates (Costar) and fluorescence measured at 520 nm using the PHERAstar microplate reader Spectra Max Plus 384 (BMG Labtech). Cell viability was assessed using GraphPad Prism SoftWare version 6.05 (GraphPad Prism, Inc). The data presented for each cell viability assay is representative of three independent experiments performed for each cell line.

2.2.10 shRNA Knockdown of BIRC6

pLKO.1 lentiviral vectors containing shRNA directed against BIRC6 (TRCN0000004157, 58, 59, 60, and 61) or a non-targeting shRNA (shCtrl) were purchased from the UNC Lenti-shRNA Core Facility. Lentivirus transduction of MYL-R cells with shRNA was done per the protocol supplied by the RNAi Consortium (http://www.broadinstitute.org/rnai/public/resources/protocols). Briefly, MYL-R cells were seeded at $5x10^5$ cells/mL in 5 mL growth media containing 8 µg/mL polybrene, and incubated with 1 mL of viral shRNA overnight. Stably transduced cells were selected for by exposure to 2 µg/mL puromycin in cell culture (57). The cells were harvested one week after selection and immunoblot analysis performed to determine which shRNA strain was most effective in knocking down BIRC6.

2.2.11 shRNA Knockdown of Lyn

pLKO.1 lentiviral vectors containing shRNA directed against Lyn (TRCN0000010101, 04, 05, 06, and and 07) or a non-targeting shRNA (shCtrl) were purchased from the UNC Lenti-shRNA Core Facility. Lentivirus transduction of MYL-R cells with shRNA was done per the protocol supplied by the RNAi Consortium, and as outlined above for BIRC6. One week after puromycin selection, BIRC6 mRNA and protein were analyzed by QRT-PCR and immunoblot respectively.

2.2.12 shRNA Knockdown of CDK9

shRNA directed against CDK9 (TRCN 0000000494, 495, 496, 497, and 498) or a non-targeting shRNA (shCtrl) were purchased from Thermo Scientific and packaged into pLKO.1 lentiviral vectors by the UNC Vector Core as described above (for BIRC6 and Lyn). Lentivirus transduction of MYL-R cells with shRNA was done per the protocol

supplied by the RNAi Consortium.   The transiently transduced MYL-R cells were harvested at 48 hrs post-infection and BIRC6 mRNA and protein were analyzed by qRT-PCR and immunoblot. Transient transduction was used in order to avoid substantial loss in cell viability previously observed upon knockdown of the protein and selection with puromycin.

2.2.13 Caspase-3/7 Activity Assay

BIRC6 protein was knocked down in MYL-R cells with shRNA transcripts shBIRC6-58 and shBIRC6-59. A third population of the same MYL-R cells was transduced with shCtrl. After selection and stabilization of the transduced cells with puromycin, 3×10^6 cells from each population were treated with 1 μM imatinib (Selleckchem) and a DMSO control, with an additional treatment of parental MYL-R cells with a 1 nM dasatinib (control). After 24 hours, cells were collected from each flask, lysed on ice for 10 minutes with 300 μL lysis buffer [50 mM HEPES (pH 7.4), 5 mM CHAPS, and 5 mM DTT], and lysates clarified by centrifugation at 10,000xg for 10 minutes at 4°C. Protein concentrations were normalized using the Bradford Assay. In a 96-well plate, 100 μg of protein was added to 200 μL of assay buffer [20 mM HEPES (pH 7.4), 0.1% CHAPS, 2 mM EDTA, 5 mM DTT, and 15 μM Ac-DEVD-AMC caspase-3/7 substrate (Sigma-Aldrich)] in triplicate, and the plate incubated at room temperature in the dark for 2 hours.   The fluorescence intensity from liberated AMC (7-amido-4-methylcoumarin) was measured using a PHERAstar microplate reader (BMG Labtech, Cary, NC) with 360 nm excitation and 460 nm emission filters.

2.2.14 Detection of Apoptosis by Flow Cytometry

   Apoptotic cells were detected using the simultaneous dual mitochondrial membrane potential detection and caspase activity assay kit, MitoCasp^{TM} (Cell Technology), according to the manufacturer's protocol. MitoCasp^{TM} is a cell permeable two-color stain used to simultaneously detect caspase activity and mitochondrial membrane potential (DeltaPsi, $\Delta\Psi$m) using flow cytometry. For detection of caspase activity, MitoCasp^{TM} uses cell permeable, non-toxic carboxyfluorescein (FAM) labeled fluoromethyl ketone (FMK)-peptide inhibitors of caspases that covalently bind to the active caspases thereby allowing for analyses by flow cytometry of cells containing bound inhibitors. For $\Delta\Psi$m detection, MitoCasp^{TM} uses a cell permeable, low toxicity, and low $\Delta\Psi$m independent (nonspecific) binding cationic dye that has a strong fluorescent signal in the red region. Healthy cells accumulate the dye in their mitochondria in proportion to the $\Delta\Psi$m, mostly resulting in high fluorescence intensity. Apoptotic cells have compromised $\Delta\Psi$m that prevents the dye from accumulating in the mitochondria thereby yielding low fluorescence signals.

   Briefly, three separate populations of approximately 6×10^5 cells/mL BIRC6 knockdown MYL-R cells (shCtrl, shBIRC6-58, and shBIRC6-59) were treated as described in caspase-3/7 activity assay above. After 24 hours of apoptosis induction, 300 µL of cells from each cell line was transferred to a 5 mL FACS tube prior to staining for flow cytometry analysis as described below. Appropriate controls were included as necessary. Approximately 6×10^5 cells/mL of Lyn knockdown MYL-R cells (shCtrl, shLyn-01, shLyn-04, shLyn-05, shLyn-06, and shLyn-07) were cultured overnight. The

cells were prepared for flow cytometry analysis as described above for BIRC6

knockdown cells, with appropriate controls.

2.2.15 Flow Cytometry

Cells were stained with 10 μL each of the 30X ΔΨm dye and 30X Caspase detection

reagent. Single-stain controls were included for instrument compensation and

background correction. Cells were gently vortexed and incubated for 60 min at 37°C/5 %

CO_2. They were washed twice with 2 mL of 1X Wash Buffer, and then resuspended in

300 μL of 1X Wash Buffer before filtering with 30 μm filters (Becton Dickinson, BD,

Biosciences). The cells were quickly analyzed by measuring fluorescence using the FL1

(FITC filter) channel (for caspase detection reagent) and FL2 (Phycoerytherin:PE filter)

channel (for ΔΨm dye) of a fluorescence-activated BD Fortessa flow cytometer

(Excitation: 488 nm). At least 10,000 cells were determined for each sample. The flow

cytometry data were analyzed by FlowJo v10 software.

The percent apoptotic cells represent the fraction of cells in Q3 defined by a loss in

mitochondrial membrane potential and gain in caspase activity as shown in

supplementary figure 4 (**Figure 2.S4**).

2.2.16 Detection of Cytochrome C Release

Cytochrome c release was measured using Cytochrome c Releasing Apoptosis Assay

Kit (Abcam, U.S.A.), per the manufacturer's protocol. Briefly, approximately $1x10^8$

MYL-R cells were treated with 5 nM ponatinib or DMSO for 24 hours. Cells were

harvested and washed with 10 mL cold 1X PBS. Each cell population was split into two

and one pair of cell pellets were lysed in immunoblot lysis buffer and protein

concentrations normalized using the Bradford assay. Pellets from the second set were

resuspended in 1.0 ml of the supplied 1X Cytosol Extraction Buffer Mix containing DTT

and protease inhibitors (Abcam, USA). After incubating the cells on ice for 10 minutes,

they were homogenized in an ice-cold Dounce tissue grinder (Wheaton, USA) as outlined

in the protocol (Abcam, USA). This process was repeated with fresh 1.0 ml of 1X

Cytosol Extraction Buffer Mix due to the large number of cells. Aliquots of the crude

lysates were saved before centrifuging the lysates at 10,000xg for 30 min at 4°C and

collecting the supernatant as Cytosolic Fractions. The pellets were resuspended by

vortexing for 10 seconds in 0.2-ml Mitochondrial Extraction Buffer Mix containing DTT

and protease inhibitors (Abcam, USA) and saved as Mitochondrial Fractions. Protein

concentrations for the crude lysates, Cytosolic Fractions, and Mitochondrial Fractions

were normalized using the Bradford assay and appropriate amounts of 4X Reducing

Sample Buffer added. Immunoblot analyses were performed on all lysates.

2.2.17 Statistics

Data are reported as the mean $\pm$ standard error of the mean (S.E.M); S.E.M. was

performed on all datasets to determine positive and negative error. Two-tailed student t-

test was used to make comparisons between groups, and p values below 0.05 at the 95%

confidence level were considered to be statistically significant. Calculations were

performed using GraphPad Prism and Microsoft Excel.

2.3   Results

2.3.1   BIRC6 mRNA and protein are increased in imatinib-resistant MYL-R cells

In a previous study we compared the functional kinomes of MYL and MYL-R cells

(57) using MIB/MS technology (117) and showed that Lyn was substantially up-

regulated in MYL-R compared to MYL cells (57).   Other studies showed that elevated

Lyn activity mediated imatinib resistance in these cells (52,118). Hence, I further

examined both the functional kinome and phosphoproteome of these cells to identify

phosphorylation events that may contribute to imatinib resistance (**Figure 2.1**). MYL-R

cells were treated for 1 hour with 10 nM ponatinib, a dual Bcr-Abl and Lyn inhibitor

(75,77), or DMSO and MIB/MS kinome profiling and phosphopeptide enrichment were

performed as described in Materials and Methods. This concentration of ponatinib was

sufficient to potently inhibit cell viability as shown in supplementary figure 1 (**Figure

2.S1**). Untreated MYL cells were also included. The MIB/MS technology can be used to

assess inhibitor specificity (119). With short-term (1 hour) treatment, kinases bound by

ponatinib will no longer be available to bind to inhibitor beads, and therefore show a

decrease in MIBs capture. The MIB/MS kinome profiling data showed that, as expected,

both Bcr-Abl and Lyn were potently inhibited by ponatinib treatment (**Figure 2.S2**).

Immunoblot analyses were performed on the same lysates to validate changes in Bcr-Abl

and Lyn observed from the MIB/MS data (**Figure 2.2C**). Short-term (1 hour) ponatinib

treatment of MYL-R cells suppressed both Bcr-Abl and Lyn activity as determined by

immunoblots of activating phosphorylation sites on Bcr-Abl, the Bcr-Abl substrates Crkl

and Cbl, Src Family kinases, and Lyn substrates Crkl and Cbl (**Figure 2.2C**). Total

BIRC6 and Mcl-1 proteins were not affected by short-term treatment (**Figure 2.2D**).

Immunoblotting detected both the anti-apoptotic (Mcl-1$_L$) and the pro-apoptotic (Mcl-1$_S$)

isoforms that result from differential splicing (120). Only the anti-apoptotic isoform,

Mcl-1$_L$, was included for simplicity. Titanium enrichment and phosphopeptide analysis

revealed ~4000 unique phosphopeptides. Phosphopeptide abundance was calculated

using label-free quantification with MaxQuant (121), and normalized to MYL cells. A

number of phosphopeptides determined to be enriched in MYL-R lysates decreased after ponatinib treatment (Herring, unpublished data), consistent with the change in Lyn activity in these cells (**Figure 2.2C**). From the list of phosphorylated proteins that followed the Lyn activity pattern, we identified a phosphopeptide [LEGDSDDLLEDS(480)DS(482)EEHS(486)R] from the anti-apoptotic protein BIRC6 that was multiply phosphorylated on serines 480, 482, and 486, proximal to the BIR domain (**Figure 2.2A**). Quantitation of the data showed that there was ~ a 1.6-fold increase in the BIRC6 phosphopeptide in MYL-R lysate compared to MYL lysate, and that ponatinib treatment of MYL-R cells reduced phosphopeptide abundance to levels close to those observed in MYL cells (**Figure 2.2B**).

I next examined BIRC6 mRNA expression in MYL and MYL-R cells, and compared these to another CML cell line, K562. Approximately equal numbers of MYL, MYL-R, and K562 cells were collected, and each cell population split into two parts, one for total RNA extraction and the other for immunoblot analysis. Total RNA was extracted and purified using RNeasy Mini Kit (Qiagen), and analyzed by QRT-PCR using BIRC6 and Mcl-1 TaqMan probes as described in Materials and Methods. Similarly, lysates were probed for BIRC6 protein by immunoblotting. Our data showed that BIRC6 and another anti-apoptotic protein known to be upregulated in MYL-R cells (56), Mcl-1, mRNA were significantly higher ($p < 0.05$) both in the imatinib-resistant MYL-R and K562 cell lines as compared to the imatinib-sensitive MYL cell line (**Figure 2.2F**). Similarly, Mcl-1 and BIRC6 protein levels were higher in MYL-R and K562 cells respectively (**Figure 2.2E**).

2.3.2   Knockdown of BIRC6 in MYL-R cells increases sensitivity to imatinib

Increased levels of BIRC6 have been observed in a number of human cancers and shown to correlate with poor prognostic profiles and higher incidences of disease relapse (80,82,84,115). Consistent with this, I found higher levels of BIRC6 in MYL-R cells (**Figure 2.2E and 2.2F**). Thus, I examined whether imatinib had any effect on BIRC6 protein. MYL-R cells were treated for 24 hours with increasing concentrations of imatinib. A separate population of MYL-R cells was treated with 10 nM ponatinib. Immunoblotting showed that imatinib treatment was effective in reducing BIRC6 protein only in the micro-molar range with 50% reduction at 10 μM. Phospho-Bcr-Abl and the Bcr-Abl substrate, phospho-Crkl, were similar reduced. Ponatinib, on the other hand, reduced BIRC6 protein by 60% and almost completely reduced phospho-Bcr-Abl and phospho-Crkl (**Figure 2.S3A**). Based on the above data, I investigated whether imatinib-resistance was dependent on BIRC6 expression in MYL-R cells.   I infected MYL-R cells with lentiviral particles containing five independent anti-BIRC6 shRNAs or shCtrl. Stably transduced cells were selected with puromycin, and BIRC6 protein levels were measured by immunoblotting (**Figure 2.3A**). These analyses showed that shRNA constructs shBIRC6-58 and shBIRC6-59 were the most efficient, reducing BIRC6 protein by approximately 90%. Thus all subsequent experiments used these constructs to achieve BIRC6 knockdown. Knockdown of BIRC6 did not affect Mcl-1 or total Lyn protein levels in MYL-R cells (**Figure 2.3A and 2.3E**). Further immunoblot analysis showed that while there was not a substantial decrease in either phospho-Crkl or total Crkl in BIRC6 knockdown MYL-R cells, phospho-Bcr-Abl and total Bcr-Abl were substantially reduced (**Figure 2.S3B**). This was consistent with a previous study that showed

enhanced degradation of Bcr-Abl upon disruption of survivin (BIRC5) in K562 cells (73).

To examine the effects of BIRC6 knockdown on imatinib resistance, I first examined the effects of imatinib on cell viability using an MTS assay. As expected, MYL and MYL-R cells showed substantial differences in their imatinib sensitivities with IC50 values of ~ 0.2 μM and ~3.0 μM for MYL and MYL-R cells respectively (**Figure 2.3B**). Next, BIRC6-knockdown MYL-R cells were incubated with increasing concentrations of imatinib for 72 hours and MTS assay performed. BIRC6 knockdown resulted in ~15-fold shift (IC50 ~0.2 μM) in the imatinib dose-response curve and increased imatinib sensitivity to levels similar to that observed for MYL cells (IC50 ~0.2 μM) (**Figure 2.3C**). Importantly, increases in imatinib sensitivity resulting from BIRC6 knockdown were consistent with the level of BIRC6 knockdown achieved by the individual shRNAs with shBIRC6-59 resulting in greater sensitivity, further emphasizing BIRC6's role in mediating imatinib resistance in MYL-R cells.

I next examined whether the effect of imatinib on viability of BIRC6 knockdown cells was specifically due to the induction of apoptosis. The stable BIRC6-knockdown MYL-R cell lines were treated with 1 μM imatinib for 24 hours and caspase-3/7 activity assays performed as described in Materials and Methods (**Figure 2.3D**). Data from the 24-hour treatment were reported because caspase-3/7 activity was determined to be maximal at this time-point. MYL-R parental cells (positive control) were treated with dasatinib, a dual Bcr-Abl and Src family kinase inhibitor known to induce caspase-3/7 activity in this cell line (57). BIRC6 knockdown (shBIRC6-58 and -59) caused ~ 2-fold increase in caspase-3/7 activity compared to shCtrl. Compared to shCtrl, knockdown of BIRC6

(shBIRC6-58 and -59) significantly ($p < 0.05$) increased MYL-R sensitivity to imatinib
(**Figure 2.3D**). Treatment of parental MYL-R cells and BIRC6 knockdown control cells
with imatinib showed comparable caspase-3/7 activation.   These observations
demonstrate that BIRC6 reduces apoptosis in MYL-R cells treated with imatinib.

To further characterize the response of MYL and MYL-R cells to imatinib, I treated
cells with 1 μM imatinib and measured caspase-3/7 activities at 0, 6, 12, 24, 48 and 72-hr
time points (**Figure 2.S3C**). The MYL cells yielded an early (~12 hours) peak response
to imatinib that gradually subsided. On the other hand, MYL-R cells showed a slow,
gradual response to imatinib with a lower peak response at about 48 hours.   Moreover,
consistent with lower levels of BIRC6 in MYL cells, MYL cells had a higher basal
caspase-3/7 activity than the MYL-R cells (**Figure 2.S3C**).

MYL-R cells express increased amounts of the anti-apoptotic protein Mcl-1 relative to
MYL cells (56,57). Therefore, I investigated whether the increase in imatinib sensitivity
observed in BIRC6 knockdown MYL-R cells (**Figure 2.3C**) was due to concomitant loss
of Mcl-1 protein. Separate populations of the stable BIRC6-knockdown MYL-R cell
lines were treated with DMSO or imatinib (300 nM or 1 μM) for 24 hrs. MYL-R cells
expressing shCtrl were similarly treated and immunoblot analyses performed (**Figure
2.3E**). The data showed that treatment of BIRC6-knockdown MYL-R cells with imatinib
(300 nM or 1 μM) had no effect on Mcl-1 protein, further suggesting that the anti-
apoptotic effects of BIRC6 in these cells are independent of Mcl-1.

We have also observed that MYL-R cells are resistant to cytotoxic nucleoside analogs
like gemcitabine and ARA-C (Data not shown). Therefore, I examined whether BIRC6
knockdown affected sensitivity of MYL-R cells to gemcitabine using an MTS assay

(**Figure 2.3F**). BIRC6-knockdown resulted in ~13-fold shift in the gemcitabine dose-response curve and significantly increased ($p < 0.05$) gemcitabine sensitivity (shCtrl, IC50 ~ 120 nM; shBIRC6-58, IC50 ~ 9 nM; shBIRC6-59, IC50 ~ 9 nM). Gemcitabine did not achieve absolute cell death under these experimental conditions likely due to its cytostatic mechanism of action (122). Thus, BIRC6 mediates resistance to multiple anti-cancer drugs including targeted inhibitors and cytotoxic compounds.

2.3.3   Lyn kinase regulates BIRC6 expression

MYL-R cells are characterized by the overexpression and activation of Lyn kinase which is important for their survival (52,56,57). Lyn activity is inhibited by dasatinib, a small molecule inhibitor of Bcr-Abl and other tyrosine kinases (95,96). To examine if Lyn regulates BIRC6 expression, MYL-R cells were treated with dasatinib (1 or 5 nM) for 24 hours and BIRC6 mRNA and protein were analyzed using QRT-PCR and immunoblotting respectively (**Figure 2.4A and 2.4B**). Whereas dasatinib significantly increased ($p < 0.05$) BIRC6 mRNA in MYL-R cells, BIRC6 protein was substantially reduced (**Figure 2.4A and 2.4B**). Similarly, treatment of MYL-R cells with ponatinib, a more selective inhibitor of Bcr-Abl and Lyn (123,124) (**Figure 2.S2**), recapitulated the effects on BIRC6 protein (**Figure 2.4C**). Ponatinib substantially inhibited Lyn activity as measured by autophosphorylation of Src family kinases including Lyn (PY416) (**Figure 2.4C**), and in parallel, reduced both BIRC6 and Mcl-1. To further validate the importance of Lyn in regulating BIRC6, I examined the effects of Lyn-knockdown in MYL-R cells. I tested five lentiviral Lyn targeted shRNA oligonucleotides and a non-targeting shRNA (shCtrl). Aliquots were harvested from each of the cell lines, and QRT-PCR and immunoblot analyses performed (**Figure 2.4E and 2.4D**). Anti-Lyn shRNA

constructs shLyn-01, shLyn-05, and shLyn-06 were the most efficient in knocking down

Lyn as determined by immunoblotting, reducing Lyn protein by 80-90%. A substantial

reduction in BIRC6 protein was observed in response to Lyn knockdown (**Figure 2.4D**).

By contrast, shRNA knockdown of Lyn did not affect Mcl-1 protein (**Figure 2.4D**). Loss

of BIRC6 protein was not mediated by changes in gene expression as mRNA levels were

significantly ($p < 0.05$ for shLyn-05 and -06) elevated in response to Lyn knockdown

(**Figure 2.4E**). Similarly, Mcl-1 mRNA levels were significantly increased in response

to Lyn knockdown. These data suggest that Lyn regulates BIRC6 protein at the

translational or post-translational level.

Since Lyn inhibition or knockdown reduced BIRC6 protein levels in MYL-R cells

(**Figure 2.4C and 2.4D**), I investigated whether this was sufficient to increase caspase-

3/7 activity in these cells. Lyn knockdown cells were harvested and caspase-3/7 activity

was measured (**Figure 2.4F**). Lyn knockdown resulted in significant increase ($p < 0.05$)

in caspase-3/7 activity in MYL-R cells. Cells expressing the more efficient Lyn-

knockdown oligonucleotides (shLyn-05 and shLyn-06), showed a ~5-fold increase in

caspase-3/7 activity. I next examined if a change in the mitochondrial membrane

potential contributed to the increase in caspase-3/7 activity in the Lyn-knockdown cells.

Approximately 1×10^6 of the Lyn-knockdown or control MYL-R cells were analyzed for

mitochondrial membrane potential and caspase-3/7 activity using MitoCasp^{TM} (**Figure

2.S4A**). Lyn knockdown lowered the mitochondrial membrane potential and increased

caspase-3/7 activity. Consistent with the Lyn knockdown immunoblot data, the best anti-

Lyn oligonucleotides yielded the largest reduction in mitochondrial membrane potential

and increase in caspase-3/7 activity. Furthermore, the most efficient anti-Lyn shRNA

construct (shLyn-06) yielded the highest percent of apoptotic cells as determined by the fraction of cells in quadrant 3 (Q3) (**Figure 2.S4B**). Based on the above observations, I investigated whether inhibiting Lyn with ponatinib would affect the basal level of caspase-3/7 activity. MYL-R cells were treated with ponatinib (1 nM or 5 nM or 10 nM) or 0.1% DMSO for 24 hours and caspase-3/7 activity assays performed (**Figure 2.4G**). Compared to DMSO, there was significant increase ($p < 0.05$) in basal caspase-3/7 activity with ~ 2-fold increase upon treatment with 1 nM ponatinib and ~ 8-fold increase upon treatment with 5 nM or 10 nM ponatinib. These observations support the importance of Lyn-mediated regulation of BIRC6 in MYL-R cells.

I next investigated if the observed reduction in BIRC6 protein levels in MYL-R cells upon Lyn inhibition or Lyn knockdown was through effects on BIRC6 protein stability. Two MYL-R cell populations infected with anti-Lyn shRNAs (shLyn-01 and shLyn-04) (**Figure 2.5A**) were selected and treated with cycloheximide (50 μg/mL). Cells were harvested at 0, 2, 4, 6, 24, and 48 hours after cycloheximide treatment, and immunoblotted for BIRC6 (**Figure 2.5B**). I observed that BIRC6 protein half-life was approximately the same (~24 hours) in shCtrl-infected MYL-R cells as that in the parental MYL cells (**Figure 2.5B and 2.5C**). By contrast, Lyn knockdown caused a substantial reduction in BIRC6 protein stability, with the protein half-life reduced ~4-fold to approximately 6 hours (**Figure 2.5B and 2.5D**).

2.3.4 CDK9 regulates BIRC6 mRNA levels

We previously showed that increased Lyn activity correlated with elevated Mcl-1 expression in MYL-R cells (56). Other studies demonstrated that Cyclin-dependent kinase 9 (CDK9), a critical component of the elongation factor complex P-TEFb, is

required for transcription of Mcl-1 (90,97). CDK9 regulates RNA Polymerase II (RNA Pol II) by phosphorylating it, thereby promoting transcription elongation (125). Cancer cells require continuous activity of RNA Pol II to suppress oncogene-induced apoptosis (126,127). Small molecule inhibitors of CDK9 have been shown to induce apoptosis in cancer cells by suppressing Mcl-1 (90,97). To investigate if CDK9 regulates BIRC6, I treated MYL-R cells with the CDK9 inhibitors dinaciclib, flavopiridol, and a novel CDK9 inhibitor (HY-16462), and compared Mcl-1 and BIRC6 expression. Whereas dinaciclib and flavopiridol target multiple CDKs (126,128), HY-16462 is reported to be a highly specific CDK9 inhibitor (Novartis, data not shown). All three CDK9 inhibitors significantly ($p < 0.05$) reduced BIRC6 mRNA in a dose-dependent manner with the highest concentrations yielding >5-fold reduction as determined by QRT-PCR (**Figure 2.6A**). Mcl-1 mRNA was similarly reduced. Immunoblot analysis revealed that the highest concentrations of CDK9 inhibitors strongly reduced Mcl-1 protein as previously reported (90,97,129) (**Figure 2.6B**). Consistent with loss in mRNA, I observed a decrease in BIRC6 protein after treatment with CDK9 inhibitors. The decrease in BIRC6 protein was modest compared to Mcl-1 but likely reflects differences in protein half-life. To further confirm the role of CDK9 in regulating BIRC6 expression, I used shRNA-mediated knockdown of CDK9 in MYL-R cells. Knockdown of CDK9 substantially reduced Mcl-1 protein levels (**Figure 2.6C**), but had no effect on BIRC6 (**Figure 2.6D**). These data demonstrate differential regulation of BIRC6 and Mcl-1 by CDK9 and suggest that specific inhibition of CDK9 is not sufficient to decrease BIRC6 protein levels.

2.3.5 Lyn regulates caspase-mediated degradation of BIRC6 in MYL-R cells

BIRC6 is degraded by caspases in response to cell death signals (81). I observed multiple fragments of BIRC6 after treatment of MYL-R cells with ponatinib (10 nM, 24hr) or dasatinib (1 nM, 24hr), including formation of a prominent ~52-kDa band (**Figure 2.7A**). This fragment was determined to contain the N-terminal region of BIRC6 as confirmed by the location of the antibody epitope and peptide competition experiment (**Figure 2.7A** and data not shown). Interestingly, the formation of the BIRC6 ~52-kDa immunoreactive band was significantly reduced in MYL-R cells co-treated with a pan-caspase inhibitor, Z-VAD-FMK (**Figure 2.7A**), indicating that the pan-caspase inhibitor rescued BIRC6 loss, further emphasizing the role played by caspases in BIRC6 degradation. Others previously reported that the onset of apoptosis can lead to BIRC6 degradation by proteasome and caspase cleavage (106). However, addition of a proteasome inhibitor (MG-132) had no effect on BIRC6 degradation in ponatinib-treated cells (**Figure 2.7A**). The data suggest that caspases are primarily involved in BIRC6 degradation following Lyn inhibition.

Previous studies showed that increased cell proliferation was accompanied with elevated tyrosine phosphorylation inside mitochondria mediated by activated Src family kinases (67). Additionally, active Lyn was reported to accumulate in the mitochondrial inter-membrane space where it complexes with a multi-protein complex (67). Hence, I investigated whether Lyn inhibition would trigger mitochondrial events leading to caspase activation and loss in BIRC6 protein. MYL-R cells were treated with 5 nM ponatinib or 0.1% DMSO and cytochrome c protein release analyzed by immunoblotting (**Figure 2.7C**). Ponatinib treatment resulted in 70% loss in Src family kinases activation

(PY416) and 30% loss in BIRC6 protein (**Figure 2.7B**). Total Lyn was increased by 80%. The appearance of cleaved PARP in whole cell lysates from ponatinib-treated but not DMSO-treated cells confirmed the induction of apoptosis (**Figure 2.7B**). Immunoblot analysis of cytochrome c was performed on crude lysate, cytosolic, and mitochondrial fractions. Cytochrome c bands were normalized to the respective DMSO fractions. Lysates from MYL-R cells treated with ponatinib showed a 2.7-fold increase in cytosolic cytochrome c (**Figure 2.7C**). These data suggest that Lyn reduces BIRC6 degradation by regulating mitochondrial events that are key to caspase activation.

2.4   Discussion

Acquired resistance to apoptosis is an important defining characteristic of many drug resistant cancers (52,117,130,131). While there is considerable evidence supporting BIRC6's role in mediating drug resistance in several human cancers, the mechanisms regulating its expression and stability are not well understood (82,84,105,112-115,130,131). I used a model of imatinib-resistance in CML cells to investigate the molecular determinants of acquired resistance. Phosphoproteomics of MYL and MYL-R cells identified BIRC6 as a potential regulator of imatinib resistance in MYL-R cells. Our data demonstrate three important observations: BIRC6 mediates imatinib resistance in MYL-R cells; Lyn activity regulates BIRC6 expression and stability; and inhibition or knockdown of Lyn results in caspase-mediated degradation of BIRC6.

In our MYL-R model of imatinib-resistant CML, I observed Lyn activity to be correlated with increased phosphorylation, expression, and stability of BIRC6. Lyn inhibition with ponatinib resulted in loss of Mcl-1 protein, release of cytochrome c from mitochondria, caspase activation, and degradation of BIRC6 protein. Lyn depletion with

shRNA also led to loss in BIRC6 protein. Regulation of BIRC6 degradation has been described to occur via various mechanisms including caspase-3, -6, -7, -8, and -9 cleavage (81). I observed that induction of apoptosis correlated with both the loss of full length BIRC6 and the formation of a prominent N-terminal BIRC6 fragment by immunoblot analysis. Use of the pan-caspase inhibitor, Z-VAD-FMK, prevented both loss of full length BIRC6 and fragment formation indicating that caspase activation was required for BIRC6 degradation in response to Lyn inhibition. I did not observe any role for proteasome-mediated degradation of BIRC6 in response to Lyn inhibition as suggested by the failure of the proteasome inhibitor, MG-132, to rescue BIRC6 degradation.

Our lab previously made a link between Lyn activity and increased Mcl-1 (56). In the present study, I show that BIRC6-knockdown rendered MYL-R cells several-fold more sensitive to imatinib and gemcitabine, two compounds used in cancer therapy. The increase in imatinib sensitivity after BIRC6 knockdown occurred without concomitant loss of Mcl-1. This was surprising since multiple studies have suggested that Mcl-1 is necessary for mediating drug resistance in cancers including leukemias (56,90,93,94,97,129). Mcl-1 and CDK9 inhibitors, however, have had limited success in cancer therapy (100,101,126,132-134). My data show that BIRC6 exerts a dominant role in mediating imatinib resistance independently of Mcl-1.

My study suggests that BIRC6 expression and stability in MYL-R cells is dependent on Lyn and that elevated BIRC6 levels promotes cell survival. The phosphorylated peptide derived from BIRC6 correlated with Lyn activity, exhibiting increased levels in MYL-R relative to MYL cells and decreased levels after ponatinib treatment. Notably,

short-term ponatinib treatment did not affect total BIRC6 protein suggesting that the change in BIRC6 phosphopeptide abundance was largely dependent on changes in kinase signaling. Interestingly, this peptide contains consensus caspase-8/9 and -3/7 cleavage sites that overlap with potential consensus phosphorylation motifs of certain serine/threonine kinases including CK2, PLK1, Aurora A kinase, and others (66,135-139). Treatment of MYL-R cells with a CK2 inhibitor caused a substantial reduction in BIRC6 protein (**Figure 2.S5A**). Furthermore, BIRC6 immunoprecipitation experiments showed that CK2 co-precipitated with BIRC6 (**Figure 2.S5B and 2.S5C**) as reported earlier (140). CK2 phosphorylation of caspase substrates in the vicinity of caspase recognition motifs protects proteins from caspase cleavage (66). Interestingly, the ~52-kDa N-terminal degradation fragment observed in our studies (**Figure 2.7A**) is consistent with the predicted molecular weight of the product of caspase cleavage near the identified phosphorylation sites proximal to the BIR domain. Cleavage of BIRC6 in the N-terminal region inactivates its ability to bind and inhibit caspases (81). Thus, phosphorylation of BIRC6 by CK2 may prevent BIRC6 degradation by caspases. While previous studies suggested that Lyn regulates CK2 activity in imatinib-resistant CML cells (65), I did not observe differences in CK2 activity in MYL and MYL-R cells as measured by the phosphorylation of validated CK2 substrates (141), CK2β and EEF1D (**Figure 2.S5D**). It remains to be determined if CK2 regulates BIRC6 stability through phosphorylation of these sites.

In summary, my data demonstrate that BIRC6 is enriched in imatinib-resistant CML cells (MYL-R), and that knockdown of BIRC6 was sufficient to increase imatinib sensitivity independent of Mcl-1. I showed that CDK9 inhibition suppressed both BIRC6

and Mcl-1 mRNA and protein levels. The increase in Mcl-1 protein caused by dinaciclib (10 nM, 24 hours) was likely due to activation of compensatory signaling mechanisms but was not pursued further in the present study. I next used anti-CDK9 shRNAs to test whether CDK9 specifically regulates BIRC6. Whereas Mcl-1 was reduced by >95% upon CDK9 knockdown, there was no effect on BIRC6 protein suggesting that CDK9 does not regulate BIRC6 protein. These data indicate that the effects observed with CDK9 inhibitors were likely due to off-target effects rather than specific inhibition of CDK9. CDK9 inhibitors, including those used in this study, have been reported both by their manufacturers and in the literature to have poor specificity for CDK9 (126,128,142). Thus, CDK9 inhibitors are unlikely to overcome imatinib resistance mediated by BIRC6. Taken together, these data also indicate that targeting Mcl-1 directly (Obatoclax Mesylate) or indirectly through CDK9 inhibition will have little effect on drug resistance in cells expressing high levels of BIRC6. Although there are currently no direct inhibitors of BIRC6, targeting Lyn or kinases that maintain BIRC6 expression or stability may have therapeutic potential in treating drug resistant CML or other cancers.
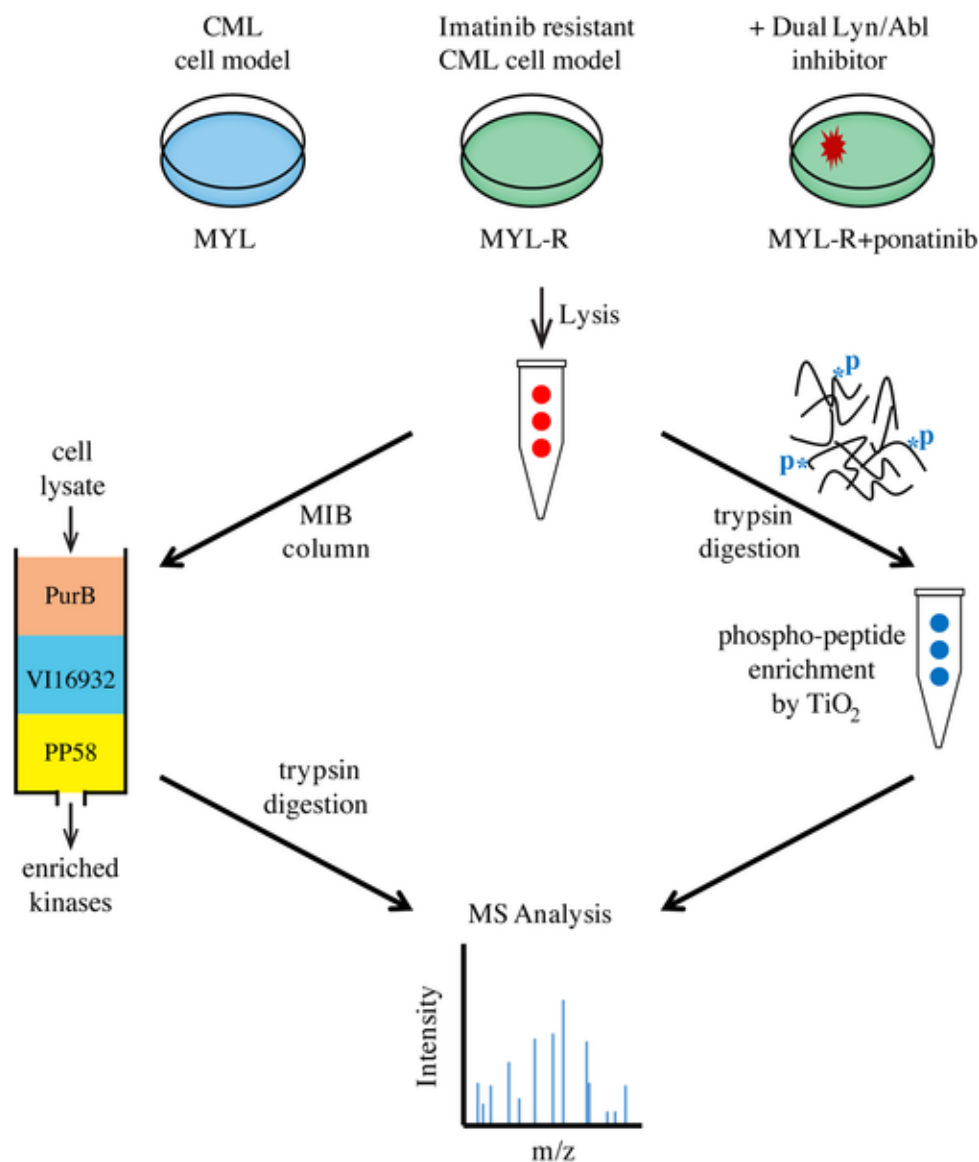
Figure 2.1. Combined MIB/MS and phosphopeptide enrichment strategy for studying proteome dynamics in CML cells.

MIB/MS was used to study kinome dynamics in MYL, MYL-R, and MYL-R cells treated with ponatinib (10 nM, 1 hr.). In parallel, phosphoproteomics was used to study global phosphorylation differences from the same cells. Identification of peptides was accomplished by LC-MS/MS and label-free quantification (LFQ) of mass spectral data was performed using MaxQuant and the integrated ANDROMEDA search engine (121).
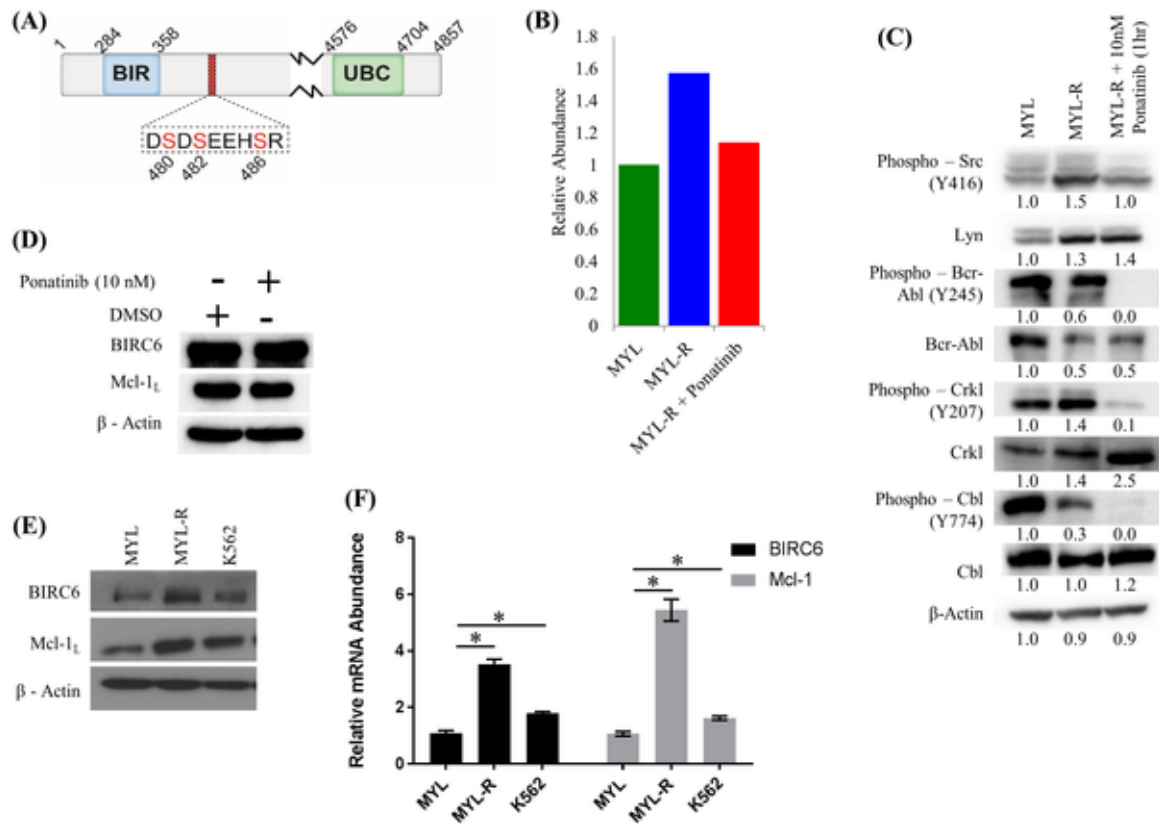
Figure 2.2. BIRC6 mRNA, protein, and BIRC6 phosphopeptide are higher in imatinib resistant MYL-R cells.

(A) Sequence and position of the BIRC6 phosphopeptide. (B) Short-term ponatinib treatment of MYL-R cells reduced BIRC6 phosphopeptide. The BIRC6 phosphopeptide was isolated from cell lysates of MYL, MYL-R, and MYL-R cells treated with 10 nM ponatinib or 0.1% DMSO for 1 hour. Label-free quantification of mass spectral data was done using MaxQuant and normalized to MYL. (C and D) Short-term ponatinib treatment suppressed Bcr-Abl and Lyn signaling in MYL-R cells. Total BIRC6 and Mcl-1 proteins were not affected. Immunoblot analyses of the same lysates were performed to validate changes in Bcr-Abl and Lyn observed from the MIB/MS data. (E and F) BIRC6 mRNA and protein were elevated in MYL-R cells compared to MYL and K562 cells. QRT-PCR and immunoblot analyses were performed as described in Materials and Methods on parental MYL, MYL-R, and K562 CML cell lines to examine BIRC6 expression. * Represents $p < 0.05$. Data are representative of three independent experiments.
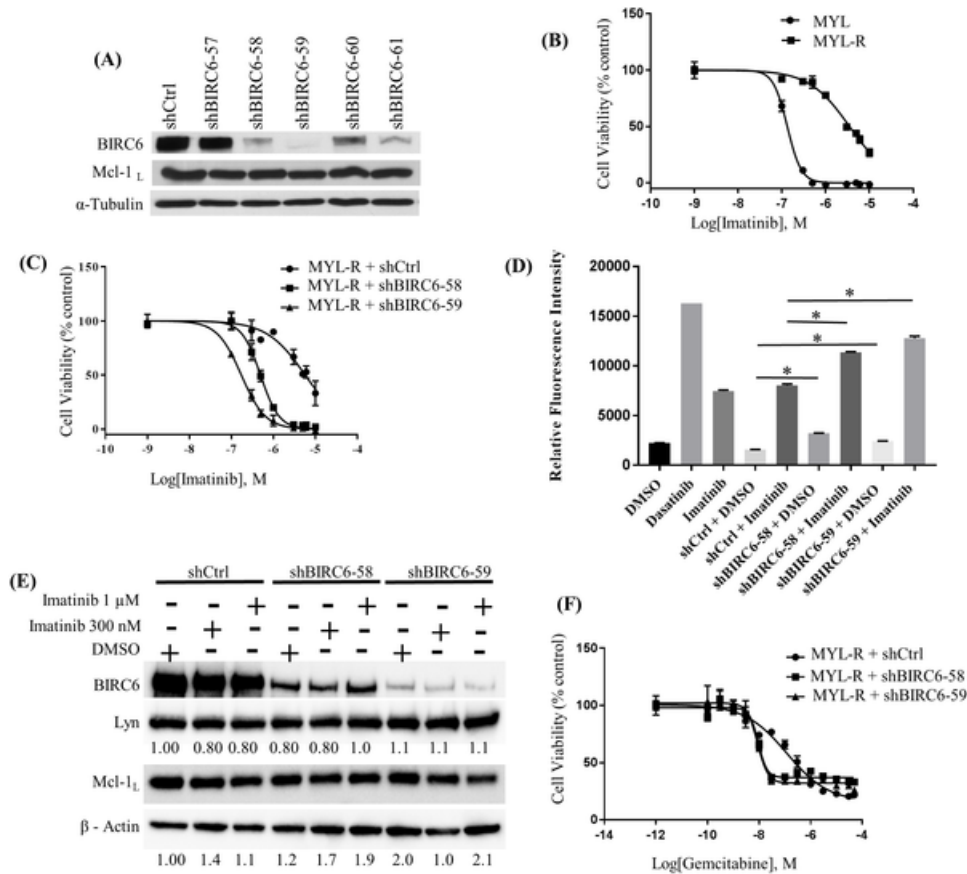
Figure 2.3. BIRC6 mediates drug resistance in MYL-R cells independently of Mcl-1.

(A) Anti-BIRC6 shRNAs were used to knock down BIRC6 in MYL-R cells. Immunoblot analyses showed that shBIRC6-58, -59, and -61 yielded efficient knockdown without affecting Mcl-1. (B) MYL-R cells were resistant to imatinib (IC50 ~3.0 μM) as compared to MYL cells (IC50 ~0.2 μM), and (C) BIRC6 knockdown sensitized MYL-R cells to imatinib (IC50 ~0.2 μM). MYL, MYL-R, and BIRC6 knockdown MYL-R cells were cultured in triplicate in 96-well plates with increasing concentrations of imatinib for 72 hours, and cell viability was assessed by MTS assay. (D) Treatment of BIRC6 knockdown MYL-R cells with imatinib showed elevation in caspase-3/7 activity. BIRC6 knockdown MYL-R cells were treated with 1 μM imatinib for 24 hours. Parental MYL-R cells were treated with DMSO or 1 nM dasatinib or 1 μM imatinib. Caspase-3/7 activity was measured using a fluorogenic substrate as described in Materials and Methods. (E) BIRC6 knockdown or imatinib treatment in MYL-R cells did not affect total Lyn or total Mcl-1 protein levels. BIRC6 knockdown MYL-R cells were treated with DMSO or 300nM or 1 μM imatinib (IM) for 24 hours, and immunoblot analyses used to measure total Lyn and total Mcl-1 proteins. (F) Knockdown of BIRC6 in MYL-R cells increased sensitivity to gemcitabine. BIRC6 knockdown MYL-R cells were cultured as described in (C) with increasing concentrations of gemcitabine for 72 hours and cell viability determined by MTS assay. The data presented in this figure are representative of at least three independent experiments, and * represents $p < 0.05$.

51
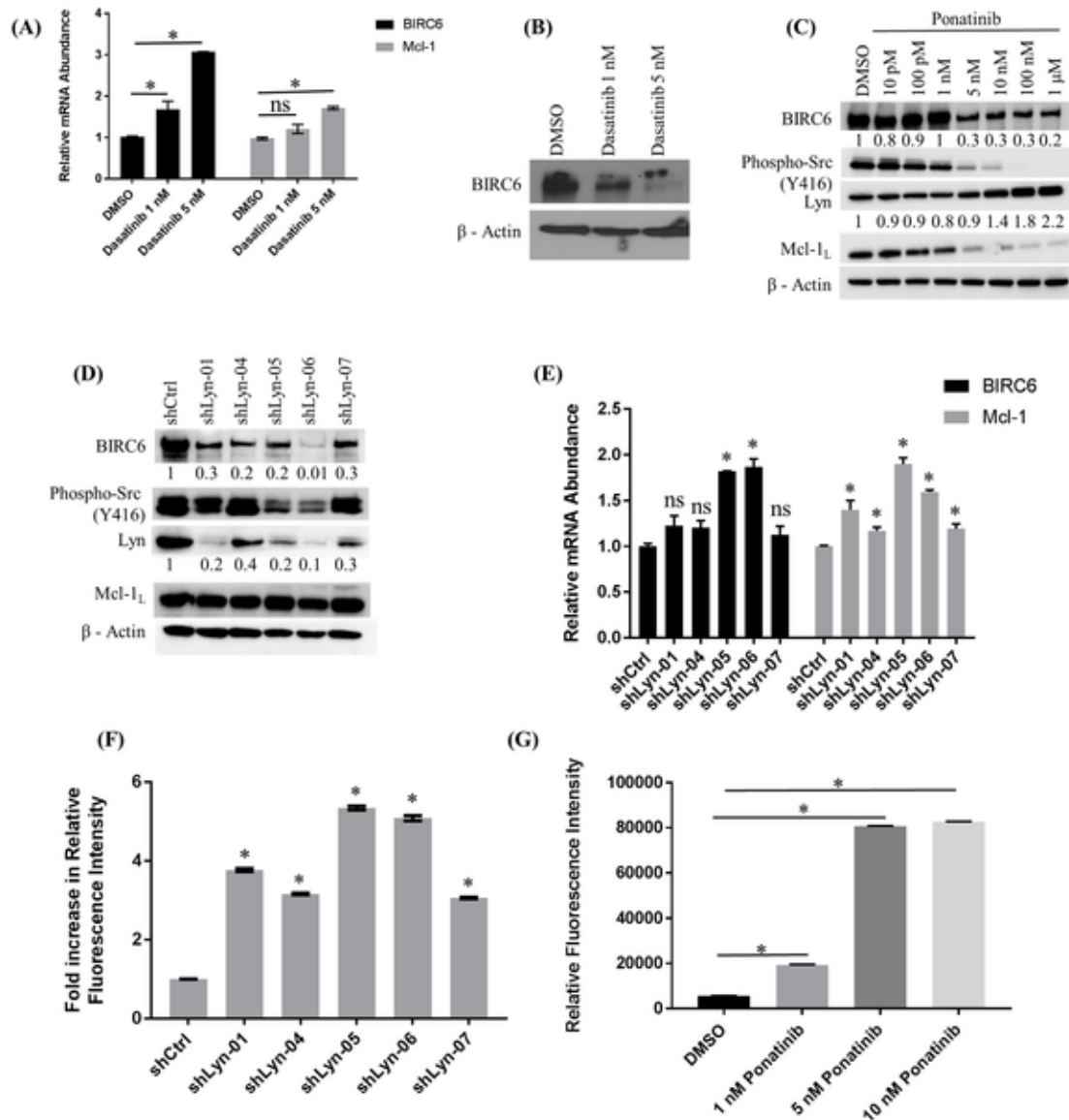
Figure 2.4. Lyn kinase regulates BIRC6 expression.

(A) Treatment of MYL-R cells with dasatinib significantly increased BIRC6 and Mcl-1 mRNA levels as determined by QRT-PCR. MYL-R cells were treated with dasatanib (1 nM or 5 nM, 24 hours) and BIRC6 and Mcl-1 mRNA levels measured by QRT-PCR. (B) Immunoblotting of lysates from the same cells showed that dasatinib treatment reduced BIRC6 protein in MYL-R cells in a dose-dependent manner. (C) Ponatinib treatment of MYL-R cells recapitulated BIRC6 protein reduction observed with dasatinib. MYL-R cells were treated for 24 hours with increasing concentrations of ponatinib and immunoblot analyses used to measure BIRC6, Mcl-1, Lyn, and phospho-Src family (Y416) protein levels. Whereas BIRC6, phospho-Src family (Y416), and Mcl-1 were reduced in a dose-dependent manner, total Lyn was increased. (D) Whereas shRNA knockdown of Lyn in MYL-R cells substantially reduced BIRC6 protein, but not Mcl-1, (E) both BIRC6 and Mcl-1 mRNA levels were significantly increased by the more

52

efficient Lyn knockdown shRNA constructs (shLyn-05 and -06). MYL-R cells were infected with lentiviral particles containing shRNA directed against Lyn. Upon selection of stably transduced cells, BIRC6 and Mcl-1 protein and mRNA levels were measured by immunoblotting and QRT-PCR. (F) Lyn knockdown in MYL-R cells was sufficient to increase caspase-3/7 activity. Data was normalized to shCtrl. (G) Ponatinib treatment of MYL-R cells significantly increased caspase-3/7 activity. MYL-R cells were treated with 1 nM, 5 nM, or 10 nM ponatinib or 0.1% DMSO for 24 hours and caspase-3/7 activity measured. The data are representative of three independent experiments, and * represents *p < 0.05*.
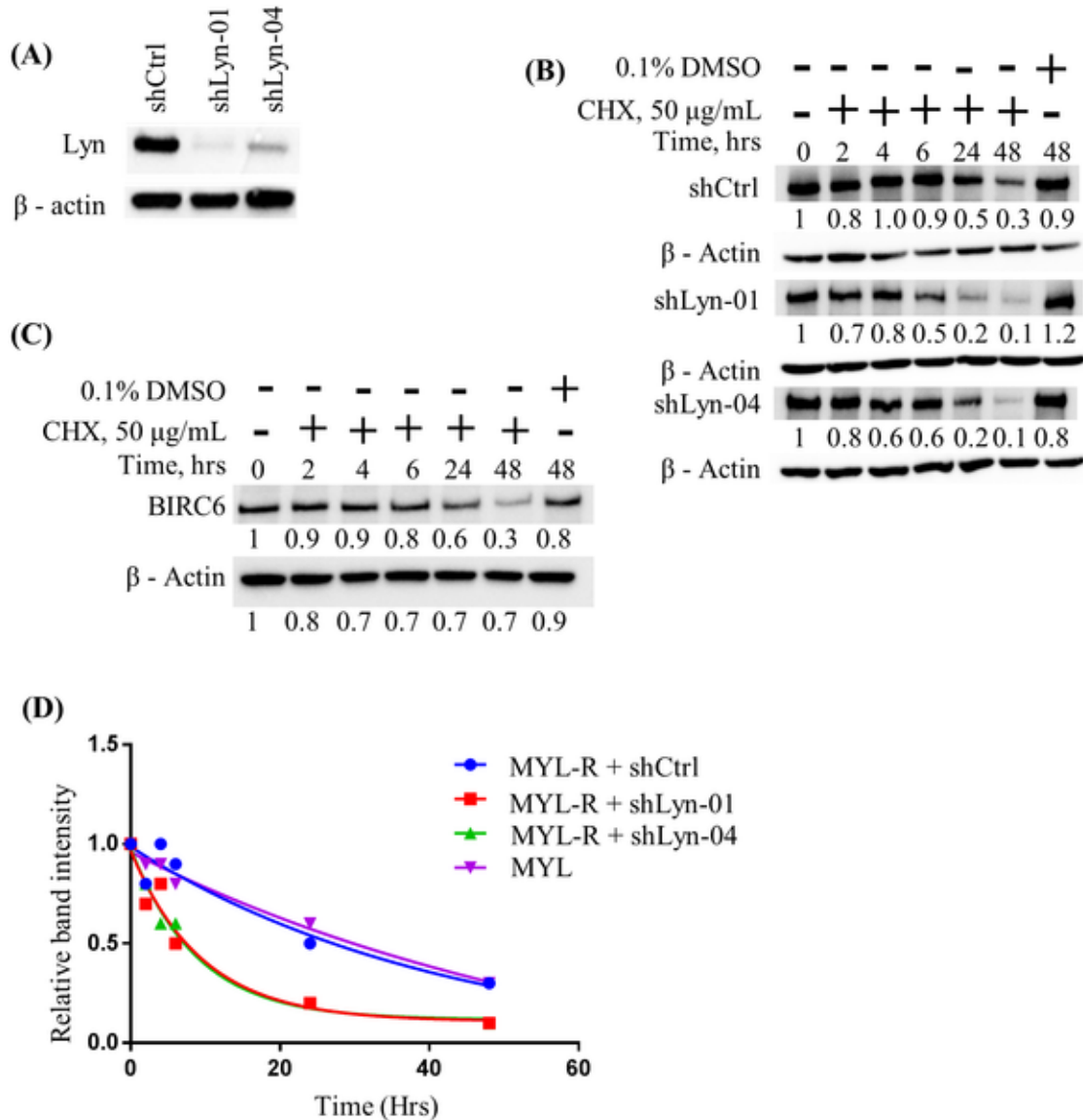
Figure 2.5. Lyn knockdown reduced the half-life of BIRC6 protein in MYL-R cells.

(A) MYL-R cells were infected with lentiviral particles containing anti-Lyn shRNA constructs (shLyn-01 and -04), and Lyn knockdown confirmed by immunoblot analysis. (B) Lyn knockdown in MYL-R cells reduced the half-life of BIRC6 4-fold (~24 hrs in shCtrl cells to ~ 6 hrs in Lyn knockdown cells). Lyn knockdown MYL-R cells were incubated with 50 μg/mL cycloheximide (CHX) in a time-course manner and BIRC6 protein determined by immunoblotting. (C) BIRC6 half-life in MYL cells was ~24 hours. MYL cells were treated with CHX as in (B) and BIRC6 protein determined by immunoblotting. (D) GraphPad[TM] Prism was used to plot change in BIRC6 stability over time upon Lyn-knockdown in MYL-R cells as described in (B). The BIRC6 stability data presented here are representative of two independent experiments.
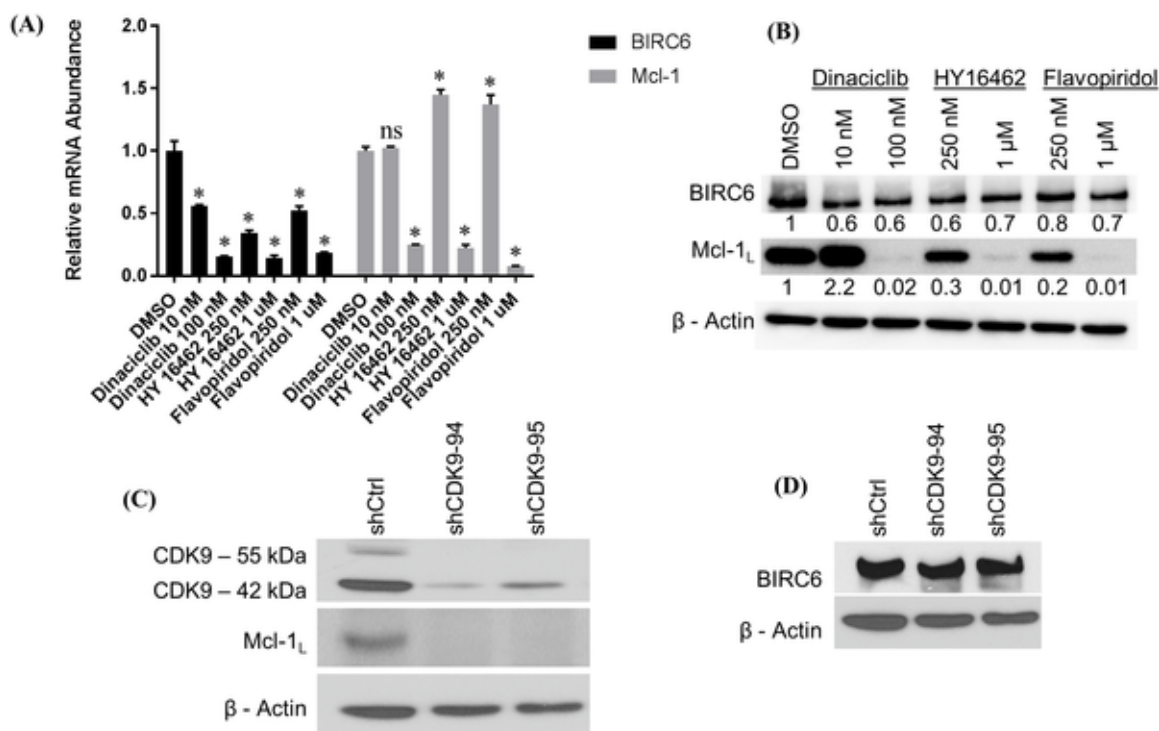
Figure 2.6. CDK9 regulates BIRC6 mRNA levels.

(A) Inhibition of CDK9 with dinaciclib, HY-16462, and flavopiridol significantly reduced BIRC6 and Mcl-1 mRNA levels in a dose-dependent manner. MYL-R cells were treated with dinaciclib (10 or 100 nM), HY-16462 (250 nM or 1 μM), and flavopiridol (250 nM or 1 μM) for 24 hours and BIRC6 and Mcl-1 mRNA measured by QRT-PCR. (B) Immunoblot analyses of lysates from the same conditions in (A) above had no substantial effect on BIRC6 protein. By contrast, Mcl-1 protein levels were reduced in a dose-dependent manner except with 10 nM dinaciclib that showed a substantial increase in Mcl-1 protein. (C and D) shRNA knockdown of CDK9 in MYL-R cells and immunoblot analysis recapitulated the data obtained in (B) above. The data presented here are representative of three independent experiments. * Represents *p* < *0.05*.
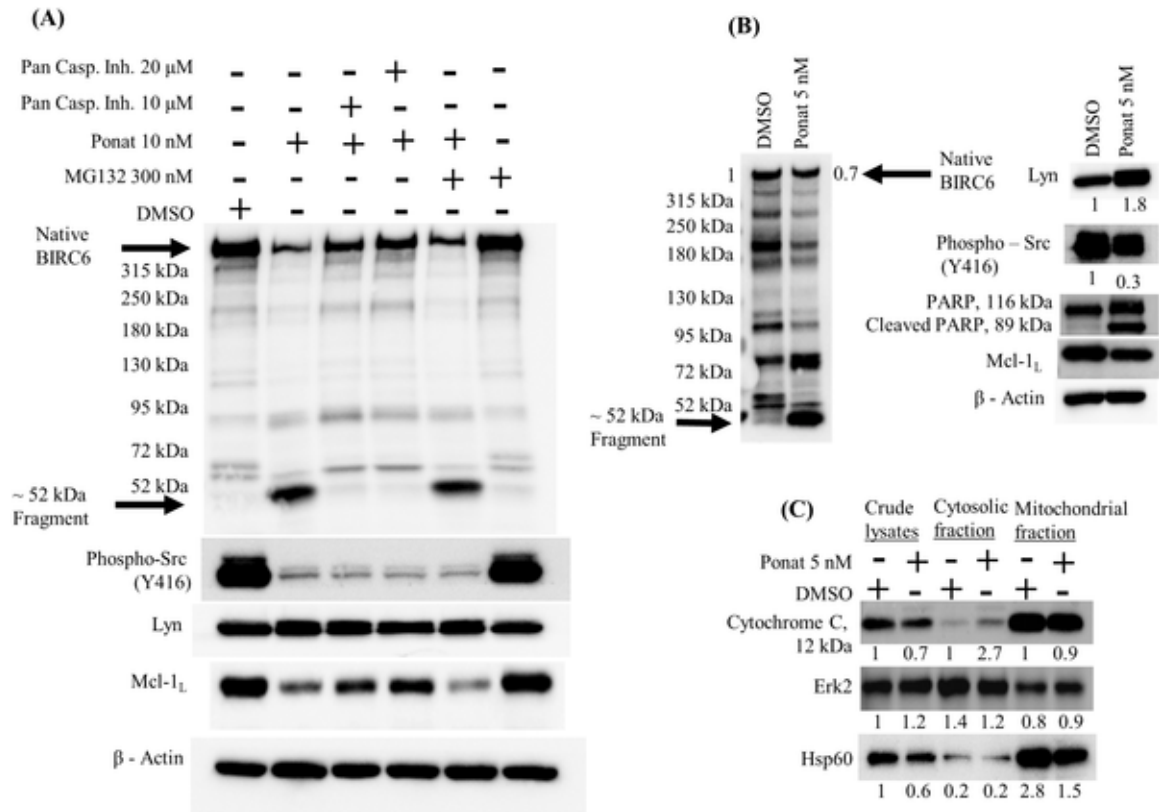
Figure 2.7. Lyn regulates caspase-mediated degradation of BIRC6 in MYL-R cells.

(A) Caspase inhibitors, but not proteasome inhibitors inhibited ponatinib-mediated BIRC6 degradation. MYL-R cells were incubated with 10 nM ponatinib or 0.1% DMSO and/or a pan-caspase inhibitor (Z-VAD-FMK 10 or 20 μM) and/or the proteasome inhibitor MG132 (300 nM) for 24 hours and BIRC6 protein examined by immunoblotting. Inhibition of Lyn (or Src family kinases) was validated by the loss in phospho-Src family (Y416). (B) Inhibition of Lyn in MYL-R cells caused a 30% reduction in BIRC6 protein and induced PARP cleavage as determined by immunoblot analyses. MYL-R cells were incubated with 5 nM ponatinib or 0.1% DMSO for 24 hours and BIRC6 protein measured. Induction of apoptosis was demonstrated by PARP cleavage. (C) Inhibition of Lyn in MYL-R cells caused cytochrome c release from mitochondria. MYL-R cells were treated with 5 nM ponatinib or 0.1% DMSO for 24 hours and mitochondria enriched using the Cytochrome C Releasing Apoptosis Assay Kit. Cytochrome c release was measured by immunoblotting cytosolic and mitochondrial fractions. Erk2 and Hsp60 were used as cytosolic and mitochondrial markers respectively. The data presented here are representative of three independent experiments.

56
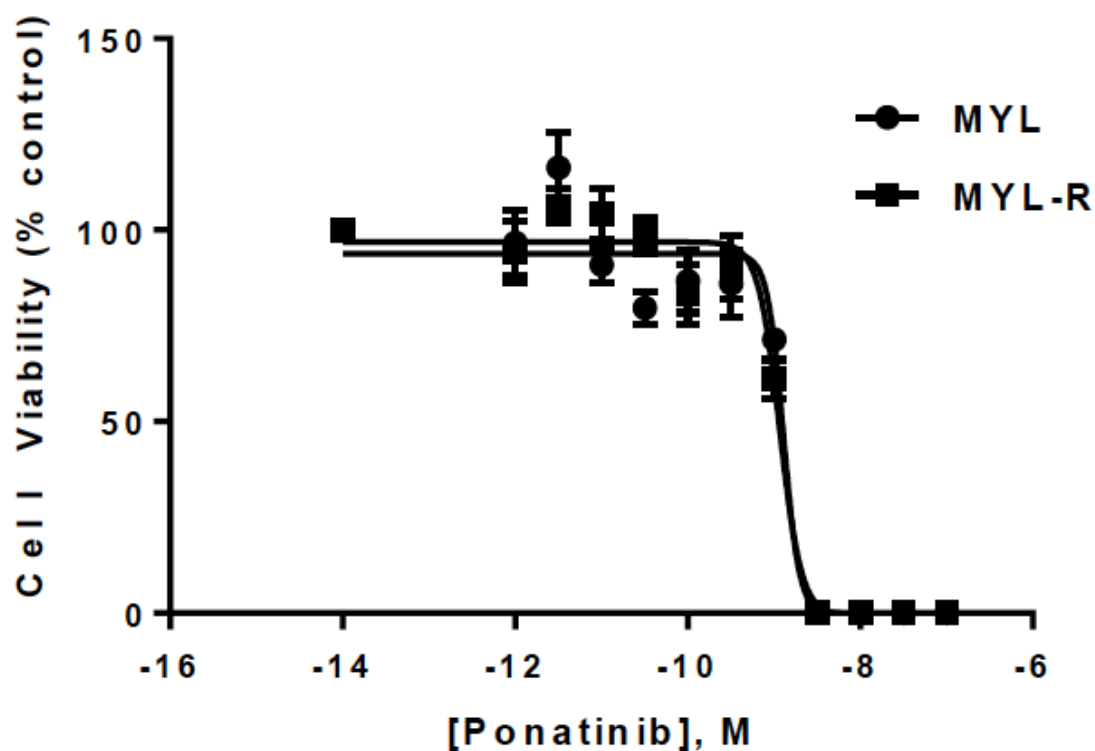
Figure 2.S1. Ponatinib is effective against imatinib-resistant CML cells (MYL-R).

MYL and MYL-R cells were cultured in triplicate in 96-well plates with increasing concentrations of ponatinib for 72 hours, and cell viability was assessed by MTS assay. MYL and MYL-R showed no difference in ponatinib sensitivity with IC50 values of ~1.3 nM and ~1.2 nM respectively.
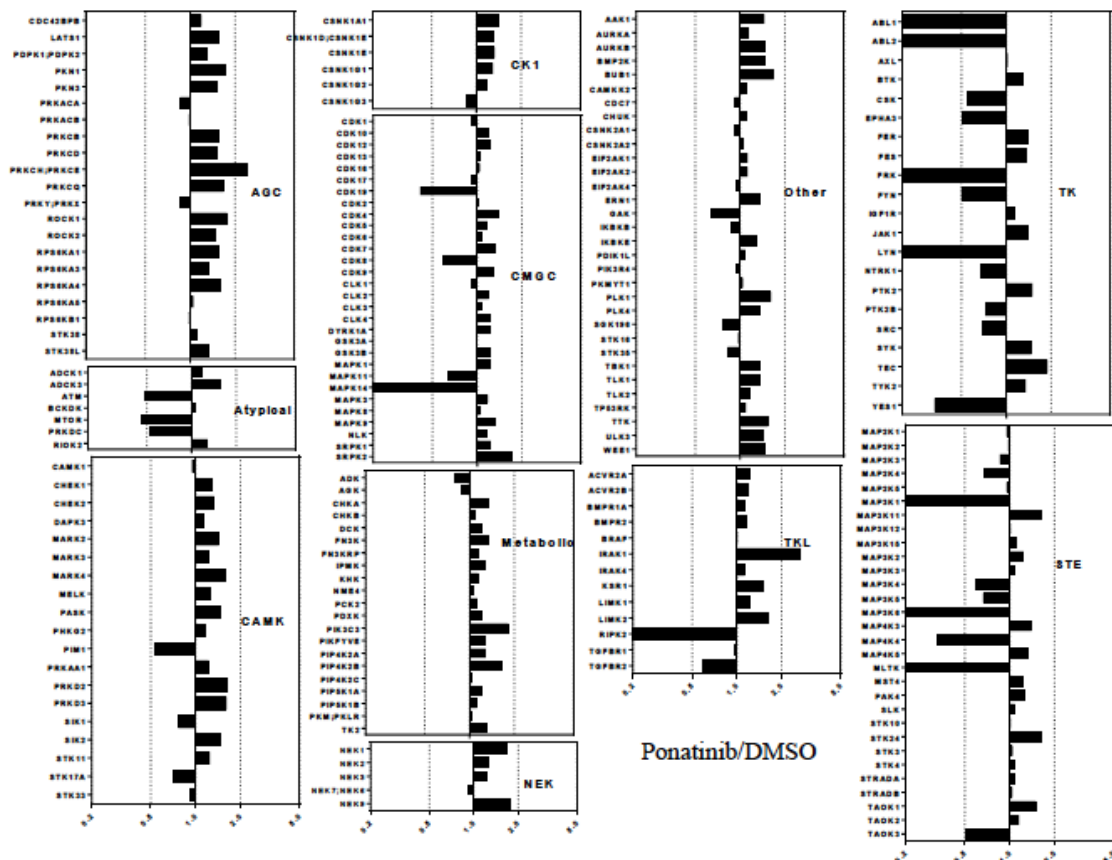
Figure 2.S2. MIB/MS analysis of lysates from MYL-R cells treated with ponatinib revealed select kinase inhibition.

MYL-R cells were treated with 10 nM ponatinib or DMSO for 1 hour and kinome changes analyzed by MIB/MS in two independent experiments. A total of ~ 230 kinases were identified in each of the two experiments. Kinases were quantified by label-free quantification using the MAXQUANT software package with integrated search engine (ANDROMEDA). Data is representative of results from the two experiments, and represent changes in the kinase abundance as determined from ratios of ponatinib/DMSO. Ratios are defined by the dashed lines where <1 and >1 respectively denote decreased and increased MIB binding of kinase in lysates from ponatinib-treated versus DMSO-treated MYL-R cells.
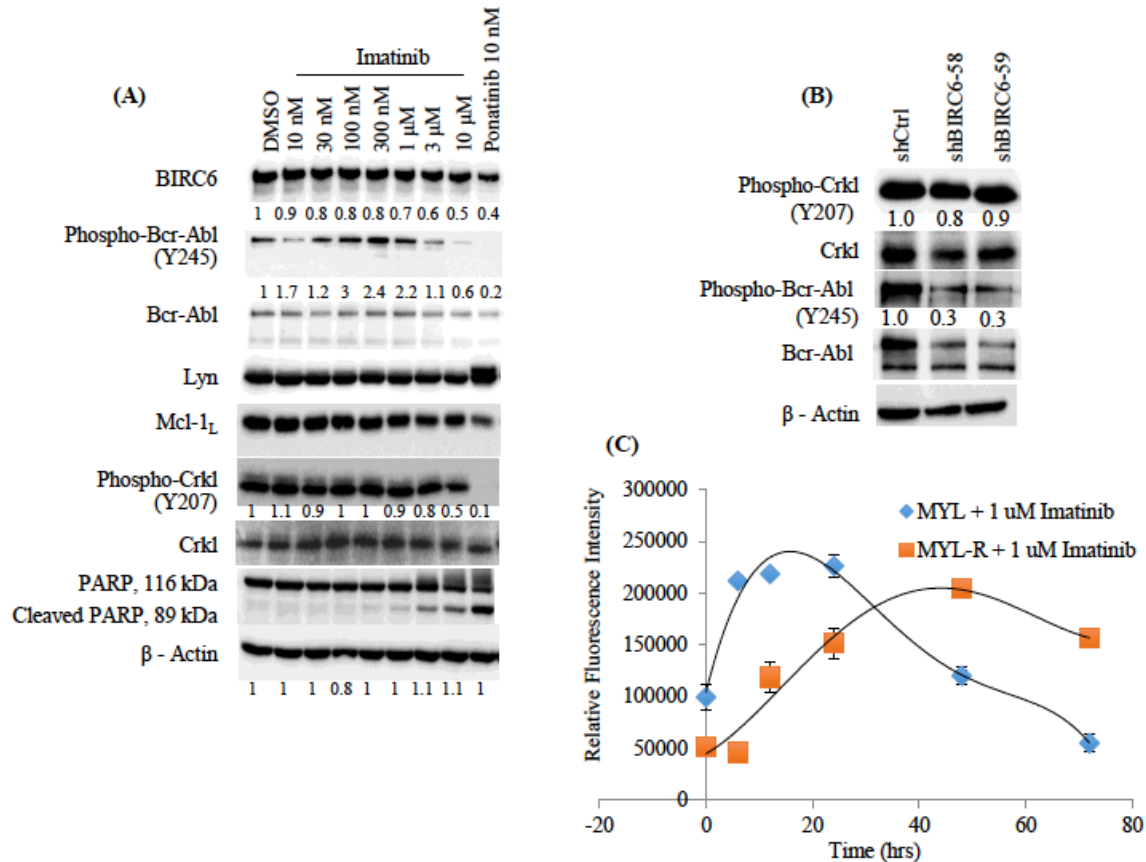
Figure 2.S3. Low doses of imatinib have no effect on BIRC6.

(A) Ponatinib more effectively suppresses Bcr-Abl and Lyn signaling, and BIRC6 protein than imatinib. MYL-R cells were treated with increasing concentrations of imatinib or 10 nM ponatinib or 0.1% DMSO for 24 hours and immunoblot analyses performed to examine the effects on BIRC6, phospho-Bcr-Abl, and Bcr-Abl/Lyn substrate, Crkl. (B) BIRC6 knockdown in MYL-R cells did not affect either phospho-Crkl or total Crkl. By contrast, BIRC6 knockdown caused substantial decrease in both phospho-Bcr-Abl and total Abl. (C) MYL-R cells had delayed activation of caspase-3/7 in response to imatinib treatment relative to MYL cells. MYL and MYL-R cells were treated with 1 μM imatinib in a time-course manner: 0, 6, 12, 24, 48 and 72 hours. Treatment was scheduled so that all cells were harvested at the 72-hr time-point. Caspase-3/7 activity was measured for each condition using a fluorogenic assay. MYL cells showed a two-fold higher basal caspase-3/7 activity relative to MYL-R cells.

59
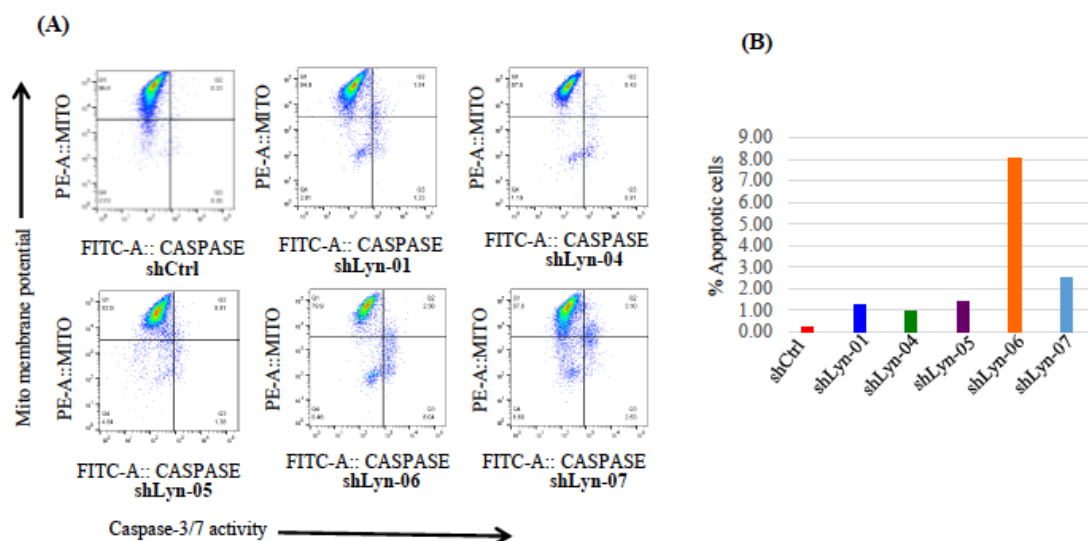
Figure 2.S4. Lyn knockdown in MYL-R cells lowered mitochondrial membrane potential and increased caspase-3/7 activity.

(A) Lyn knockdown resulted in lower membrane potential and increased caspase-3/7 activity in MYL-R cells as determined by flow cytometry. Knockdown of Lyn was achieved by infecting MYL-R cells with lentiviral particles containing shRNA directed against Lyn. Fluorescence intensities for mitochondrial membrane potential and caspase-3/7 activity for Lyn knockdown MYL-R cells (shCtrl, shLyn-01, shLyn-04, shLyn-05, shLyn-06, and shLyn-07) were measured using the MitoCasp^{TM} dual sensor. (B) The most efficient anti-Lyn shRNA construct (shLyn-06) yielded the highest percent of apoptotic cells as determined by the fraction of cells in quadrant 3 (Q3).
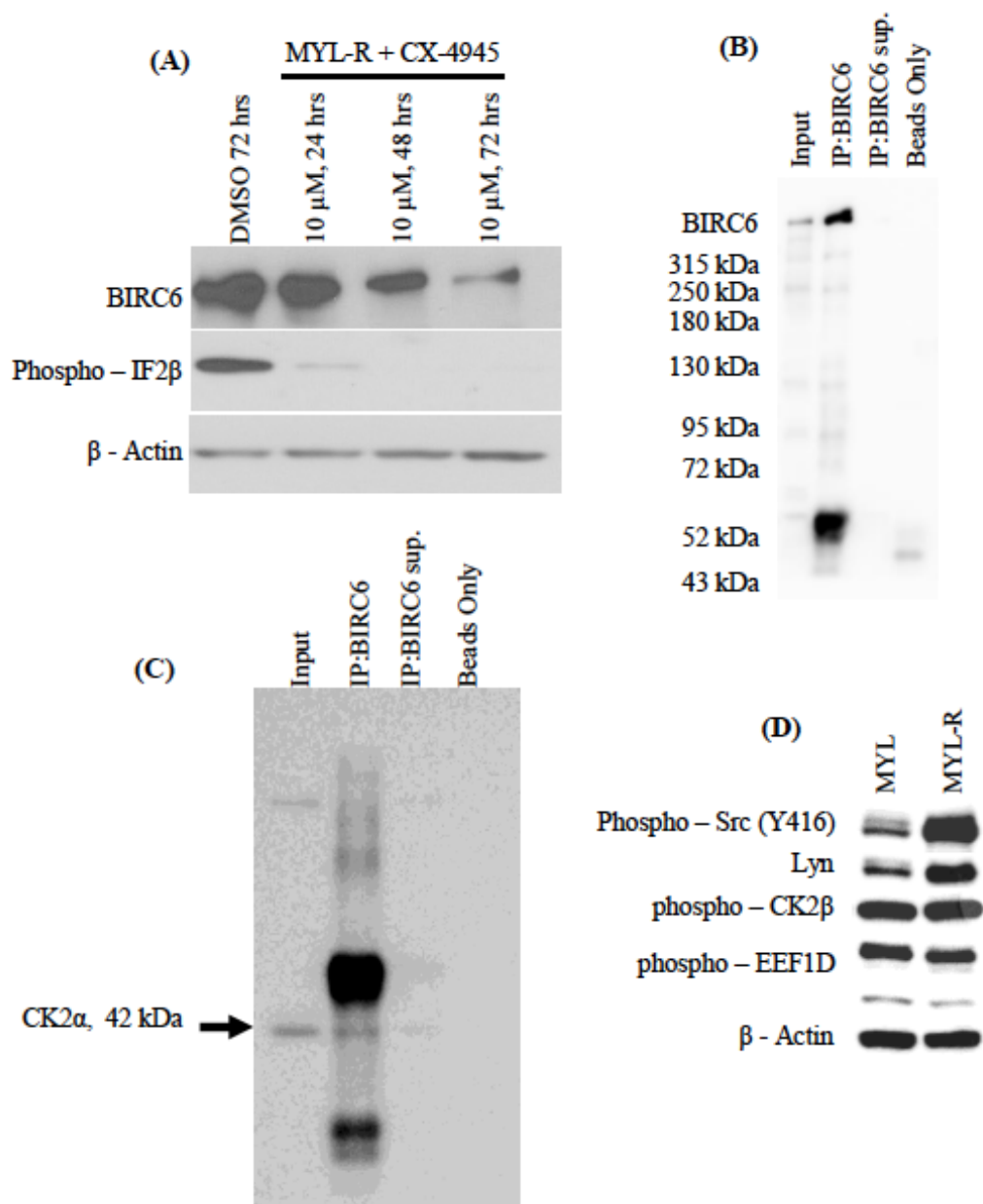
Figure 2.S5. CK2 regulates BIRC6 protein.

(A) CK2 inhibition substantially reduced BIRC6 protein. MYL-R cells were treated with CX-4945, a small molecule inhibitor of CK2, in a time-course manner and cells harvested after 24, 48, and 72 hours. Immunoblot analyses were performed to examine BIRC6 protein and activation level of a validated CK2 substrate (phospho-IF2β). (B) BIRC6 was immunoprecipitated from lysates of MYL-R cells. The supernatant and beads-only lanes showed no BIRC6 protein as determined by immunoblot analysis, and (C) CK2 co-immunoprecipitated with BIRC6. CK2α was present in the BIRC6 IP but not in the beads-only control. (D) Baseline CK2 activity is the same in both MYL and MYL-R

cells. MYL and MYL-R cells were lysed and immunoblot analyses performed to determine the activity level of CK2 (phospho-CK2β) and the level of active CK2 substrate (phospho-EEF1D). The data showed that CK2 activity was the same in MYL and MYL-R cells.

Target	shRNA sequence, 5'-3'
Non-targeting vector	None
Lyn_1	TTCATGAGGTTGGCTTCTTCC
Lyn_4	TTCCCATAGGTGACAATTTCG
Lyn_5	AAACGTTGGTCTCTCTTCTGC
Lyn_6	TTCTAAGGTGTTGAGTTTGGC
Lyn_7	TTCGTGGAGAGATGTAATAGC
CDK9_94	TTCTAACGGACCAAACTGTGC
CDK9_95	ATTAGCAGCCTTCATGTCCCT
BIRC6_58	AATGCACTGTAGAAAGAACGC
BIRC6_59	ATTTGCACCATTCACTACAGC

Table 2.1. shRNA oligonucleotides used in Chapter 2.

CHAPTER 3. LYN REGULATES CREATINE UPTAKE IN AN IMATINIB-RESISTANT CML CELL LINE

3.1   Introduction

The defining characteristic of Philadelphia chromosome-positive chronic myelogenous leukemia (Ph+ CML) is the presence of the Bcr-Abl fusion protein resulting from the reciprocal translocation of chromosomes 9 and 22 (143,144). Bcr-Abl protein possesses constitutive kinase activity and is the principal cause of CML development and progression (145,146). A major advance in CML cancer therapy was the approval of imatinib mesylate (Gleevec, Novartis), a 2-phenylaminopyrimidine compound that selectively inhibits the enzymatic activity of the Bcr-Abl protein (147,148). While imatinib has been extremely successful in the treatment and management of CML, the development of acquired imatinib-resistance in patients remains a clinical problem (149).

Multiple Bcr-Abl-dependent mechanisms contribute to imatinib resistance including increased transcript and protein expression levels, gene amplification, extra chromosomal aberrations, and specific point mutations ("gate-keeper") that sterically inhibit imatinib binding to the inactive configuration of Bcr-Abl (52,150-155). In addition to alterations in molecular signaling events, Bcr-Abl is linked to cellular metabolic alterations that underlie enhanced cell proliferation and viability (156). Hematopoietic cells transfected with Bcr-Abl show increased GLUT1 transporter expression and glucose uptake (157). Metabolomics studies demonstrated that imatinib treatment alters glucose carbon flux

63

involved in the *de novo* synthesis of nucleic and fatty acids thereby limiting Bcr-Abl transformed cells of important macromolecule substrates essential for proliferation (158). In addition, imatinib treatment also results in increased mitochondrial activity, reduced glycolytic activity, and internalization of the GLUT1 transporter in Bcr-Abl-positive CML cells that consequently leads to reduced glucose uptake (159-161). In fact, an important hallmark of imatinib-resistance in CML cell lines is up-regulated glucose uptake mediated by increased glycolytic activity and retention of GLUT1 transporters in the cell membrane. The increased glucose metabolism phenotype in these cell lines is further evidenced by high lactate synthesis and elevations in phosphocholine, which are believed to support enhanced cell proliferation (162).

Bcr-Abl-independent mechanisms such as the overexpression of the Src-family kinase Lyn or Hck also contribute to imatinib resistance in CML (52-54,145,146,163). Our lab previously showed that increased Lyn activity in imatinib-resistant CML cells (MYL-R) leads to upregulation of anti-apoptotic proteins such as Mcl-1 and BIRC6 resulting in increased imatinib resistance (11,56,147,148). Furthermore, using high-resolution NMR spectrometry to analyze water-soluble metabolites revealed that in addition to the commonly observed alterations in glucose metabolism, there was a significant elevation of intracellular creatine in the imatinib-resistant MYL-R cells (68,149). Over 50% of the creatine was in the form of phosphocreatine under these conditions, and considering its role as a high-energy phosphate donor, it was speculated that elevated phosphocreatine might confer a survival advantage on MYL-R cells. In the present study, I investigated the molecular mechanisms involved in the accumulation of creatine in MYL-R cells. The results of these studies demonstrate that MYL-R creatine

levels were dependent both on creatine uptake from the media and the Na^+/K^+-ATPase activity. Moreover, I now provide evidence for the direct involvement of Lyn in creatine uptake through phosphorylation and regulation of the Na^+/K^+-ATPase pump. Thus, these studies demonstrate a pivotal role for the Na^+/K^+ ATPase pump in regulating creatine uptake and suggest that increased creatine uptake and metabolism may be an important cellular adaptation mechanism utilized by the imatinib-resistant CML sub-line (MYL-R cells).

3.2   Materials and Methods

3.2.1   Cells, Cell Culture and Reagents

The human chronic myelogenous leukemia cell line, MYL, and its imatinib-resistant sub-line, MYL-R, were generous gifts from Dr. Hideo Tanaka (Department of Haematology and Oncology, Hiroshima University, Hiroshima, Japan) (52,150-155). Cells were cultured in culture flasks suspended in RPMI 1640 medium (Gibco® by Life Technologies™, U.S.A.) supplemented with 10% fetal bovine serum (Atlanta Biologicals; Norcross, GA), and 1% antibiotic/antimycotic (Invitrogen; Carlsbad, Ca) as previously described (68,156). Cells were maintained at 37 °C in a humidified 5% CO_2 atmosphere in concentrations of approximately $0.6x10^6$ cells mL^{-1}. Culture medium was replaced every 2 to 4 days. Similar to what was originally reported, MYL-R cells can be maintained in imatnib-free culture medium for up to ~6 months without a change in their sensitivity to imatinib treatment (52,157). For most experiments described here, cells were harvested by low-speed centrifugation and washed with cold 1X PBS prior to lysis.

For the labeled glycine experiments, an additional 10 mg/L 2-^{13}C-glycine (Cambridge Isotope Laboratory, Tewksbury, MA) was added to the growth medium that already

contained 10 mg/L unlabeled glycine, thereby resulting in a 50% labeled glycine pool. As a control, more unlabeled glycine was added, resulting in a final concentration of 20 mg/L. MYL and MYL-R cells were maintained under these culture conditions for 5 days prior to extraction.

Reagents were obtained from the following sources: ponatinib and dasatinib were from LC Laboratories (Woburn, MA); imatinib was from Selleckchem (Houston, TX). Ouabain, DMSO, and 3-Guanidinopropionic acid were from Sigma-Aldrich (St. Louis, MO). Polyethylenimine (P.E.I.) was from Polysciences Inc. (Warrington, PA). The primary human antibodies used include: SLC6A8 and creatine kinase B (Abcam, Cambridge, MA), Phospho-Na$^+$/K$^+$-ATPase α1 (Tyr10), Na$^+$/K$^+$-ATPase, phospho-Src (Y416), PTMScan® Phospho-Tyrosine (Cell Signaling Technology, CST, Danvers, MA).), Lyn and β-actin (Santa Cruz Biotechnology, SCBT, Dallas, TX); with secondary antibodies, anti-mouse and anti-rabbit IgG-HRP conjugated (Promega {Madison, WI}). The primary antibodies were diluted following supplier recommendations: 1:200 to 1:1000 in 5% BSA in TBS-T. Secondary antibodies were diluted at 1:10,000 in 5% dry, non-fat milk in TBS-T.

The Lyn overexpression plasmids {pEGFP-Lyn wild type and -Lyn mutant (Y508F)} were kind gifts from Dr. Klaus Hahn's Lab (Department of Pharmacology, UNC-Chapel Hill School of Medicine, Chapel Hill, NC, U.S.A.). pEGFP-Lyn kinase dead (K275R) was made from p-EGFP-Lyn-wild type using site-directed mutagenesis.

For experiments examining creatine depletion, cells were grown in RPMI medium containing 10% heat-inactivated dialyzed FBS (Sigma-Aldrich Company, St. Louis, MO) in place of normal FBS for 5 days prior to extraction.

3.2.2 Cell Treatments

Approximately 15 x 10^6 cells were grown and exposed to different drugs to examine the regulation of creatine uptake. Fewer cells, approximately 2 X 10^6, were used in experiments for immunoblot analyses. Drug dose-response experiments were initially performed with different compounds to determine the effective concentrations. For ouabain, cells were incubated in increasing concentrations, starting at 1.0 nM and increased by order of 10 until the concentration of 10 mM was achieved. Separate populations of the cells were also treated with dasatinib or ponatinib (Selleckchem), dual Bcr-Abl and Src family tyrosine kinase inhibitors. The creatine competitive inhibitor, 3-Guanidinopropionic Acid (Sigma-Aldrich, St. Louis, MO), was reconstituted in media (above) and a 30-mM concentration used to treat MYL-R cells. Cells were treated for 24 h before metabolite extraction. The drugs/compounds were reconstituted in regular media (3-Guanidinopropionic acid), hot, autoclaved water (ouabain), and DMSO (imatinib, ponatinib, dasatinib); likewise regular media, diH$_2$O, and DMSO were also used as the vehicle controls.

3.2.3 Cell Extraction and NMR Sample Preparation

Following cell treatments or incubations, cells were harvested by low-speed centrifugation and the metabolites were extracted using a cold methanol extraction method, as previously described (68,158). Briefly, the cells were collected by centrifugation and washed three times with cold PBS. Following removal of the last wash, 500 mL of ice-cold 50% methanol was added to the cell pellet and vortexed. The cell extracts were then incubated for 30 minutes on dry ice and then allowed to thaw for 10 minutes on ice. The extracts were clarified by centrifugation at 16,000g for 10

minutes at 4° C. The methanol extract (supernatant) was collected and transferred to a

new microcentrifuge tube, while an additional 500 mL of 50% methanol was added to the

pellet for a second extraction. The second 50% methanol extract was collected and

combined with the previous (first) extract. The total cell extract was evaporated to

dryness using a SpeedVac lyophilizer.

Prior to NMR spectroscopy, the evaporated cell extract pellet was dissolved in 600

µL of D_2O containing 0.5 mM (final concentration) trimethylsilyl-2,2,3,3-

tetradeuteropropionic acid (TSP) and transferred to a 5 mm NMR tube for high resolution

NMR analysis. For the MYL-R NMR studies on the regulation of creatine uptake, the

pellet was suspended in 70 µL of D_2O containing 0.1 mM TSP.

3.2.4   1D ^{1}H and 2D ^{1}H-$\{^{13}C\}$ HSQC NMR Spectroscopy

1D ^{1}H NMR spectra characterizing the metabolic differences between MYL and

MYL-R were acquired at 16.4T using a Varian INOVA NMR spectrometer (700 MHz

^{1}H, Varian Instruments) equipped with a 5 mm indirect cold probe. The FIDs were

acquired using a one-pulse sequence with a total repetition time (TR) of 12.65s, number

of transients (nt) of 64 and 1024, and a 90° flip angle. 2D ^{1}H-$\{^{13}C\}$ heteronuclear single

quantum coherence (HSQC) NMR spectra were acquired at 14.1 T NMR spectrometer

equipped with 5 mm indirect HCN probe using 256 increments and zero filled in f1 and

f2 to 4.096 points and with a shifted sine bell apodization.

For the MYL-R creatine regulation analysis, 1D ^{1}H NMR spectra were acquired at

14.1T using a Varian INOVA NMR spectrometer (599.64 MHz ^{1}H, Agilent) equipped

with a 5 mm indirect cold probe. The 5 mm probe is a Varian pulsed field gradient,

inverse detection probe. The micro-coil probe is a Protasis/MRM 10 ll capillary NMR

probe (Magnetic Resonance Micro- sensors, Savoy, IN). Samples were introduced into the micro-coil using a Protasis High-throughput Sample Automation System (Protasis, Marlboro, MA). A simple presaturation pulse sequence was used which included a 1 s solvent presaturation, followed by an Ernst angle optimized read pulse and a 2.3 s acquisition delay. The Ernst angle was based upon an assumed average metabolite T1 of three seconds. A sweep width of 7,195.5 Hz was digitized with 16,384 complex points. A total of 256 transients were collected requiring a total of approximately 20 min.

3.2.5   Spectral Processing, Pattern Recognition and Metabolite determination

All NMR spectra were processed using ACD/1D NMR Manager, version 12.0 (Advanced Chemistry Development, Inc., Toronto, ON, Canada). Imported FIDs were zero filled to at least 32,000 points and an exponential line broadening of 0.1 to 1.0 Hz was applied prior to Fourier transformation. Spectra were phased, baseline corrected, and referenced to the TSP peak at 0.00 ppm. TSP (at 0.75 ppm and upfield), residual methanol, water, and formate were excluded from binning process. Metabolite identification and quantification were performed using Chenomx software (version 6.1; Chenomx Inc., Edmonton, Canada), as previously described (Dewar et al., 2010).

3.2.6   shRNA Knockdown of Lyn

pLKO.1 lentiviral vectors containing shRNA directed against Lyn (TRCN0000010101, 04, 05, 06, and and 07) or a non-targeting shRNA (shCtrl) were purchased from the UNC Lenti-shRNA Core Facility. Lentivirus transduction of MYL-R cells with shRNA was done per the protocol supplied by the RNAi Consortium (http://www.broadinstitute.org/rnai/public/resources/protocols), and as previously described (11,159-161). Briefly, MYL-R cells were seeded at $5x10^5$ cells/mL in 5 mL

growth media containing 8 μg/mL polybrene, and incubated overnight with 1 mL of anti-

Lyn viral shRNA (shLyn-01, -05, and -06) known to efficiently knock down Lyn. Non-

targeting viral shRNA (shCtrl) was used as control. Stably transduced cells were selected

for by exposure to 2 μg/mL puromycin in cell culture (57,162). Aliquots of the cells

were harvested one week after selection and immunoblot analyses performed to confirm

Lyn knockdown. The rest of the cells were expanded in puromycin for another one week

to obtain enough cells (~20M) per condition for NMR analyses of total creatine pool.

3.2.7   Western Blotting Conditions

Cells were harvested by centrifugation, washed once in cold 1X PBS, and lysed in a

modified RIPA (RIPA, no SDS) buffer (150 mM NaCl, 9.1 mM Na_2HPO_4, 1.7 mM

NaH_2PO_4, 1% NP-40, and 0.5% deoxycholic acid; adjusted to pH 7.4) and supplemented

with 2 mM sodium orthovanadate, 10 mM NaF, 0.0125 μM calyculin A, and cOmplete

Protease Inhibitor Cocktail (Roche Diagnostics, U.S.A.). The lysates were clarified by

centrifugation and the protein concentrations were normalized using a Bradford assay

(BIO-RAD). Samples for gel electrophoresis were prepared by adding protein lysates to

Laemmli sample buffer (final concentration: 0.25 M Tris pH 6.8, 10% glycerol, 5% β-

mercaptoethanol, 0.001 μg/mL Bromophenol blue) and 30 μg of protein were loaded into

each well of an SDS-polyacrylamide gel for protein separations. Proteins were

transferred to polyvinylidene difluoride (PVDF) membranes (BIO-RAD) which were

then blocked for 1 hr with 5% non-fat dry milk or 5 % BSA dissolved in Tris-buffered

saline supplemented with Tween-20 (TBS-T). The membranes were then incubated in

primary antibodies at 4° C overnight, washed 3 times with TBST, then incubated with

anti-mouse / anti-rabbit IgG-HRP conjugated secondary antibodies for 1 hr at room

temperature. The membranes were rinsed 3 times with TBS-T then developed using Clarity ™ ECL Western Substrate (BIO-RAD), and imaged using a ChemiDoc ™ Touch Imaging System (BIO-RAD).

3.2.8 Cell Transfection

HEK293 cells were passaged and split into four 60 mm plates a day before transfection. The following day, the cells were transfected with Lyn expression vectors: wild type or mutant (Y508F) or kinase dead (K275R), using polyethylenimine (PEI) transfection reagent (Polysciences Inc., Warrington, PA). A total of 5 μg DNA was used for each transfection. The fourth 60 mm plate was transfected with empty vector (mock). The cells were harvested 24 hours after transfection, washed in cold 1X PBS, and lysed in cold Western blot lysis buffer (above). Western blot analysis was performed as described above to examine the effect of Lyn overexpression on Na^+/K^+-ATPase (Tyr10) phosphorylation.

3.2.9 Cell Viability (MTS Assay)

MYL and MYL-R cells were maintained in normal growth medium (10% FBS) or regular media containing various concentrations of cyclocreatine (CCr), a competitive inhibitor of creatine known to have high affinity for the Na^+/creatine symporter(164). Cyclocreatine was dissolved in regular cell growth medium at a stock concentration of 100 mM. In triplicate, CCr was added to $10 \times 10^3/100$ μL MYL or MYL-R cells in increasing concentrations in a 96-well plate. Regular cell culture medium was used as the vehicle control. After 48-hr incubation at 37°C with 5% CO_2, cell viability was determined by MTS assay performed according to the manufacturer's instructions (CellTiter 96® AQueous One Solution Reagent, Promega, Madison, WI). The

absorbance was read at 490 nm using a SpectraMAX plate reader (Molecular Devices, Sunnyvale, CA). Trypan blue exclusion assay was performed using the Trypan blue reagent, and cells were counted using a hemacytometer (Hausser Scientific, Horsham, PA). Triplicate counts were obtained and used to determine cell proliferation. Data was analyzed for significant differences using a paired t-test.

3.2.10 Rubidium Uptake Assay

Rb$^+$ uptake measurements were performed by Dr. Andrew Ghio's lab (EPA, UNC-Chapel Hill). Approximately 15M MYL-R cells were treated for 24 hours with dasatinib (1 nM) or ouabain (100 nM) or DMSO. From every condition, approximately 4M cells were pelleted (enough for 1M cells per time point), resuspended in 4x1.5 mL tubes and washed once with Rb$^+$-free uptake buffer. Then, the cells were resuspended in fresh uptake buffer supplemented with 5 mM RbCl and incubated at room temperature for different time-points: 0, 15, and 30 minutes. The fourth tube had cells resuspended only in Rb$^+$-free uptake buffer, and was incubated for 30 min. O-min time-point cells were pelleted immediately after resuspending the cells in fresh uptake buffer containing 5 mM RbCl. The cells were washed X3 with Rb$^+$-free buffer, and 1 mL metal free HCl added on removal of third wash. Cells from other time-points were similarly processed. The rest of the procedure to determine Rb concentration in each sample tube was done as previously described (165).

3.2.11 Statistical Analyses

Data are reported as the mean $\pm$ standard error of the mean (S.E.M); S.E.M. was performed on all datasets to determine positive and negative error. Two-tailed student t-test was used to make comparisons between groups, and p values below 0.05 at the 95%

confidence level were considered to be statistically significant. Calculations were performed using GraphPad Prism and Microsoft Excel.

3.3 RESULTS

3.3.1 Increased steady state levels of creatine in MYL-R cells detected by ^{1}H NMR

^{1}H NMR spectroscopy was used to examine the metabolic differences between the CML cell line MYL and its imatinib-resistant counterpart, MYL-R (52,68). Consistent with our previous study, the 1D ^{1}H spectra obtained from MYL and MYL-R cell extracts demonstrated increased levels of intracellular creatine in the MYL-R cells as shown in supplementary figure 1B (**Figure 3.S1B**) compared to MYL cells (in **Figure 3.S1A**). We observed the ^{3}H of the creatine methyl group (*) at a chemical shift of 3.023 ppm and the ^{2}H of the methylene group (**) at a chemical shift of 3.92 ppm as shown in supplementary figure 1B (**Figure 3.S1B**). To verify the identity of creatine, 2D ^{1}H-{^{13}C} HSQC NMR was performed on the MYL-R cell extracts and this confirmed the creatine signal by correlating the ^{1}H and ^{13}C resonances (**Figure 3.S1**, inset).

3.3.2 De novo synthesis does not account for elevated creatine levels in MYL-R cells

In order to determine if *de novo* synthesis was contributing to the elevated levels of creatine observed in MYL-R cells, both MYL and MYL-R cells were maintained in total growth medium (RPMI + 10%FBS) with or without the addition of 2-^{13}C-glycine for 5 days. Glycine and arginine are required for the biosynthesis of creatine and therefore, incubation with 2-^{13}C-glycine, results in creatine labeled at the 2-position through this two-part reaction (**Figure 3.1A**) (166). After 5 days, the cells were harvested, metabolites extracted, and ^{1}H NMR spectra of each cell extract were obtained. Following

incubation in medium containing 50% 2-^{13}C-glycine, the percent incorporation of labeled

glycine in the cell extracts was found to be $31.3 \pm 4.1\%$ and $31.0 \pm 2.6\%$ for MYL and

MYL-R cells, respectively. These data indicate that there were no statistically significant

differences in the ability of each cell type to synthesize labeled creatine *de novo*. Shown

in **Figure 3.1B** are the stacked ^{1}H NMR spectra from MYL-R cells incubated with (blue)

or without (black) labeled 2-^{13}C-glycine. The proton peaks representing the unlabeled

(^{12}C) glycine and creatine were observed at 3.56 and 3.93 ppm, respectively. As

expected, satellite peaks from 2-^{13}C-glycine were only observed in MYL-R cells

incubated with labeled glycine (blue line). However, we did not observe any satellite

peaks associated with creatine under these conditions indicating that *de novo* synthesis

does not account for the elevated creatine levels observed in MYL-R cells.

3.3.3 Media creatine is a major source of intracellular creatine in both MYL and MYL-R cells

Since enhanced *de novo* creatine synthesis was not observed in MYL-R cells, I

examined whether uptake from the cell culture medium was a potential source of

creatine. ^{1}H NMR analysis of RPMI and RPMI + 10% FBS media indicated that FBS is a

significant source of creatine at an average concentration of 37.4 ± 3.04 μM (see

Supplemental Data). Dialyzed FBS (dFBS) is depleted of creatine and other small

molecules, including growth factors, cytokines, and metabolites. Incubating MYL and

MYL-R cells in RPMI medium supplemented with 10% dFBS resulted in a significant

decline in creatine in both cell types (**Figure 3.2**). Addition of 100 mM creatine to the

dFBS containing culture medium, restored the total creatine pool (creatine and

phosphocreatine) in the MYL cells to basal levels, whereas the increase in the total

creatine pool was nearly 2-fold greater in MYL-R cells compared to MYL-R cells

incubated in RPMI + 10% FBS (**Figure 3.2**).

3.3.4 Creatine transporter and creatine kinase B protein levels are comparable in MYL and MYL-R cells

Whereas creatine is imported into the cell through SLC6A8 transporter, creatine

kinase, brain-type (CKB) phosphorylates creatine both in the extracellular and

intracellular spaces to generate phosphocreatine, a source of high-energy phosphate used

to generate ATP in low-energy states(167). CKB is expressed mainly in the brain and

distributed to other tissues of the body. Its overexpression in many tumor types has been

linked to adverse prognostic outcomes(168). Hence, I compared the protein levels of

both the creatine transporter (SLC6A8) and creatine kinase B in MYL and MYL-R cells

to determine if these proteins contributed to the increased total creatine pool in MYL-R

cells (**Figure 3.S1B**). Untreated MYL and MYL-R cells were harvested and prepared for

Western blotting as described in Materials and Methods. Western blot analyses showed

that SLC6A8 and creatine kinase B protein levels were comparable in MYL and MYL-R

cells (**Figure 3.3A**), suggesting that the observed increase in total creatine pool was

independent of the expression levels of the two proteins.

3.3.5 Role of the Na^+/K^+-ATPase in regulating creatine uptake in MYL-R cells

Since our data indicated that the total creatine pool in MYL-R cells was dependent on

uptake from the media, I examined possible mechanisms for this regulation.

Extracellular creatine uptake is mediated by a Na^+/creatine symporter, SLC6A8

(166,169-171), and import of creatine is dependent on a gradient which requires both Na^+

and Cl^- ions(172). Since earlier studies showed that creatine uptake was dependent on

the activity of the Na^+-K^+-ATPase pump, I tested the requirement for this protein in

creatine uptake in MYL-R cells (**Figure 3.3B**). MYL-R cells were incubated with increasing concentrations of ouabain, a glycoside that directly binds to and inhibits the Na^+-K^+-ATPase. As expected, oubain significantly *(P<0.05)* depleted the total creatine pool in MYL-R cells at 100 nM or greater concentrations (**Figure 3.3C**). Similar results were obtained with digitoxin, another well-established Na^+-K^+-ATPase inhibitor (data not shown). A rubidium uptake assay further confirmed that these drug treatments directly inhibited Na^+/K^+-ATPase activity (**Figure 3.3D**). Compared to DMSO treatment, 100 nM ouabain substantially lowered Rb uptake in MYL-R cells resuspended in rubidium-free uptake buffer supplemented with 5 mM RbCl. Thus, these studies demonstrate the importance of Na^+/K^+-ATPase activity in affecting creatine levels in MYL-R cells.

3.3.6   Role of Lyn in mediating creatine uptake in MYL-R cells

Studies from our lab and others have demonstrated that Lyn is an important tyrosine kinase for the survival of MYL-R cells (52,57),(11,56). Immunoprecipitation data have shown that Lyn is able to bind in a complex with the Na^+, K^+-ATPase pump resulting in phosphorylation and activation of the pump(173-175). Further studies have revealed that phosphorylation of the α-subunit of Na^+/K^+-ATPase on Tyr10 (pY10) is critical to the enzyme's activity(174,175). To test the potential involvement of Lyn in the regulation of the Na^+/K^+-ATPase, MYL-R cells were incubated with dasatinib, a broad tyrosine kinase inhibitor known to inhibit Lyn, and the intracellular creatine pool measured. Compared to DMSO, dasatinib treatment substantially reduced total intracellular creatine pool in MYL-R cells (**Figure 3.S2A**). Western blot analyses were used to compare both Lyn activation (as measured by pY416) and Na^+/K^+-ATPase α-1 activation (as measured by pY10) in MYL and MYL-R cells. As reported earlier, both total Lyn and phospho-SFK

(P-Y416) were substantially higher in the MYL-R compared to the MYL cells (**Figure 3.4A**). Phospho-Na$^+$/K$^+$-ATPase α-1 (pY10) was also substantially higher in MYL-R compared to MYL cells whereas total Na$^+$/K$^+$-ATPase protein was comparable in the two cell lines (**Figure 3.4A**). Ponatinib, a more selective Bcr-Abl and Lyn inhibitor(11,76), inhibited Lyn activity (pY416) and significantly reduced the amount of creatine in MYL-R cells (**Figure 3.4C & 3.4B**). While phospho-Na$^+$/K$^+$-ATPase α-1 (pY10) was substantially reduced by this treatment, neither the Na$^+$/K$^+$-ATPase nor the SLC6A8 protein was affected (Fig 4C). Finally, incubation of MYL-R cells with dasatinib or ouabain caused ~65% and ~95% inhibition of creatine uptake respectively (**Figure 3.S2B**).

   To further study the role of Lyn in creatine uptake, I developed a lentiviral shRNA system to investigate the effects of Lyn knockdown. While three knockdown constructs (shLyn-01, -05, and -06) were effective as determined by Western blot analyses (**Figure 3.4E**), two constructs (shLyn-01 and shLyn-06) were selected for further studies, and the amount of intracellular creatine measured as described above. As observed with Lyn inhibition (**Figure 3.4B**), Lyn knockdown substantially reduced the amount of intracellular creatine observed in these cells compared to the vector control (**Figure 3.4D**). ShLyn-06, the shRNA construct most effective at reducing Lyn protein, most efficiently reduced intracellular creatine levels (**Figure 3.4D**). These data support the requirement of Lyn for creatine uptake in MYL-R cells.

3.3.7   Reduced Na$^+$/K$^+$-ATPase tyrosine phosphorylation correlates with Lyn inhibition or Lyn knockdown

   Since tyrosine 10 has been identified as a key phosphorylation site involved in regulating the Na$^+$/K$^+$-ATPase pump activity(175,176), I examined the effects of Lyn

knockdown on the phosphorylation of this site using a commercially available antibody (anti-phospho-Na$^+$/K$^+$-ATPase α1 (pY10), Cell Signaling Technology). Lyn knockdown substantially reduced phosphorylation of the Na$^+$/K$^+$-ATPase pump on tyrosine 10 (pY10), consistent with inhibition of pump activity (**Figure 3.4E**). Conversely, overexpression of Lyn in HEK293 cells resulted in substantial increase in phospho-Na$^+$/K$^+$-ATPase α1 (pY10) (**Figure 3.5**). Compared to the empty vector or wild-type Lyn or kinase dead (K275R) Lyn, transfection of constitutively active Lyn (Y508F) into HEK293 cells dramatically increased Na$^+$/K$^+$-ATPase α1 (Tyr10) phosphorylation (**Figure 3.5**). Phospho-STAT5A (pY694), a known readout for Lyn activity, was strongly increased in HEK293 cells expressing constitutively active (Y508F) Lyn. Taken together, these data are consistent with Lyn mediating the phosphorylation and activation of the Na$^+$/K$^+$-ATPase pump.

3.3.8   Inhibitors of creatine uptake reduce cell viability

I next investigated the effect of intracellular creatine depletion on cell viability. MYL and MYL-R cells were treated for 48 hours with increasing concentrations of cyclocreatine (CCr), a competitive inhibitor of creatine with high affinity for the Na$^+$/creatine symporter(164). Cell viability, calculated as a percentage of the cells maintained in regular media only (0 mM CCr), was determined as described in Materials and Methods. Creatine depletion altered the viability of the MYL and MYL-R cells in a dose-dependent manner (**Figure 3.6**). Under normal culture conditions (0 mM CCr), the percent of viable MYL and MYL-R cells were the same after 48 hours of treatment. There was a dose-dependent loss in cell viability over the 48-hr period for both the MYL and MYL-R cells as shown in **Figure 3.6**. The loss in viability was substantially higher

(~80%) for the MYL-R cells compared to the MYL cells (~20%) when treated with 50 mM CCr for 48 hours (**Figure 3.6**). In addition to demonstrating that MYL-R cells have a higher creatine uptake than MYL cells, these studies suggest that creatine may also play a critical role in maintaining cell viability. Similarly, I tested the effect of Beta-Guanidinopropionic Acid or 3-Guanidinopropionic Acid (3-GPA), a creatine analog(177), on creatine uptake by MYL-R cells. Treatment of MYL-R cells with 3-GPA (30 mM, 24 Hr) reduced total intracellular creatine pool ten-fold; comparable to untreated MYL cells (**Figure 3.S3**). MTS assay studies following treatment of MYL-R cells with increasing concentrations of 3-GPA revealed loss in cell viability at ≥30 mM concentrations (data not shown).

3.3.9 Discussion

Similar to that originally reported by Ito *et al*., studies from our lab have shown that increased Lyn activity is one of the major drivers of drug resistance in MYL-R cells(11,52,56). Since our previous study demonstrated a substantial accumulation of creatine (and phosphocreatine) in MYL-R cells compared to MYL cells, the objective of the current study was to investigate the molecular basis for this difference. A second goal was to determine if increased creatine levels was important for MYL-R cell viability. Lastly, I sought to determine if hyperactivation of Lyn in MYL-R cells contributed to the increased accumulation of creatine in these cells. The results of these studies demonstrate three important findings. First, the accumulation of creatine was dependent on uptake from the extracellular media, a rich source of creatine, and not dependent on *de novo* synthesis. Second, our data demonstrate an essential role for the Na^+/K^+-ATPase pump in creatine uptake in MYL-R cells and suggest that Lyn-dependent tyrosine

phosphorylation is required for this effect. Lastly, my results suggest that the increased

accumulation of creatine (and phosphocreatine) may be important for cell viability.

Multiple mechanisms are known to contribute to the development of imatinib-

resistance in CML. While mutations in Bcr-Abl are frequent, additional mechanisms of

resistance are now established, including hyperactivation of Lyn of Hck kinases and

overexpression of anti-apoptotic proteins(11,52-54,56-58,163). The development of

second and third generation inhibitors targeting these kinases, in addition to Bcr-Abl, has

been promising. Despite these clinical advances, the exact mechanisms by which Lyn or

other Src family kinases contribute to acquired drug resistance are poorly understood.

The MYL-R cells are a well characterized model system to investigate the potential

role of Lyn kinase in imatinib resistance(52). Our phosphoproteomics analyses also

revealed changes in tyrosine phosphorylation of the Na^+/K^+-ATPase in a manner

consistent with Lyn activation and inhibition (data not shown). Western blot analyses for

phospho-Na^+/K^+-ATPase (pY10) confirmed Lyn-dependent changes in the

phosphorylation of this protein (**Figure 3.4 and 3.5**). Consistent with studies

demonstrating the importance of Y10 phosphorylation, inhibition or knockdown of Lyn

reduced the uptake of creatine in MYL-R cells (**Figure 3.4B and 3.4D**).

Metabolic reprogramming is a hallmark of a variety of human cancers(68,178-180).

While high levels of creatine and phosphocreatine have been reported in human

breast(181,182) and colorectal(167) cancers, the importance of these high-energy

intermediates on drug resistance have not been extensively explored. While our previous

studies demonstrated that MYL-R cells had elevated creatine(68), the current study now

suggests that this may exert a protective effect that contributes to enhanced cell viability.

Though outside the scope of this study, our observations are consistent with other studies that have shown the creatine/phosphocreatine system to be protective against apoptosis by regulating mitochondrial oxidative phosphorylation(69). Additionally, the creatine/phosphocreatine system acts as an ATP buffering system where excess ATP in the cell is abstracted by creatine (Cr) to produce pools of phosphocreatine (PCr), a high-energy reservoir used by the cell when needed. Thus, the system functions to ensure energy/ATP homeostasis in the cell(183).

As demonstrated in **Figure 3.6**, creatine uptake is needed to mediate MYL-R cell viability given that the recorded intracellular creatine does not come from *de novo* synthesis from glycine (**Figure 3.1**). MYL-R cells were also treated with dasatinib and bryostatin 1, therapeutic agents also used in the treatment of CML (184,185), to determine their effects on creatine uptake. Bryostatin 1 first activates and then inhibits protein kinase C (PKC). Both PKC and protein kinase A (PKA), have been reported to phosphorylate the α-subunit of the Na^+/K^+-ATPase on serine and threonine residues. Phosphorylation on these residues may not account for the observed basal phosphorylation level of this subunit in various cells (175). This is supported by our current data that shows treatment of MYL-R cells with bryostatin 1 increased the total intracellular creatine pool compared to the DMSO-treated cells (**Figure 3.S2A**). By contrast, treatment of MYL-R cells with dasatinib or ouabain substantially reduced the total intracellular creatine pool, with ouabain registering ~10-fold reduction (**Figure 3.S2A**). Additionally, dasatinib and ouabain treatments inhibited creatine uptake by ~65% and ~95% respectively compared to DMSO treatment (**Figure 3.S2B**). Given that dasatinib is a Lyn inhibitor and ouabain inhibits the Na^+/K^+-ATPase pump, our data

81

suggest that Lyn and possibly other tyrosine kinases can mediate creatine regulation in MYL-R cells. Taken together, these data suggest that targeting Lyn or kinases that activate the Na^+/K^+-ATPase pump and are required for increased uptake of creatine may have therapeutic potential in treating drug resistant CML or other cancers.
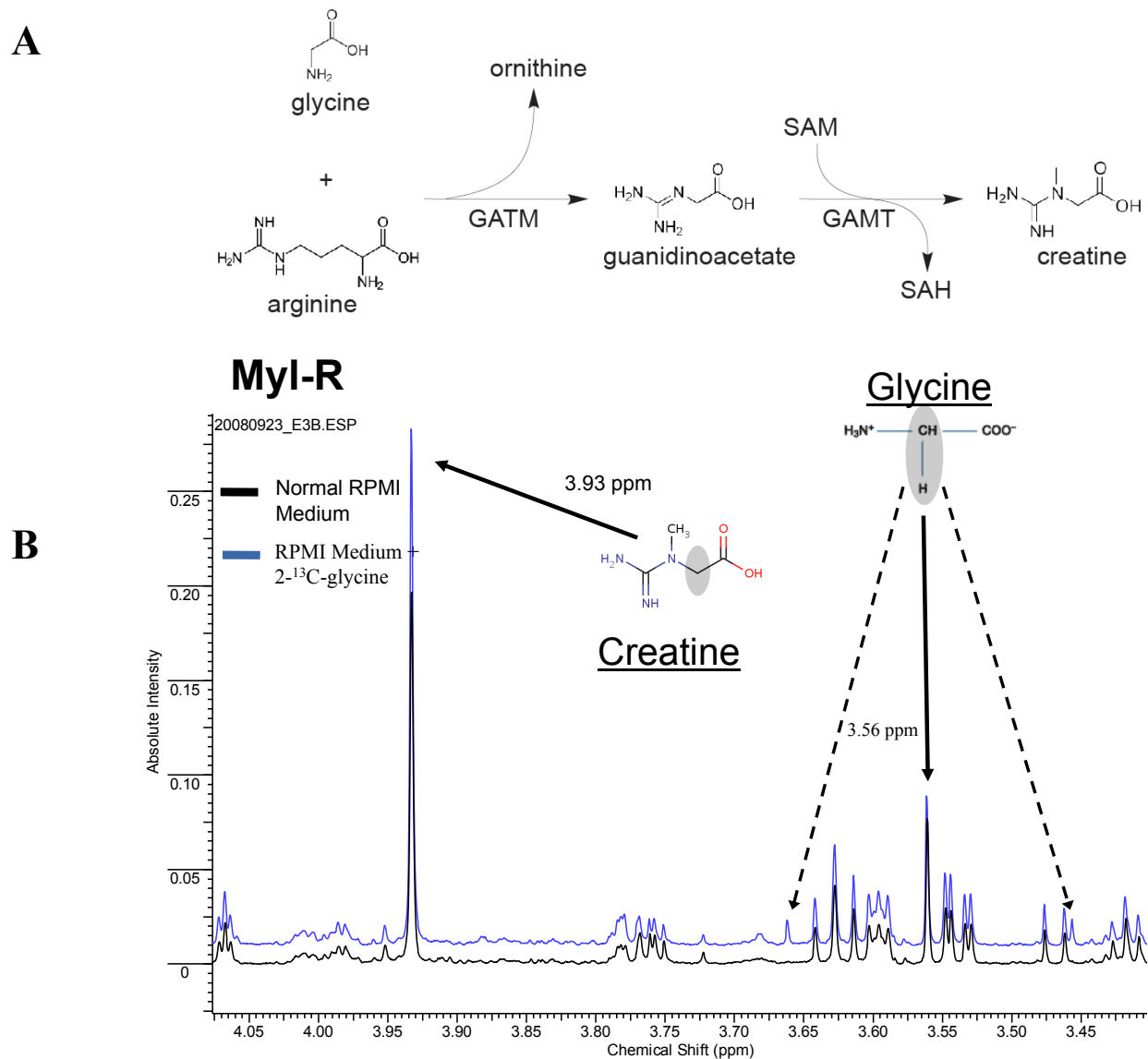
Figure 3.1. Increased intracellular creatine in MYL-R cells is due to uptake from cell media, and not de novo synthesis.

(A) Glycine and arginine are required for the biosynthesis of creatine in a two-part reaction. MYL and MYL-R cells were maintained in total growth medium with or without the addition of 2-^{13}C-glycine for 5 days. (B) Analysis of ^{1}H NMR spectra of each cell extract revealed that there was no statistically significant difference in percent incorporation of labeled glycine in the cell extracts from MYL and MYL-R cells. Whereas satellite peaks from 2-^{13}C-glycine were only observed in MYL-R cells incubated with heavy glycine, satellite peaks associated with creatine under these conditions were not observed.
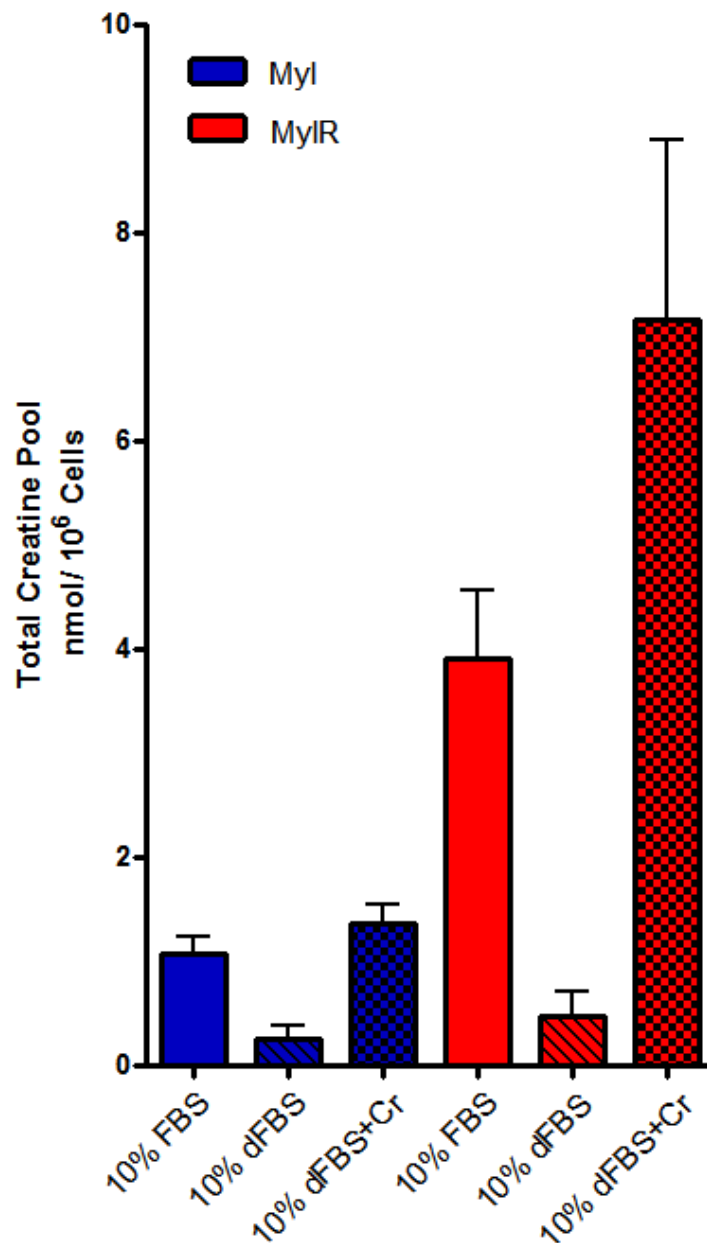
Figure 3.2. Media creatine is responsible for observed differences between MYL and MYL-R cells.

MYL and MYL-R cells were cultured in RPMI medium supplemented with 10% dFBS and intracellular creatine concentrations analyzed as described in Materials and Methods. Compared to cells cultured in RPMI medium supplemented with 10% FBS, there was significant reduction in creatine in both cell lines. Addition of 100 μM creatine to the dFBS-containing media restored creatine in MYL cells to normal levels and increased creatine levels in MYL-R cells by ~2-fold over that observed with 10% FBS. Approximately 50M MYL or MYL-R cells were cultured in RPMI media supplemented

with 10% dFBS five days prior to extraction. Creatine was added to each cell population in 10% dFBS to a final concentration of 100 μM two days prior to extraction. Cells were collected and metabolites extracted for ^{1}H NMR analysis of total intracellular creatine. Metabolites from MYL and MYL-R cells cultured under normal conditions (10% FBS) were similarly analyzed for comparison. Error was determined based on data from three independent experiments.

Figure 3.3. The Na⁺/K⁺-ATPase pump is required for creatine uptake by MYL-R cells.

(A) Creatine kinase B (CKB) and SLC6A8 protein levels are comparable in MYL and MYL-R cells. Western blot analysis was performed as described in Materials and Methods on parental MYL and MYL-R cells to examine CKB and SLC6A8 protein levels. (B) Model diagram depicting creatine uptake and subsequent phosphorylation by CKB to generate phosphocreatine. (C) Treatment of MYL-R cells with increasing concentrations of ouabain significantly reduced total intracellular creatine in a dose-dependent manner as determined by ^{1}H NMR analysis. MYL-R cells were treated for 24 hours with increasing concentrations of ouabain and ^{1}H NMR used to measure total creatine. (D) Treatment of MYL-R cells with dasatinib or ouabain substantially reduced rubidium (Rb) uptake as determined using the Rb uptake assay. After MYL-R cells were treated for 24 hours with DMSO or dasatinib (1 nM) or ouabain (100 nM), approximately 1M cells per condition were counted out, pelleted and washed in Rb-free uptake buffer. Cells were then resuspended in uptake buffer supplemented with 5 mM RbCl and incubated at room temperature over increasing time-points as described in Materials and Methods. Rb⁺ uptake was measured as described by Frazier et al., 2011(165). Rubidium uptake measurements were performed courtesy of Dr. Andrew Ghio's lab (EPA, UNC Chapel Hill, NC). The data presented in this figure are averages of three independent experiments, and * represents $p < 0.05$.
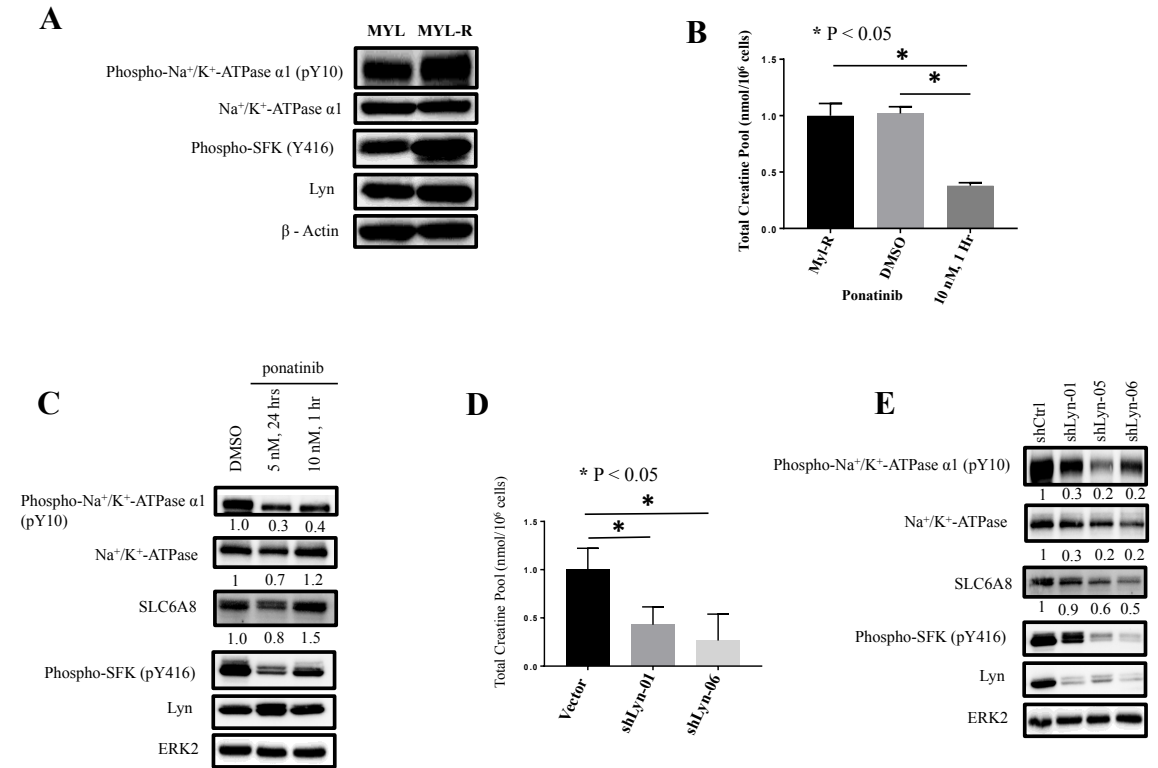
Figure 3.4. Lyn regulates creatine uptake in MYL-R cells.

(A) Activities for Lyn and Na^+/K^+-ATPase were elevated in MYL-R compared to MYL cells. Immunoblot analyses were performed on lysates of parental MYL and MYL-R cells to compare activity of Na^+/K^+-ATPase in the two cell lines. (B and C) Lyn inhibition significantly reduced total creatine pool in MYL-R cells. Approximately 15M MYL-R cells were treated for 1 hour with DMSO or ponatinib (10 nM) and total intracellular creatine concentrations determined using ^{1}H NMR as outlined in Materials and Methods. Untreated MYL-R cells were similarly analyzed for comparison. Similarly, Lyn inhibition reduced both Na^+/K^+-ATPase and Lyn activities as determined by immunoblot analyses. The creatine transporter, SLC6A8, and Na^+/K^+-ATPase protein levels were not affected. (D and E) Lyn knockdown significantly reduced total intracellular creatine pool in MYL-R cells. Similarly reduced by the more efficient Lyn knockdown shRNA constructs (shLyn-01, shLyn-05, and shLyn-06) were Na^+/K^+-ATPase and Lyn activities, together with SLC6A8 and Na^+/K^+-ATPase protein levels. Approximately 15M MYL-R cells were infected with lentiviral particles containing shRNA directed against Lyn. Upon selection of stably transduced cells, total intracellular creatine levels were measured using ^{1}H NMR, and Na^+/K^+-ATPase and Lyn activities, together with SLC6A8 and Na^+/K^+-ATPase protein levels were measured by immunoblotting. The data are the averages of three independent experiments, and * represents $p < 0.05$.

Phospho-Na⁺/K⁺-ATPase α1 (pY10)

Na⁺/K⁺-ATPase α1

Phospho-SFK (Y416)

Lyn

Phospho-STAT5A (Y694)

STAT5A

SLC6A8

Creatine Kinase B

β - Actin

1 2 3 4

Lane Id:

1. pEGFP
2. pEGFP-Lyn-WT-YPET
3. pEGFP-Lyn-mut-YF-YPET
4. pEGFP-Lyn-KD(K275R)-YPET
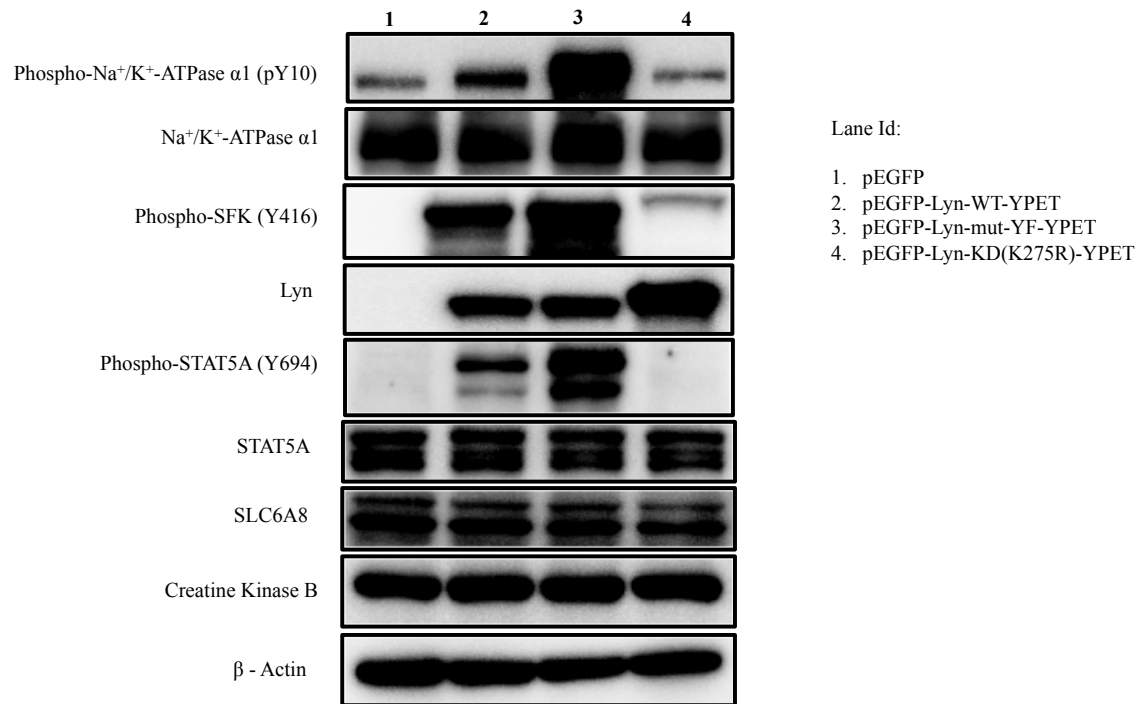
Figure 3.5. Lyn mediates the phosphorylation and activation of the Na⁺/K⁺-ATPase pump.

Transfection of constitutively active Lyn (Y508F) into HEK293 cells increased phospho-Na⁺/K⁺-ATPase α1 (pY10) levels. Phospho-STAT5A (pY694) levels were measured as an indication of Lyn activity and were similarly increased. No changes in Na⁺/K⁺-ATPase, SLC6A8 or STAT5A protein levels were observed under these conditions. HEK293 cells were transiently transfected with wild type or constitutively active (Y508F) or kinase dead (K275R) Lyn DNA as described in Materials and Methods. Na⁺/K⁺-ATPase, STAT5A and Lyn activities, together with SLC6A8, STAT5A and Na⁺/K⁺-ATPase protein levels were measured by immunoblotting.
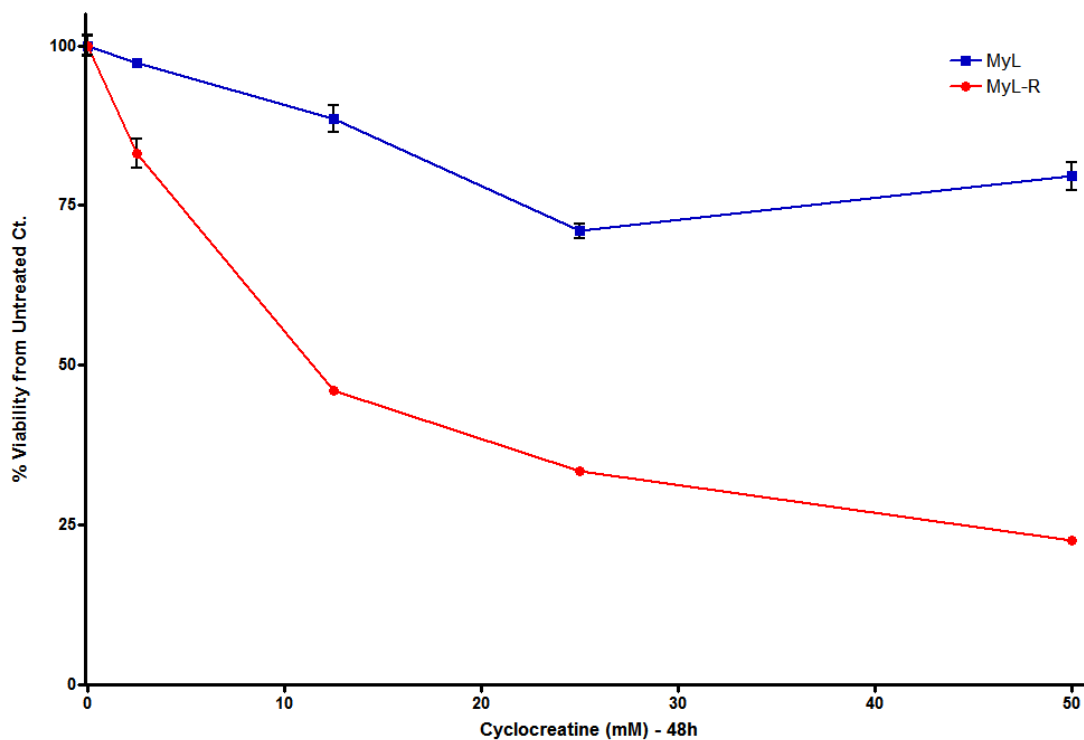
Figure 3.6. Depletion of intracellular creatine pool substantially reduces MYL-R cell viability.

Treatment of MYL-R cells with cyclocreatine (CCr) reduced cell viability in a dose-dependent manner compared to MYL cells. MYL and MYL-R cells were treated for 48 hours with increasing concentrations of CCr. Cell viability was determined in triplicate using the MTS Assay as described in Materials and Methods.
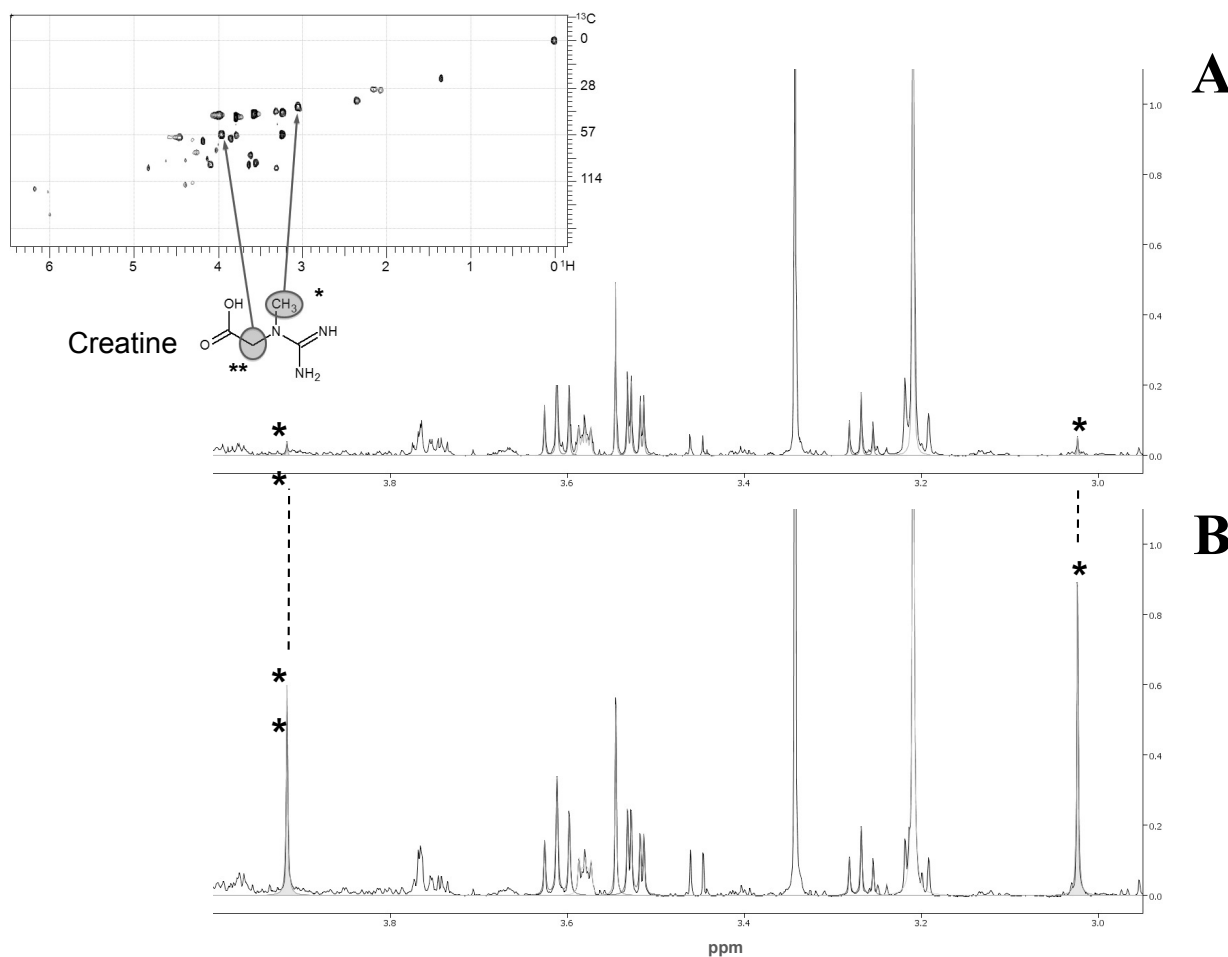
Figure 3.S1. Quantification of intracellular creatine in MYL (A) and MYL-R (B) cells.

^{1}H NMR analysis showed that intracellular creatine was significantly higher in MYL-R compared to MYL cells (68). Creatine concentrations from the ^{1}H NMR processed spectra were determined using Chenomx software and calculated as mmol/10[6] cells. Two-tailed student's t test was used to test for significance ($p < 0.05$) in the difference in total intracellular creatine between MYL and MYL-R cells (68).
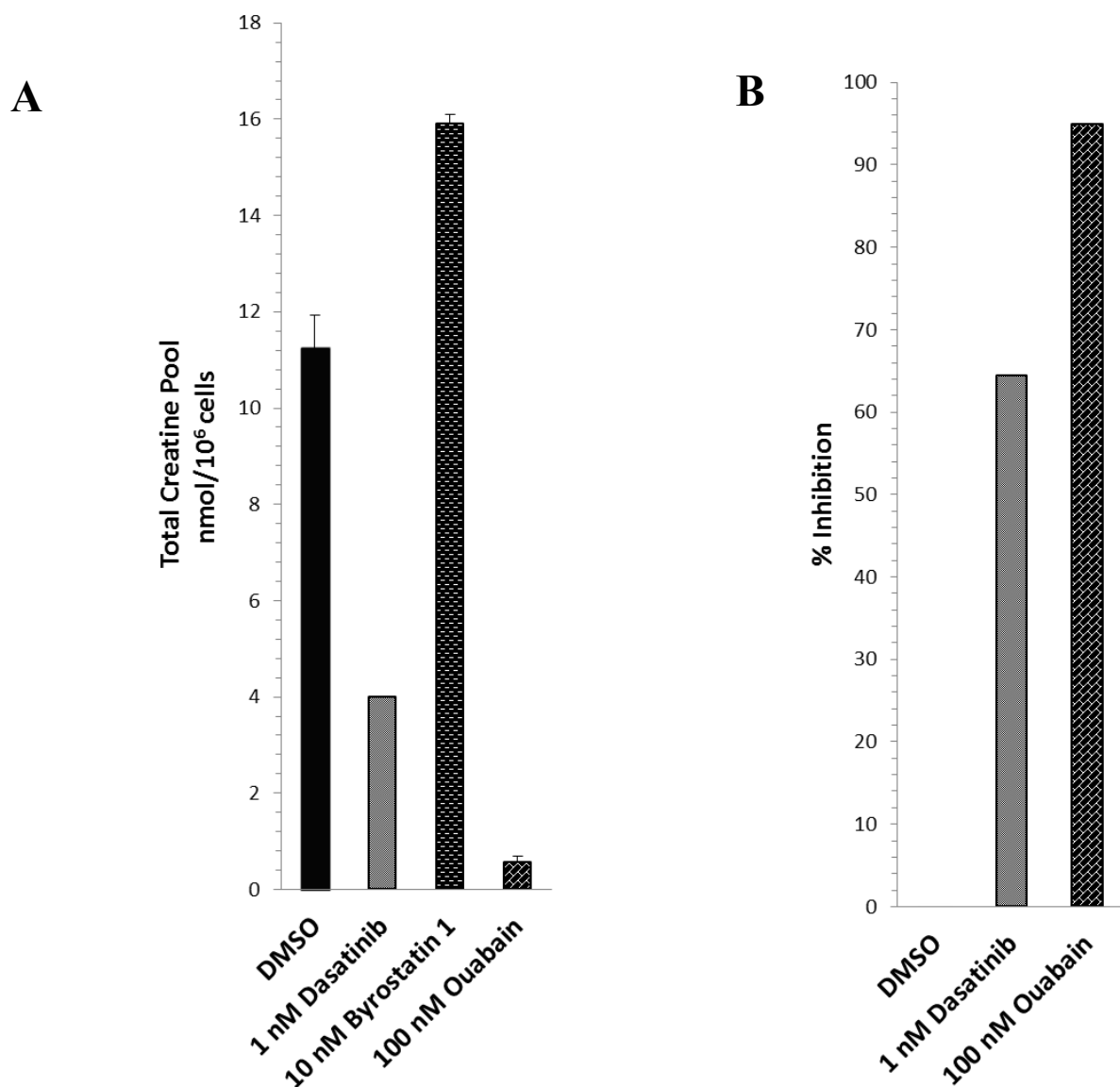
Figure 3.S2. Lyn and Na$^+$/K$^+$-ATPase inhibitors suppress creatine uptake in MYL-R cells.

(A) Lyn and Na$^+$/K$^+$-ATPase inhibitors reduced total creatine pool in MYL-R cells. My-R cells were treated overnight with 1 nM dasatinib or 0.1% DMSO or 10 nM bryostatin 1 or 100 nM ouabain and total intracellular creatine examined by ^{1}H NMR. Creatine quantification was performed as described in Materials and Methods. Inhibition of Lyn or Na$^+$/K$^+$-ATPase with dasatinib or ouabain substantially reduced total intracellular creatine. Conversely, treatment of MYL-R cells with bryostatin 1 increased total intracellular creatine levels above those recorded for DMSO. (B) Percent inhibition of intracellular creatine was calculated from the values obtained in (A), with ouabain registering ~100% inhibition.
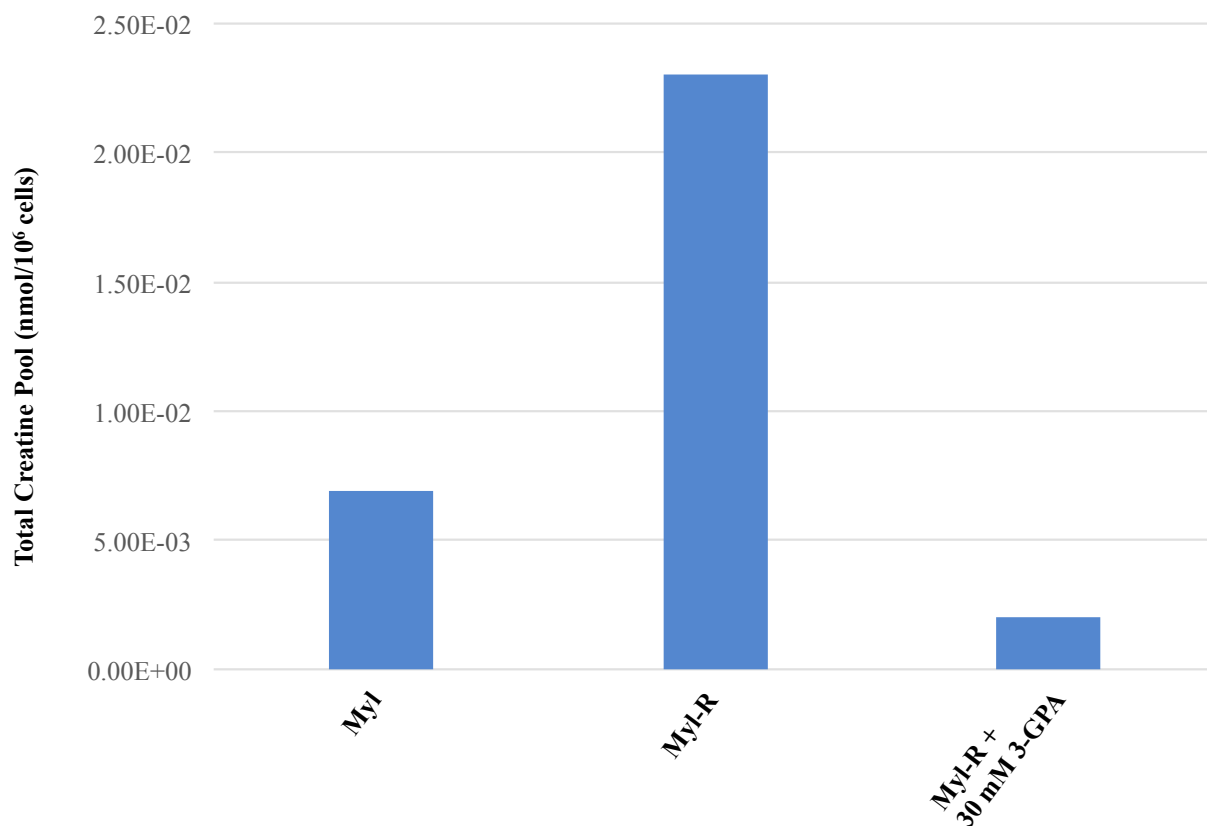
Figure 3.S3. Competitive inhibitors of creatine transport reduce creatine levels in MYL-R cells.

Treatment of MYL-R cells with 3-Guanidinopropionic acid (3-GPA) reduced total intracellular creatine pool ten-fold, comparable to untreated MYL cells. MYL-R cells were treated for 24 hours with 3-GPA (30 mM), and total intracellular creatine pool determined using ^{1}H NMR as outlined in Materials and Methods. Untreated MYL and MYL-R cells were similarly analyzed for comparison.

Target	shRNA sequence, 5'-3'
Non-targeting vector	None
Lyn_1	TTCATGAGGTTGGCTTCTTCC
Lyn_5	AAACGTTGGTCTCTCTTCTGC
Lyn_6	TTCTAAGGTGTTGAGTTTGGC

Table 3.1. shRNA oligonucleotides used in Chapter 3.

CHAPTER 4. CONCLUSIONS AND FUTURE DIRECTIONS

4.1   Conclusions

The emergence of acquired resistance to cancer therapy has presented monumental challenges to successful treatment of various human cancers, making it critical to fully understand the drivers of this phenomenon (11,178). In this regard, we in the Graves lab have adopted multi-omics approaches aimed at unraveling some of the adaptation mechanisms utilized by various human cancers to evade molecularly targeted therapies. We have used transcriptomics, proteomics, and metabolomics to accomplish these studies both in solid and liquid tumors. In this dissertation, and as shown in **Figure 4.1**, I have described two mechanisms by which an alternative kinase (Lyn), activated in a Bcr-Abl initiated CML, promotes cell survival. To successfully accomplish the studies described herein, I have collaborated with others and used the multi-omics approaches outlined in **Figure 4.1.**

Whereas our MIB-MS analyses of imatinib-sensitive (MYL) and imatinib-resistant (MYL-R) CML cells confirmed Lyn to be up-regulated in MYL-R compared to MYL cells, phosphopeptide analyses revealed that increased Lyn activity in MYL-R cells resulted in downstream substrate changes that promote drug resistance. For example, expression of anti-apoptotic proteins were found to be up-regulated (11,56,57). Zimmerman et al showed in a previous study that increased Lyn activity resulted in increased expression of Mcl-1, an anti-apoptotic protein. As illustrated in **Figure 4.2**, I showed that increased Lyn activity in MYL-R cells led to increased expression and

stability of BIRC6, an anti-apoptotic protein known to bind and inactivate active caspases (11). The stability of BIRC6 was regulated via phosphorylation in a Lyn-dependent manner. Thus, increased expression and stability of anti-apoptotic proteins is one mechanism by which Lyn promotes drug resistance in MYL-R cells.

Altered metabolism is a hallmark of a variety of human cancers and is thought to promote drug resistance by yet undefined mechanisms (68,178-180,186). High intracellular ATP levels, however, have been linked to drug resistance in many human cancer cells (186). Our lab previously showed that total intracellular pool was 5-fold higher in MYL-R than MYL cells (68). Accordingly, I have demonstrated in this dissertation that increased Lyn activity plays a critical role in regulating creatine uptake by MYL-R cells. In collaborations using metabolomics (^{1}H-NMR spectroscopy) approach as shown in **Figure 4.1**, and Western blot analyses, I have shown that Lyn phosphorylates and activates the Na^+/K^+-ATPase pump resulting in the establishment of a membrane gradient required for Na^+ and creatine symport. As shown in **Figure 4.3**, upon uptake into the cell, creatine is phosphorylated by creatine kinase to produce phosphocreatine, a high-energy source that supports cell survival via maintenance of ATP homeostasis (183,186). Consistent with these observations, my data showed that creatine uptake inhibition resulted in reduced MYL-R cell viability.

Although not very exhaustive, our studies have highlighted some of the many ways in which increased Lyn activity enriches our understanding of the molecular mechanisms underlying Bcr-Abl-initiated CML progression into imatinib-resistance (**Fig 4.4**). More research, however, remains to be done to fully understand Lyn's role in promoting drug resistance in CML.

4.2   Future Directions

Data from my studies highlight novel targets that may be critical to the development of effective therapies for drug-resistant CML. In furtherance of these studies, I propose the following experiments:

(1) Develop approaches to study BIRC6 and caspases interactions as a first step to inform more robust assays to screen for potential inhibitors of the BIR domain of BIRC6. Validation of key residues involved in these interactions will be important in designing peptide-based inhibitors of BIRC6. Already, research is ongoing in this area to develop inhibitors of the BIR regions of IAPs (187).

Lyn being a tyrosine kinase, the multiple serine phosphorylation events observed close to the BIR domain of BIRC6 (**Figure 2.2A**) were not due to direct action by Lyn, but the result of multiple signaling cascades regulated by Lyn. Since direct inhibitors of BIRC6 are not available, it is important to interrogate further the involved signaling proteins downstream of Lyn that may be targeted in an effort to eliminate BIRC6 and make the cancer cells more sensitive to therapy.

(2) For the creatine studies, overexpress Lyn in MYL cells and use ^{1}H-NMR analysis to investigate if there is any impact on creatine uptake. Compare to MYL-R cells. Investigate if MYL cells show any changes in imatinib-sensitivity. Additionally, perform cell viability assays to compare cell viability between the two cell lines.

Previous findings showed that phosphocreatine was important for maintaining the integrity of the mitochondrial membrane thereby protecting cells against apoptosis (69). Our creatine uptake inhibitor data show that depletion of creatine reduced MYL-R cell viability (**Figure 3.6**). Therefore, it is important to investigate if and how creatine (or

phosphocreatine) may be promoting drug resistance in MYL-R cells. Incubation of

MYL-R cells with inhibitors of creatine uptake (like cyclocreatine and 3-GPA) and

investigating changes in mitochondrial membrane potential will probably be a critical

step in addressing this question.
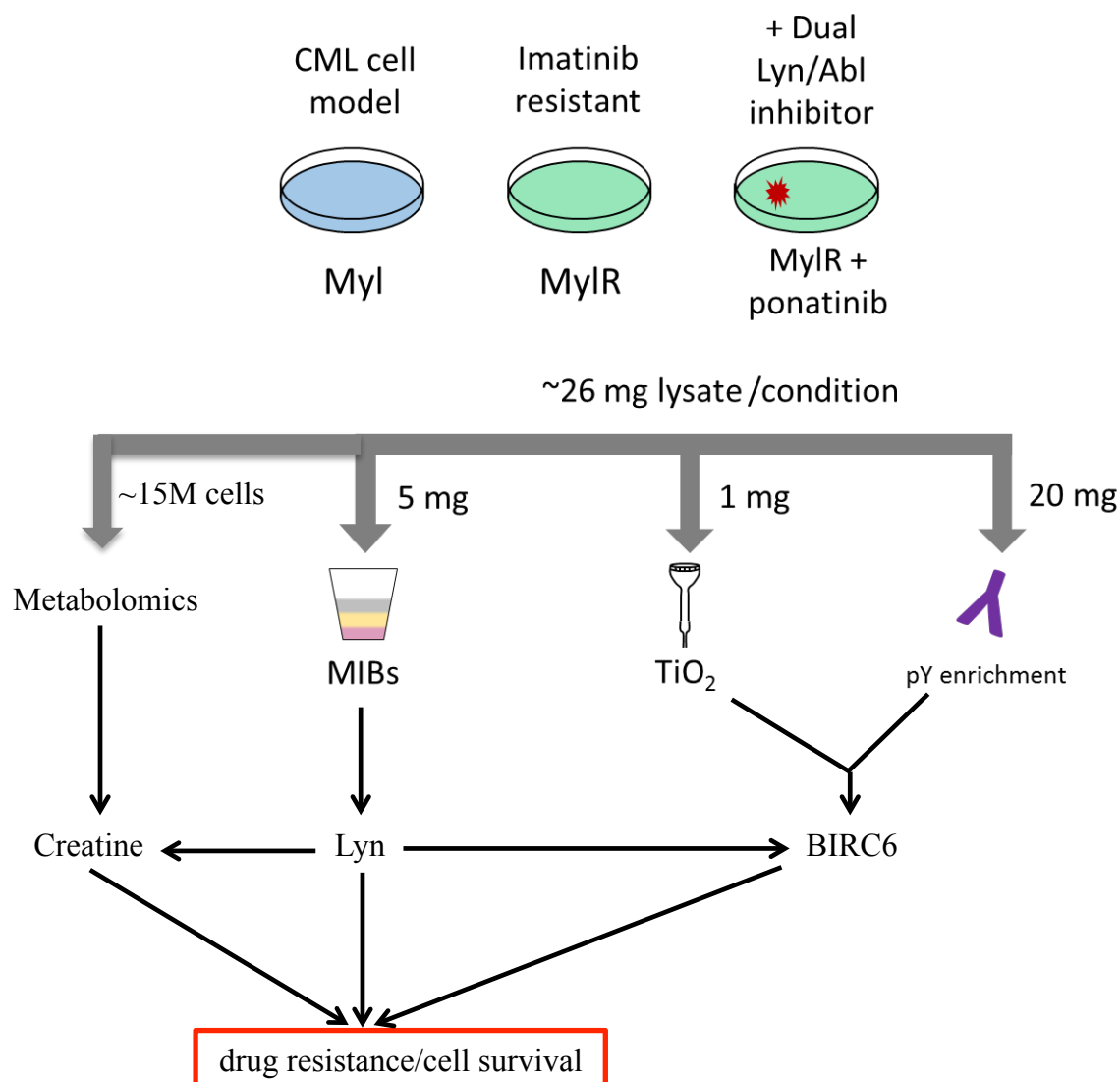
Figure 4.1. MIB/MS, phosphopeptide enrichment, and metabolomics approaches for studying drug resistance mechanisms in CML.

MIB/MS was used to study kinome dynamics in MYL, MYL-R, and MYL-R cells treated with ponatinib (10 nM, 1 hr.). In parallel, phosphoproteomics was used to study global phosphorylation differences from the same cells. Identification of peptides was accomplished by LC-MS/MS and label-free quantification (LFQ) of mass spectral data was performed using MaxQuant and the integrated ANDROMEDA search engine (121). Metabolomics was used to study metabolon dynamics in MYL, MYL-R, Lyn-knockdown MYL-R, and MYL-R cells treated with 3-GPA or ponatinib or dasatinib or bryostatin or ouabain. Identification of metabolites was accomplished using. ^{1}H-NMR spectral data were acquired using 1D ^{1}H and 2D ^{1}H-$\{^{13}$C$\}$ HSQC NMR Spectroscopy, and the metabolites were identified and quantitated using Chenomx software (version 6.1; Chenomx Inc., Edmonton, Canada).
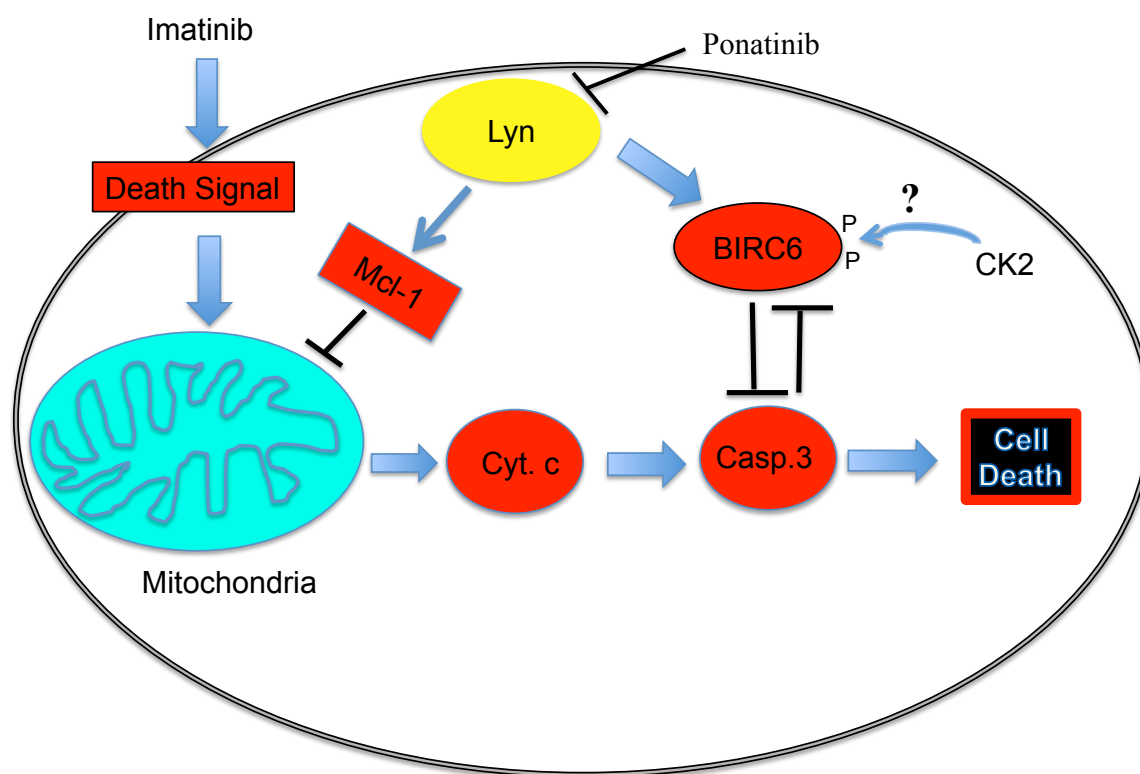
Figure 4.2. Lyn regulates BIRC6 expression and stability in MYL-R cells.

Schematic depiction of how activation of Lyn in Bcr-Abl-initiated CML leads to up-regulation of BIRC6 expression and stability thereby preventing the cells from going into apoptosis when challenged with imatinib. BIRC6 stability is enhanced via multiple phosphorylations in regions that overlap with caspase cleavage motifs, thus abrogating caspase-mediated degradation of the protein.
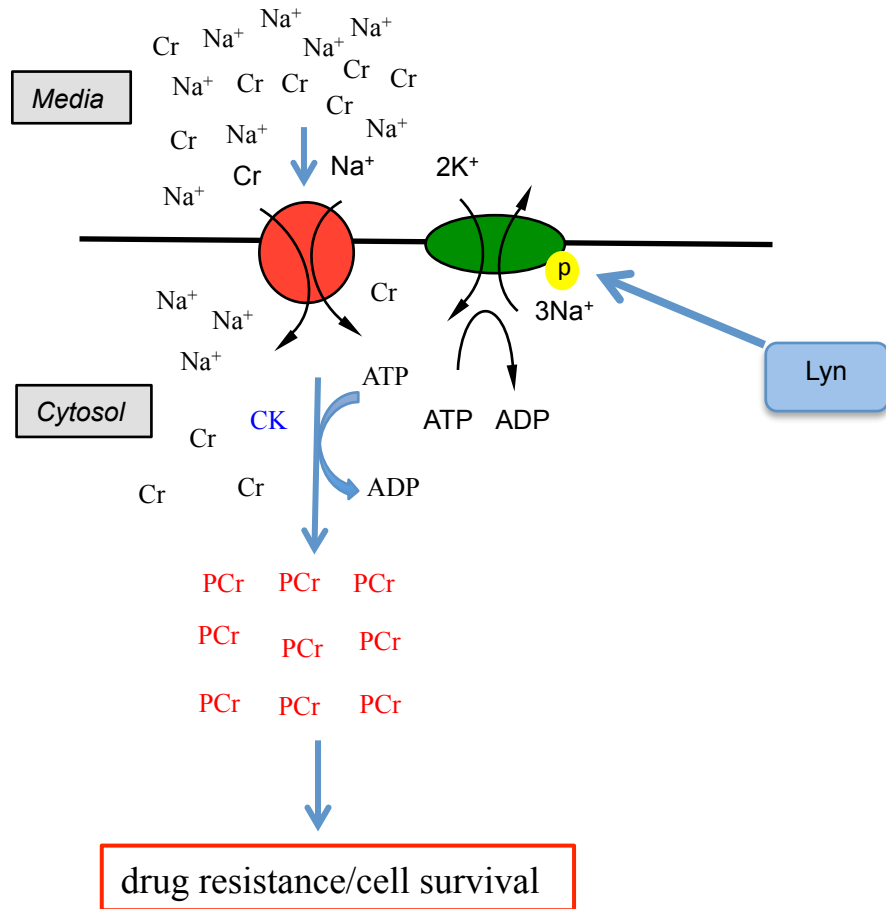
Figure 4.3. Creatine uptake by MYL-R cells.

Model showing creatine uptake machinery in MYL-R cells comprising of Lyn, the Na^+/creatine symporter (SLC6A8), and the Na^+/K^+-ATPase pump. Lyn phosphorylation and activation of the Na^+/K^+-ATPase pump allows for the establishment of a membrane gradient that facilitates inflow of Na^+ accompanied with creatine. Intracellular creatine is phosphorylated by creatine kinase (CK) to produce phosphocreatine, a high-energy molecule known to promote cancer cell survival.
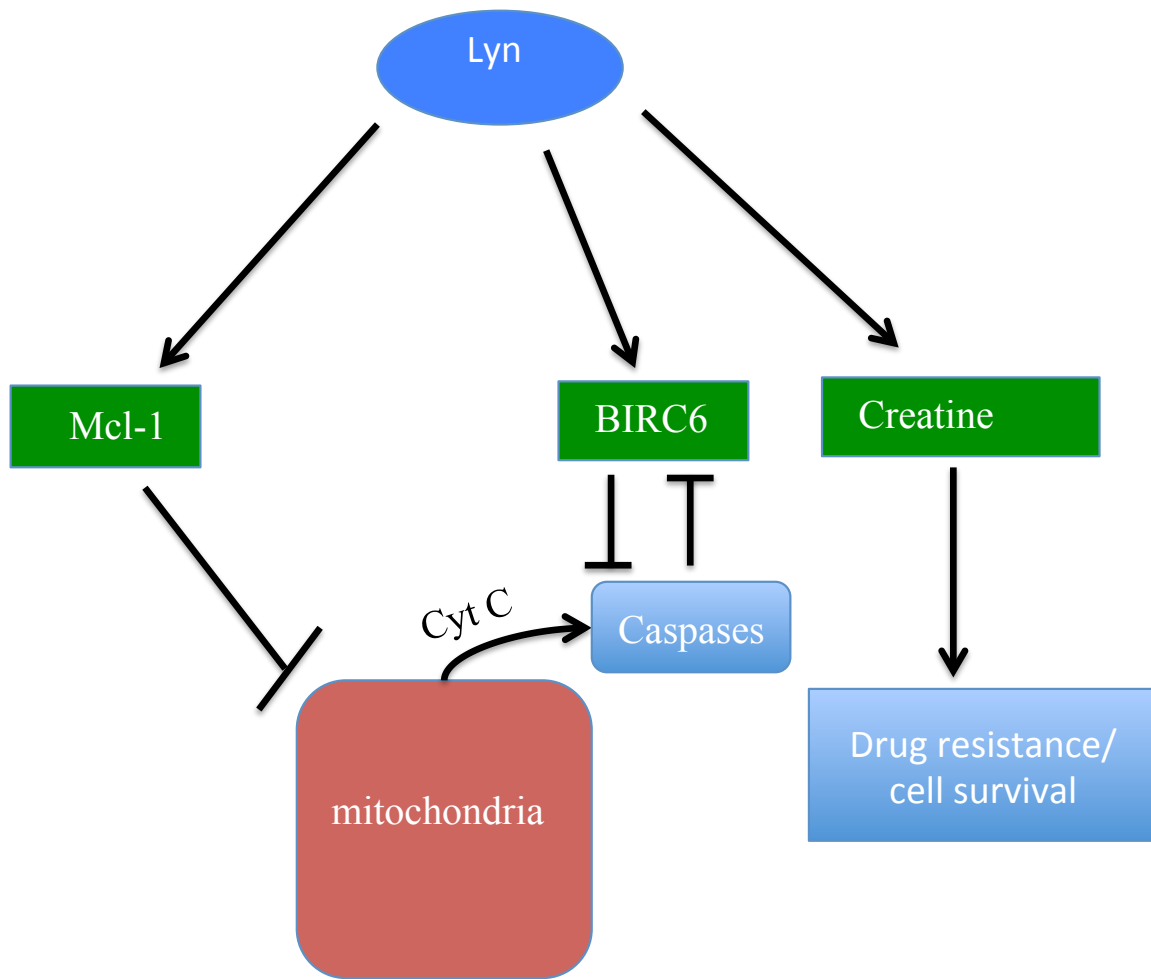
Figure 4.4. Adaptation mechanisms regulated by Lyn in MYL-R cells.

Simplified depiction of some of the Lyn-mediated survival pathways utilized by drug-resistant CML cells (MYL-R). Our lab uses MYL-R cells as a model system for studying drug resistance in CML.

REFERENCES

1. Sawyers CL. Chronic myeloid leukemia. New England Journal of Medicine. Mass Medical Soc; 1999;340(17):1330–40.

2. Cortes J. Natural history and staging of chronic myelogenous leukemia. Hematol Oncol Clin North Am. 2004 Jun;18(3):569–84–viii.

3. Melo JV, Barnes DJ. Chronic myeloid leukaemia as a model of disease evolution in human cancer. Nat Rev Cancer. 2007 Jun;7(6):441–53.

4. Jabbour E, Kantarjian H. Chronic myeloid leukemia: 2018 update on diagnosis, therapy and monitoring. Am J Hematol. 2018 Mar;93(3):442–59.

5. Siegel RL, Miller KD, Jemal A. Cancer statistics, 2018. CA A Cancer Journal for Clinicians. 2018 Jan;68(1):7–30.

6. Ren R. Mechanisms of BCR-ABL in the pathogenesis of chronic myelogenous leukaemia. Nat Rev Cancer. 2005 Mar;5(3):172–83.

7. Jabbour EJ, Cortes JE, Kantarjian HM. Resistance to tyrosine kinase inhibition therapy for chronic myelogenous leukemia: a clinical perspective and emerging treatment options. Clin Lymphoma Myeloma Leuk. 2013 Oct;13(5):515–29.

8. Pasic I, Lipton JH. Current approach to the treatment of chronic myeloid leukaemia. Leuk Res. 2017 Jan 11;55:65–78.

9. Goga A, McLaughlin J, Afar D, Saffran DC, Witte ON. Alternative signals to RAS for hematopoietic transformation by the BCR-ABL oncogene. Cell. 1995.

10. Ma L, Shan Y, Bai R, Xue L, Eide CA. A therapeutically targetable mechanism of BCR-ABL–independent imatinib resistance in chronic myeloid leukemia. Science translational …. 2014.

11. Okumu DO, East MP, Levine M, Herring LE, Zhang R, Gilbert TSK, et al. BIRC6 mediates imatinib resistance independently of Mcl-1. PLoS ONE. 2017;12(5):e0177871.

12. Tilbrook PA, Ingley E, Williams JH, Hibbs ML, Klinken SP. Lyn tyrosine kinase is essential for erythropoietin-induced differentiation of J2E erythroid cells. EMBO J. 1997 Apr 1;16(7):1610–9.

13. Tilbrook PA, Palmer GA, Bittorf T, McCarthy DJ, Wright MJ, Sarna MK, et al. Maturation of erythroid cells and erythroleukemia development are affected by the kinase activity of Lyn. Cancer Res. 2001 Mar 15;61(6):2453–8.

14. Ingley E. Functions of the Lyn tyrosine kinase in health and disease. Cell Commun Signal. 2012 Jul 17;10(1):21.

15.   Gocek E, Moulas AN, Studzinski GP. Non-receptor protein tyrosine kinases signaling pathways in normal and cancer cells. Crit Rev Clin Lab Sci. 2014 Jun;51(3):125–37.

16.   Tie SR, McCarthy DJ, Kendrick TS, Louw A, Le C, Satiaputra J, et al. Regulation of sarcoma cell migration, invasion and invadopodia formation by AFAP1L1 through a phosphotyrosine-dependent pathway. Oncogene. 2016 Apr 21;35(16):2098–111.

17.   Resh MD. Fatty acylation of proteins: new insights into membrane targeting of myristoylated and palmitoylated proteins. Biochim Biophys Acta. 1999 Aug 12;1451(1):1–16.

18.   Liang X, Lu Y, Wilkes M, Neubert TA, Resh MD. The N-terminal SH4 region of the Src family kinase Fyn is modified by methylation and heterogeneous fatty acylation: role in membrane targeting, cell adhesion, and spreading. J Biol Chem. 2004 Feb 27;279(9):8133–9.

19.   Chong Y-P, Chan AS, Chan K-C, Williamson NA, Lerner EC, Smithgall TE, et al. C-terminal Src kinase-homologous kinase (CHK), a unique inhibitor inactivating multiple active conformations of Src family tyrosine kinases. J Biol Chem. 2006 Nov 3;281(44):32988–99.

20.   Ingley E. Src family kinases: regulation of their activities, levels and identification of new pathways. Biochim Biophys Acta. 2008 Jan;1784(1):56–65.

21.   Plani-Lam JHC, Slavova-Azmanova NS, Kucera N, Louw A, Satiaputra J, Singer P, et al. Csk-binding protein controls red blood cell development via regulation of Lyn tyrosine kinase activity. Experimental Hematology. 2017 Feb;46:70–82.e10.

22.   Rider LG, Raben N, Miller L, Jelsema C. The cDNAs encoding two forms of the LYN protein tyrosine kinase are expressed in rat mast cells and human myeloid cells. Gene. 1994 Jan 28;138(1-2):219–22.

23.   Hibbs ML, Stanley E, Maglitto R, Dunn AR. Identification of a duplication of the mouse Lyn gene. Gene. 1995 Apr 24;156(2):175–81.

24.   Yi TL, Bolen JB, Ihle JN. Hematopoietic cells express two forms of lyn kinase differing by 21 amino acids in the amino terminus. Mol Cell Biol. 1991 May;11(5):2391–8.

25.   Sato I, Obata Y, Kasahara K, Nakayama Y, Fukumoto Y, Yamasaki T, et al. Differential trafficking of Src, Lyn, Yes and Fyn is specified by the state of palmitoylation in the SH4 domain. Journal of Cell Science. 2009 Apr 1;122(Pt 7):965–75.

26.   Kasahara K, Nakayama Y, Ikeda K, Fukushima Y, Matsuda D, Horimoto S, et al.

Trafficking of Lyn through the Golgi caveolin involves the charged residues on alphaE and alphaI helices in the kinase domain. The Journal of Cell Biology. 2004 Jun 7;165(5):641–52.

27. Ikeda K, Nakayama Y, Ishii M, Obata Y, Kasahara K, Fukumoto Y, et al. Requirement of the SH4 and tyrosine-kinase domains but not the kinase activity of Lyn for its biosynthetic targeting to caveolin-positive Golgi membranes. Biochim Biophys Acta. 2009 Oct;1790(10):1345–52.

28. Ikeda K, Nakayama Y, Togashi Y, Obata Y, Kuga T, Kasahara K, et al. Nuclear localization of Lyn tyrosine kinase mediated by inhibition of its kinase activity. Exp Cell Res. 2008 Nov 1;314(18):3392–404.

29. Frame MC. Src in cancer: deregulation and consequences for cell behaviour. Biochim Biophys Acta. 2002 Jun 21;1602(2):114–30.

30. Abrams CS, Zhao W. SH3 domains specifically regulate kinase activity of expressed Src family proteins. J Biol Chem. 1995 Jan 6;270(1):333–9.

31. Scapini P, Pereira S, Zhang H, Lowell CA. Multiple roles of Lyn kinase in myeloid cell signaling and function. Immunol Rev. 2009 Mar;228(1):23–40.

32. Yamanashi Y, Mori S, Yoshida M, Kishimoto T, Inoue K, Yamamoto T, et al. Selective expression of a protein-tyrosine kinase, p56lyn, in hematopoietic cells and association with production of human T-cell lymphotropic virus type I. Proc Natl Acad Sci USA. 1989 Sep;86(17):6538–42.

33. Lamagna C, Hu Y, DeFranco AL, Lowell CA. B cell-specific loss of Lyn kinase leads to autoimmunity. J Immunol. 2014 Feb 1;192(3):919–28.

34. Chin H, Arai A, Wakao H, Kamiyama R, Miyasaka N, Miura O. Lyn physically associates with the erythropoietin receptor and may play a role in activation of the Stat5 pathway. Blood. 1998 May 15;91(10):3734–45.

35. Radha V, Nambirajan S, Swarup G. Association of Lyn tyrosine kinase with the nuclear matrix and cell-cycle-dependent changes in matrix-associated tyrosine kinase activity. Eur J Biochem. 1996 Mar 1;236(2):352–9.

36. Kubota S, Morii M, Yuki R, Yamaguchi N, Yamaguchi H, Aoyama K, et al. Role for Tyrosine Phosphorylation of A-kinase Anchoring Protein 8 (AKAP8) in Its Dissociation from Chromatin and the Nuclear Matrix. Journal of Biological Chemistry. 2015 Apr 24;290(17):10891–904.

37. Bates RC, Edwards NS, Burns GF, Fisher DE. A CD44 survival pathway triggers chemoresistance via lyn kinase and phosphoinositide 3-kinase/Akt in colon carcinoma cells. Cancer Res. 2001 Jul 1;61(13):5275–83.

38. Goldenberg-Furmanov M, Stein I, Pikarsky E, Rubin H, Kasem S, Wygoda M, et

al. Lyn is a target gene for prostate cancer: sequence-based inhibition induces regression of human tumor xenografts. Cancer Res. 2004 Feb 1;64(3):1058–66.

39. Guan H, Zhou Z, Gallick GE, Jia S-F, Morales J, Sood AK, et al. Targeting Lyn inhibits tumor growth and metastasis in Ewing's sarcoma. Mol Cancer Ther. 2008 Jul;7(7):1807–16.

40. Slattery ML, Mullany LE, Sakoda L, Samowitz WS, Wolff RK, Stevens JR, et al. The NF-κB signalling pathway in colorectal cancer: associations between dysregulated gene and miRNA expression. J Cancer Res Clin Oncol. 2018 Feb;144(2):269–83.

41. Liu WM, Huang P, Kar N, Burgett M, Muller-Greven G, Nowacki AS, et al. Lyn facilitates glioblastoma cell survival under conditions of nutrient deprivation by promoting autophagy. PLoS ONE. 2013;8(8):e70804.

42. Kim YJ, Hong S, Sung M, Park MJ, Jung K, Noh K-W, et al. LYN expression predicts the response to dasatinib in a subpopulation of lung adenocarcinoma patients. Oncotarget. 2016 Dec 13;7(50):82876–88.

43. Sutton P, Borgia JA, Bonomi P, Plate JMD. Lyn, a Src family kinase, regulates activation of epidermal growth factor receptors in lung adenocarcinoma cells. Mol Cancer. 2013;12:76.

44. Roseweir AK, Qayyum T, Lim Z, Hammond R, MacDonald AI, Fraser S, et al. Nuclear expression of Lyn, a Src family kinase member, is associated with poor prognosis in renal cancer patients. BMC Cancer. 2016 Mar 16;16:229.

45. Stettner MR, Wang W, Nabors LB, Bharara S, Flynn DC, Grammer JR, et al. Lyn kinase activity is the predominant cellular SRC kinase activity in glioblastoma tumor cells. Cancer Res. 2005 Jul 1;65(13):5535–43.

46. Liu S, Hao X, Ouyang X, Dong X, Yang Y, Yu T, et al. Tyrosine kinase LYN is an oncotarget in human cervical cancer: A quantitative proteomic based study. Oncotarget. 2016 Nov 15;7(46):75468–81.

47. Tabariès S, Annis MG, Hsu BE, Tam CE, Savage P, Park M, et al. Lyn modulates Claudin-2 expression and is a therapeutic target for breast cancer liver metastasis. Oncotarget. 2015 Apr 20;6(11):9476–87.

48. Thaper D, Vahid S, Nip KM, Moskalev I, Shan X, Frees S, et al. Targeting Lyn regulates Snail family shuttling and inhibits metastasis. Oncogene. 2017 Jul 13;36(28):3964–75.

49. Torigoe T, O'Connor R, Santoli D, Reed JC. Interleukin-3 regulates the activity of the LYN protein-tyrosine kinase in myeloid-committed leukemic cell lines. Blood. 1992 Aug 1;80(3):617–24.

50. Santos Dos C, Demur C, Bardet V, Prade-Houdellier N, Payrastre B, Récher C. A critical role for Lyn in acute myeloid leukemia. Blood. 2008 Feb 15;111(4):2269–79.

51. Okamoto M, Hayakawa F, Miyata Y, Watamoto K, Emi N, Abe A, et al. Lyn is an important component of the signal transduction pathway specific to FLT3/ITD and can be a therapeutic target in the treatment of AML with FLT3/ITD. Leukemia. 2007 Mar;21(3):403–10.

52. Ito T, Tanaka H, Kimura A. Establishment and characterization of a novel imatinib-sensitive chronic myeloid leukemia cell line MYL, and an imatinib-resistant subline MYL-R showing overexpression of Lyn. European journal of haematology. Wiley Online Library; 2007;78(5):417–31.

53. Donato NJ, Wu JY, Stapley J, Gallick G, Lin H, Arlinghaus R, et al. BCR-ABL independence and LYN kinase overexpression in chronic myelogenous leukemia cells selected for resistance to STI571. Blood. 2003 Jan 15;101(2):690–8.

54. Dai Y, Rahmani M, Corey SJ, Dent P, Grant S. A Bcr/Abl-independent, Lyn-dependent form of imatinib mesylate (STI-571) resistance is associated with altered expression of Bcl-2. J Biol Chem. 2004 Aug 13;279(33):34227–39.

55. Nam S, Williams A, Vultur A, List A, Bhalla K, Smith D, et al. Dasatinib (BMS-354825) inhibits Stat5 signaling associated with apoptosis in chronic myelogenous leukemia cells. Mol Cancer Ther. AACR; 2007;6(4):1400–5.

56. Zimmerman EI, Dollins CM, Crawford M, Grant S, Nana-Sinkam SP, Richards KL, et al. Lyn kinase-dependent regulation of miR181 and myeloid cell leukemia-1 expression: implications for drug resistance in myelogenous leukemia. Molecular Pharmacology. 2010 Nov;78(5):811–7.

57. Cooper MJ, Cox NJ, Zimmerman EI, Dewar BJ, Duncan JS, Whittle MC, et al. Application of multiplexed kinase inhibitor beads to study kinome adaptations in drug-resistant leukemia. PLoS ONE. 2013;8(6):e66755.

58. Donato NJ, Wu JY, Stapley J, Lin H, Arlinghaus R, Aggarwal BB, et al. Imatinib mesylate resistance through BCR-ABL independence in chronic myelogenous leukemia. Cancer Res. 2004 Jan 15;64(2):672–7.

59. Wu J, Meng F, Lu H, Kong L, Bornmann W, Peng Z, et al. Lyn regulates BCR-ABL and Gab2 tyrosine phosphorylation and c-Cbl protein stability in imatinib-resistant chronic myelogenous leukemia cells. Blood. 2008 Apr 1;111(7):3821–9.

60. Steinberg M. Dasatinib: a tyrosine kinase inhibitor for the treatment of chronic myelogenous leukemia and philadelphia chromosome-positive acute lymphoblastic leukemia. Clin Ther. 2007 Nov;29(11):2289–308.

61. Illmer T, Schaich M, Platzbecker U, Freiberg-Richter J, Oelschlägel U, Bonin

von M, et al. P-glycoprotein-mediated drug efflux is a resistance mechanism of chronic myelogenous leukemia cells to treatment with imatinib mesylate. Leukemia. 2004 Mar;18(3):401–8.

62. Liu P, Cheng H, Roberts TM, Zhao JJ. Targeting the phosphoinositide 3-kinase pathway in cancer. Nat Rev Drug Discov. 2009 Aug;8(8):627–44.

63. Mohapatra B, Ahmad G, Nadeau S, Zutshi N, An W, Scheffe S, et al. Protein tyrosine kinase regulation by ubiquitination: critical roles of Cbl-family ubiquitin ligases. Biochim Biophys Acta. 2013 Jan;1833(1):122–39.

64. Suzuki Y, Imai Y, Nakayama H, Takahashi K, Takio K, Takahashi R. A serine protease, HtrA2, is released from the mitochondria and interacts with XIAP, inducing cell death. Mol Cell. 2001 Sep;8(3):613–21.

65. Borgo C, Cesaro L, Salizzato V, Ruzzene M, Massimino ML, Pinna LA, et al. Aberrant signalling by protein kinase CK2 in imatinib-resistant chronic myeloid leukaemia cells: biochemical evidence and therapeutic perspectives. Mol Oncol. 2013 Dec;7(6):1103–15.

66. Duncan JS, Turowec JP, Duncan KE, Vilk G, Wu C, Lüscher B, et al. A peptide-based target screen implicates the protein kinase CK2 in the global regulation of caspase signaling. Sci Signal. 2011;4(172):ra30.

67. Gringeri E, Carraro A, Tibaldi E, D'Amico FE, Mancon M, Toninello A, et al. Lyn-mediated mitochondrial tyrosine phosphorylation is required to preserve mitochondrial integrity in early liver regeneration. Biochem J. 2010 Jan 15;425(2):401–12.

68. Dewar BJ, Keshari K, Jeffries R, Dzeja P, Graves LM, Macdonald JM. Metabolic assessment of a novel chronic myelogenous leukemic cell line and an imatinib resistant subline by H NMR spectroscopy. Metabolomics. 2010 Sep;6(3):439–50.

69. Sun Z, Lan X, Ahsan A, Xi Y, Liu S, Zhang Z, et al. Phosphocreatine protects against LPS-induced human umbilical vein endothelial cell apoptosis by regulating mitochondrial oxidative phosphorylation. Apoptosis. 2016 Mar;21(3):283–97.

70. Bhamidipati PK, Kantarjian H, Cortes J, Cornelison AM, Jabbour E. Management of imatinib-resistant patients with chronic myeloid leukemia. Ther Adv Hematol. 2013 Apr;4(2):103–17.

71. Carter BZ, Mak PY, Mu H, Zhou H, Mak DH, Schober W, et al. Combined targeting of BCL-2 and BCR-ABL tyrosine kinase eradicates chronic myeloid leukemia stem cells. Sci Transl Med. 2016 Sep 7;8(355):355ra117.

72. Carter BZ, Mak DH, Schober WD, Cabreira-Hansen M, Beran M, McQueen T,

et al. Regulation of survivin expression through Bcr-Abl/MAPK cascade: targeting survivin overcomes imatinib resistance and increases imatinib sensitivity in imatinib-responsive CML cells. Blood. 2006 Feb 15;107(4):1555–63.

73. Wang Z, Sampath J, Fukuda S, Pelus LM. Disruption of the inhibitor of apoptosis protein survivin sensitizes Bcr-abl-positive cells to STI571-induced apoptosis. Cancer Res. 2005 Sep 15;65(18):8224–32.

74. Kantarjian H, O'Brien S, Jabbour E, Garcia-Manero G, Quintas-Cardama A, Shan J, et al. Improved survival in chronic myeloid leukemia since the introduction of imatinib therapy: a single-institution historical experience. Blood. 2012 Mar 1;119(9):1981–7.

75. Wu P, Nielsen TE, Clausen MH. FDA-approved small-molecule kinase inhibitors. Trends Pharmacol Sci. 2015 Jul;36(7):422–39.

76. Wu P, Nielsen TE, Clausen MH. Small-molecule kinase inhibitors: an analysis of FDA-approved drugs. Drug Discov Today. 2016 Jan;21(1):5–10.

77. Cassuto O, Dufies M, Jacquel A, Robert G, Ginet C, Dubois A, et al. All tyrosine kinase inhibitor-resistant chronic myelogenous cells are highly sensitive to ponatinib. Oncotarget. 2012 Dec;3(12):1557–65.

78. O'Hare T, Deininger MW, Eide CA, Clackson T, Druker BJ. Targeting the BCR-ABL signaling pathway in therapy-resistant Philadelphia chromosome-positive leukemia. Clin Cancer Res. AACR; 2011;17(2):212–21.

79. Oberoi-Khanuja TK, Murali A, Rajalingam K. IAPs on the move: role of inhibitors of apoptosis proteins in cell migration. Cell Death Dis. 2013;4:e784.

80. Luk SUI, Xue H, Cheng H, Lin D, Gout PW, Fazli L, et al. The BIRC6 gene as a novel target for therapy of prostate cancer: dual targeting of inhibitors of apoptosis. Oncotarget. 2014 Aug 30;5(16):6896–908.

81. Bartke T, Pohl C, Pyrowolakis G, Jentsch S. Dual role of BRUCE as an antiapoptotic IAP and a chimeric E2/E3 ubiquitin ligase. Mol Cell. 2004 Jun 18;14(6):801–11.

82. Wang L, Chen Y-J, Hou J, Wang Y-Y, Tang W-Q, Shen X-Z, et al. Expression and clinical significance of BIRC6 in human epithelial ovarian cancer. Tumour Biol. 2014 May;35(5):4891–6.

83. Ribe EM, Serrano-Saiz E, Akpan N, Troy CM. Mechanisms of neuronal death in disease: defining the models and the players. Biochem J. 2008 Oct 15;415(2):165–82.

84. Sung KW, Choi J, Hwang YK, Lee SJ, Kim H-J, Lee SH, et al. Overexpression

of Apollon, an antiapoptotic protein, is associated with poor prognosis in childhood de novo acute myeloid leukemia. Clin Cancer Res. 2007 Sep 1;13(17):5109–14.

85.   Huang J, Lyu H, Wang J, Liu B. MicroRNA regulation and therapeutic targeting of survivin in cancer. Am J Cancer Res. 2015;5(1):20–31.

86.   Chen X, Duan N, Zhang C, Zhang W. Survivin and Tumorigenesis: Molecular Mechanisms and Therapeutic Strategies. J Cancer. 2016;7(3):314–23.

87.   Mobahat M, Narendran A, Riabowol K. Survivin as a preferential target for cancer therapy. Int J Mol Sci. 2014;15(2):2494–516.

88.   Blanc-Brude OP, Mesri M, Wall NR, Plescia J, Dohi T, Altieri DC. Therapeutic targeting of the survivin pathway in cancer: initiation of mitochondrial apoptosis and suppression of tumor-associated angiogenesis. Clin Cancer Res. 2003 Jul;9(7):2683–92.

89.   Deveraux QL, Reed JC. IAP family proteins—suppressors of apoptosis. Genes Dev. 1999.

90.   Thomas D, Powell JA, Vergez F, Segal DH, Nguyen N-YN, Baker A, et al. Targeting acute myeloid leukemia by dual inhibition of PI3K signaling and Cdk9-mediated Mcl-1 transcription. Blood. 2013 Aug 1;122(5):738–48.

91.   Bose P, Grant S. Mcl-1 as a Therapeutic Target in Acute Myelogenous Leukemia (AML). Leukemia Research Reports. 2013 Jan 1;2(1):12–4.

92.   Sharma A, Singh K, Mazumder S, Hill BT, Kalaycio M, Almasan A. BECN1 and BIM interactions with MCL-1 determine fludarabine resistance in leukemic B cells. Cell Death Dis. 2013;4:e628.

93.   Akgul C. Mcl-1 is a potential therapeutic target in multiple types of cancer. Cell Mol Life Sci. 2009 Apr;66(8):1326–36.

94.   Hussain S-RA, Cheney CM, Johnson AJ, Lin TS, Grever MR, Caligiuri MA, et al. Mcl-1 is a relevant therapeutic target in acute and chronic lymphoid malignancies: down-regulation enhances rituximab-mediated apoptosis and complement-dependent cytotoxicity. Clin Cancer Res. 2007 Apr 1;13(7):2144–50.

95.   Kim A, Seong KM, Kang HJ, Park S, Lee S-S. Inhibition of Lyn is a promising treatment for mantle cell lymphoma with bortezomib resistance. Oncotarget. 2015 Nov 10;6(35):38225–38.

96.   Schwarz LJ, Fox EM, Balko JM, Garrett JT, Kuba MG, Estrada MV, et al. LYN-activating mutations mediate antiestrogen resistance in estrogen receptor-positive breast cancer. J Clin Invest. 2014 Dec;124(12):5490–502.

97. Polier G, Ding J, Konkimalla BV, Eick D, Ribeiro N, Köhler R, et al. Wogonin and related natural flavones are inhibitors of CDK9 that induce apoptosis in cancer cells by transcriptional suppression of Mcl-1. Cell Death Dis. 2011;2:e182.

98. Belmar J, Fesik SW. Small molecule Mcl-1 inhibitors for the treatment of cancer. Pharmacol Ther. 2015 Jan;145:76–84.

99. Chen L, Fletcher S. Mcl-1 inhibitors: a patent review. Expert Opin Ther Pat. 2017 Feb;27(2):163–78.

100. Gores GJ, Kaufmann SH. Selectively targeting Mcl-1 for the treatment of acute myelogenous leukemia and solid tumors. Genes Dev. 2012 Feb 15;26(4):305–11.

101. Lee S, Wales TE, Escudero S, Cohen DT, Luccarelli J, Gallagher CG, et al. Allosteric inhibition of antiapoptotic MCL-1. Nat Struct Mol Biol. 2016 Jun;23(6):600–7.

102. Hunter AM, LaCasse EC, Korneluk RG. The inhibitors of apoptosis (IAPs) as cancer targets. Apoptosis. 2007 Sep;12(9):1543–68.

103. Hao Y, Sekine K, Kawabata A, Nakamura H, Ishioka T, Ohata H, et al. Apollon ubiquitinates SMAC and caspase-9, and has an essential cytoprotection function. Nat Cell Biol. 2004 Sep;6(9):849–60.

104. Hauser HP, Bardroff M, Pyrowolakis G, Jentsch S. A giant ubiquitin-conjugating enzyme related to IAP apoptosis inhibitors. The Journal of Cell Biology. 1998 Jun 15;141(6):1415–22.

105. Lopergolo A, Pennati M, Gandellini P, Orlotti NI, Poma P, Daidone MG, et al. Apollon gene silencing induces apoptosis in breast cancer cells through p53 stabilisation and caspase-3 activation. Br J Cancer. Nature Publishing Group; 2009;100(5):739–46.

106. Qiu X-B, Goldberg AL. The membrane-associated inhibitor of apoptosis protein, BRUCE/Apollon, antagonizes both the precursor and mature forms of Smac and caspase-9. J Biol Chem. 2005 Jan 7;280(1):174–82.

107. Pohl C, Jentsch S. Final stages of cytokinesis and midbody ring formation are controlled by BRUCE. Cell. 2008 Mar 7;132(5):832–45.

108. Ge C, Che L, Ren J, Pandita RK, Lu J, Li K, et al. BRUCE regulates DNA double-strand break response by promoting USP8 deubiquitination of BRIT1. Proc Natl Acad Sci USA. 2015 Mar 17;112(11):E1210–9.

109. Kikuchi R, Ohata H, Ohoka N, Kawabata A, Naito M. APOLLON Protein Promotes Early Mitotic CYCLIN A Degradation Independent of the Spindle Assembly Checkpoint. J Biol Chem. ASBMB; 2014;289(6):3457–67.

110.   Lotz K, Pyrowolakis G, Jentsch S. BRUCE, a giant E2/E3 ubiquitin ligase and inhibitor of apoptosis protein of the trans-Golgi network, is required for normal placenta development and mouse survival. Mol Cell Biol. 2004 Nov;24(21):9339–50.

111.   Hitz C, Vogt-Weisenhorn D, Ruiz P, Wurst W, Floss T. Progressive loss of the spongiotrophoblast layer of Birc6/Bruce mutants results in embryonic lethality. Genesis. 2005 Jun;42(2):91–103.

112.   Van Houdt WJ, Emmink BL, Pham TV, Piersma SR, Verheem A, Vries RG, et al. Comparative proteomics of colon cancer stem cells and differentiated tumor cells identifies BIRC6 as a potential therapeutic target. Mol Cell Proteomics. 2011 Dec;10(12):M111.011353.

113.   Lamers F, Schild L, Koster J, Speleman F, Øra I, Westerhout EM, et al. Identification of BIRC6 as a novel intervention target for neuroblastoma therapy. BMC Cancer. 2012;12:285.

114.   Dong X, Lin D, Low C, Vucic EA, English JC, Yee J, et al. Elevated expression of BIRC6 protein in non-small-cell lung cancers is associated with cancer recurrence and chemoresistance. J Thorac Oncol. 2013 Feb;8(2):161–70.

115.   Tang W, Xue R, Weng S, Wu J, Fang Y. BIRC6 promotes hepatocellular carcinogenesis: Interaction of BIRC6 with p53 facilitating p53 degradation. J Cancer. 2014.

116.   Druker BJ. Imatinib as a paradigm of targeted therapies. Adv Cancer Res. 2004;91:1–30.

117.   Duncan JS, Whittle MC, Nakamura K, Abell AN, Midland AA, Zawistowski JS, et al. Dynamic reprogramming of the kinome in response to targeted MEK inhibition in triple-negative breast cancer. Cell. 2012 Apr 13;149(2):307–21.

118.   Wang Q, Zimmerman EI, Toutchkine A, Martin TD, Graves LM, Lawrence DS. Multicolor monitoring of dysregulated protein kinases in chronic myelogenous leukemia. ACS Chem Biol. 2010 Sep 17;5(9):887–95.

119.   Godl K, Wissing J, Kurtenbach A, Habenberger P, Blencke S, Gutbrod H, et al. An efficient proteomics method to identify the cellular targets of protein kinase inhibitors. Proc Natl Acad Sci USA. 2003 Dec 23;100(26):15434–9.

120.   Bingle CD, Craig RW, Swales BM, Singleton V, Zhou P, Whyte MK. Exon skipping in Mcl-1 results in a bcl-2 homology domain 3 only gene product that promotes cell death. J Biol Chem. 2000 Jul 21;275(29):22136–46.

121.   Cox J, Mann M. MaxQuant enables high peptide identification rates, individualized p.p.b.-range mass accuracies and proteome-wide protein quantification. Nat Biotechnol. 2008 Dec;26(12):1367–72.

122. de Sousa Cavalcante L, Monteiro G. Gemcitabine: metabolism and molecular mechanisms of action, sensitivity and chemoresistance in pancreatic cancer. Eur J Pharmacol. 2014 Oct 15;741:8–16.

123. Okabe S, Tauchi T, Tanaka Y, Ohyashiki K. Efficacy of ponatinib against ABL tyrosine kinase inhibitor-resistant leukemia cells. Biochem Biophys Res Commun. 2013 Jun 7;435(3):506–11.

124. Roskoski R. Src protein-tyrosine kinase structure, mechanism, and small molecule inhibitors. Pharmacol Res. 2015 Apr;94:9–25.

125. Peterlin BM, Price DH. Controlling the elongation phase of transcription with P-TEFb. Mol Cell. 2006 Aug 4;23(3):297–305.

126. Bose P, Simmons GL, Grant S. Cyclin-dependent kinase inhibitor therapy for hematologic malignancies. Expert Opin Investig Drugs. 2013 Jun;22(6):723–38.

127. Phatnani HP, Greenleaf AL. Phosphorylation and functions of the RNA polymerase II CTD. Genes Dev. 2006 Nov 1;20(21):2922–36.

128. Yeh Y-Y, Chen R, Hessler J, Mahoney E, Lehman AM, Heerema NA, et al. Up-regulation of CDK9 kinase activity and Mcl-1 stability contributes to the acquired resistance to cyclin-dependent kinase inhibitors in leukemia. Oncotarget. 2015 Feb 20;6(5):2667–79.

129. Polier G, Giaisi M, Köhler R, Müller WW, Lutz C, Buss EC, et al. Targeting CDK9 by wogonin and related natural flavones potentiates the anti-cancer efficacy of the Bcl-2 family inhibitor ABT-263. Int J Cancer. 2014 Jun 4.

130. Fulda S. Tumor resistance to apoptosis. Int J Cancer. 2009 Feb 1;124(3):511–5.

131. Foo J, Michor F. Evolution of acquired resistance to anti-cancer therapy. J Theor Biol. 2014 Aug 21;355:10–20.

132. Malumbres M, Barbacid M. Cell cycle, CDKs and cancer: a changing paradigm. Nat Rev Cancer. 2009 Mar;9(3):153–66.

133. Belmar J, Fesik SW. Small molecule Mcl-1 inhibitors for the treatment of cancer. Pharmacol Ther. 2015 Jan;145:76–84.

134. Lu H, Xue Y, Guoying KY, Arias C, Lin J, Fong S. Compensatory induction of MYC expression by sustained CDK9 inhibition via a BRD4-dependent mechanism. Elife. 2015.

135. Litchfield DW. Protein kinase CK2: structure, regulation and role in cellular decisions of life and death. Biochem J. 2003 Jan 1;369(Pt 1):1–15.

136. Miyata Y. Protein kinase CK2 in health and disease: CK2: the kinase controlling

the Hsp90 chaperone machinery. Cell Mol Life Sci. 2009 Jun;66(11-12):1840–9.

137.   Nakajima H, Toyoshima-Morimoto F, Taniguchi E, Nishida E. Identification of a consensus motif for Plk (Polo-like kinase) phosphorylation reveals Myt1 as a Plk1 substrate. J Biol Chem. 2003 Jul 11;278(28):25277–80.

138.   Kelly KR, Ecsedy J, Medina E, Mahalingam D, Padmanabhan S, Nawrocki ST, et al. The novel Aurora A kinase inhibitor MLN8237 is active in resistant chronic myeloid leukaemia and significantly increases the efficacy of nilotinib. J Cell Mol Med. 2011 Oct;15(10):2057–70.

139.   Marin O, Bustos VH, Cesaro L, Meggio F, Pagano MA, Antonelli M, et al. A noncanonical sequence phosphorylated by casein kinase 1 in beta-catenin may play a role in casein kinase 1 targeting of important signaling proteins. Proc Natl Acad Sci USA. 2003 Sep 2;100(18):10193–200.

140.   Zhang M, Han G, Wang C, Cheng K, Li R, Liu H, et al. A bead-based approach for large-scale identification of in vitro kinase substrates. Proteomics. 2011 Dec;11(24):4632–7.

141.   Gyenis L, Duncan JS, Turowec JP, Bretner M, Litchfield DW. Unbiased functional proteomics strategy for protein kinase inhibitor validation and identification of bona fide protein kinase substrates: application to identification of EEF1D as a substrate for CK2. J Proteome Res. 2011 Nov 4;10(11):4887–901.

142.   Arend KC, Lenarcic EM, Vincent HA, Rashid N, Lazear E, McDonald IM, et al. Kinome Profiling Identifies Druggable Targets for Novel Human Cytomegalovirus (HCMV) Antivirals. Mol Cell Proteomics. 2017 Apr;16(4 suppl 1):S263–76.

143.   Rowley JD. Letter: A new consistent chromosomal abnormality in chronic myelogenous leukaemia identified by quinacrine fluorescence and Giemsa staining. Nature. 1973 Jun 1;243(5405):290–3.

144.   Melo JV, Gordon DE, Cross NC, Goldman JM. The ABL-BCR fusion gene is expressed in chronic myeloid leukemia. Blood. 1993 Jan 1;81(1):158–65.

145.   Daley GQ, Van Etten RA, Baltimore D. Induction of chronic myelogenous leukemia in mice by the P210bcr/abl gene of the Philadelphia chromosome. Science. 1990 Feb 16;247(4944):824–30.

146.   Evans CA, Owen-Lynch PJ, Whetton AD, Dive C. Activation of the Abelson tyrosine kinase activity is associated with suppression of apoptosis in hemopoietic cells. Cancer Res. 1993 Apr 15;53(8):1735–8.

147.   Deininger MW, Goldman JM, Lydon N, Melo JV. The tyrosine kinase inhibitor CGP57148B selectively inhibits the growth of BCR-ABL-positive cells. Blood. 1997 Nov 1;90(9):3691–8.

148. Druker BJ, Tamura S, Buchdunger E, Ohno S, Segal GM, Fanning S, et al. Effects of a selective inhibitor of the Abl tyrosine kinase on the growth of Bcr-Abl positive cells. Nat Med. 1996 May;2(5):561–6.

149. Apperley JF. Part I: mechanisms of resistance to imatinib in chronic myeloid leukaemia. Lancet Oncol. 2007 Nov;8(11):1018–29.

150. Mahon FX, Deininger MW, Schultheis B, Chabrol J, Reiffers J, Goldman JM, et al. Selection and characterization of BCR-ABL positive cell lines with differential sensitivity to the tyrosine kinase inhibitor STI571: diverse mechanisms of resistance. Blood. 2000 Aug 1;96(3):1070–9.

151. Campbell LJ, Patsouris C, Rayeroux KC, Somana K, Januszewicz EH, Szer J. BCR/ABL amplification in chronic myelocytic leukemia blast crisis following imatinib mesylate administration. Cancer Genet Cytogenet. 2002 Nov;139(1):30–3.

152. le Coutre P, Tassi E, Varella-Garcia M, Barni R, Mologni L, Cabrita G, et al. Induction of resistance to the Abelson inhibitor STI571 in human leukemic cells through gene amplification. Blood. 2000 Mar 1;95(5):1758–66.

153. Hochhaus A, Kreil S, Corbin AS, La Rosée P, Müller MC, Lahaye T, et al. Molecular and chromosomal mechanisms of resistance to imatinib (STI571) therapy. Leukemia. 2002 Nov;16(11):2190–6.

154. Gorre ME, Mohammed M, Ellwood K, Hsu N, Paquette R, Rao PN, et al. Clinical resistance to STI-571 cancer therapy caused by BCR-ABL gene mutation or amplification. Science. 2001 Aug 3;293(5531):876–80.

155. Shah NP, Nicoll JM, Nagar B, Gorre ME, Paquette RL, Kuriyan J, et al. Multiple BCR-ABL kinase domain mutations confer polyclonal resistance to the tyrosine kinase inhibitor imatinib (STI571) in chronic phase and blast crisis chronic myeloid leukemia. Cancer Cell. 2002 Aug;2(2):117–25.

156. Klawitter J, Kominsky DJ, Brown JL, Klawitter J, Christians U, Leibfritz D, et al. Metabolic characteristics of imatinib resistance in chronic myeloid leukaemia cells. Br J Pharmacol. 2009 Sep;158(2):588–600.

157. Bentley J, Walker I, McIntosh E, Whetton AD, Owen-Lynch PJ, Baldwin SA. Glucose transport regulation by p210 Bcr-Abl in a chronic myeloid leukaemia model. Br J Haematol. 2001 Jan;112(1):212–5.

158. Boren J, Cascante M, Marin S, Comín-Anduix B, Centelles JJ, Lim S, et al. Gleevec (STI571) influences metabolic enzyme activities and glucose carbon flow toward nucleic acid and fatty acid synthesis in myeloid tumor cells. J Biol Chem. 2001 Oct 12;276(41):37747–53.

159. Klawitter J, Anderson N, Klawitter J, Christians U, Leibfritz D, Eckhardt SG, et

al. Time-dependent effects of imatinib in human leukaemia cells: a kinetic NMR-profiling study. Br J Cancer. 2009 Mar 24;100(6):923–31.

160. Gottschalk S, Anderson N, Hainz C, Eckhardt SG, Serkova NJ. Imatinib (STI571)-mediated changes in glucose metabolism in human leukemia BCR-ABL-positive cells. Clin Cancer Res. 2004 Oct 1;10(19):6661–8.

161. Barnes K, McIntosh E, Whetton AD, Daley GQ, Bentley J, Baldwin SA. Chronic myeloid leukaemia: an investigation into the role of Bcr-Abl-induced abnormalities in glucose transport regulation. Oncogene. 2005 May 5;24(20):3257–67.

162. Kominsky DJ, Klawitter J, Brown JL, Boros LG, Melo JV, Eckhardt SG, et al. Abnormalities in glucose uptake and metabolism in imatinib-resistant human BCR-ABL-positive cells. Clin Cancer Res. 2009 May 15;15(10):3442–50.

163. Ptasznik A, Nakata Y, Kalota A, Emerson SG, Gewirtz AM. Short interfering RNA (siRNA) targeting the Lyn kinase induces apoptosis in primary, and drug-resistant, BCR-ABL1(+) leukemia cells. Nat Med. 2004 Nov;10(11):1187–9.

164. Maril N, Degani H, Rushkin E, Sherry AD, Cohn M. Kinetics of cyclocreatine and Na(+) cotransport in human breast cancer cells: mechanism of activity. Am J Physiol. 1999 Oct;277(4 Pt 1):C708–16.

165. Frazier MD, Mamo LB, Ghio AJ, Turi JL. Hepcidin expression in human airway epithelial cells is regulated by interferon-γ. Respir Res. 2011 Aug 2;12:100.

166. Wyss M, Kaddurah-Daouk R. Creatine and creatinine metabolism. Physiol Rev. 2000 Jul;80(3):1107–213.

167. Loo JM, Scherl A, Nguyen A, Man FY, Weinberg E, Zeng Z, et al. Extracellular metabolic energetics can promote cancer progression. Cell. 2015 Jan 29;160(3):393–406.

168. Lillie JW, O'Keefe M, Valinski H, Hamlin HA, Varban ML, Kaddurah-Daouk R. Cyclocreatine (1-carboxymethyl-2-iminoimidazolidine) inhibits growth of a broad spectrum of cancer cells derived from solid tumors. Cancer Res. 1993 Jul 1;53(13):3172–8.

169. Loike JD, Somes M, Silverstein SC. Creatine uptake, metabolism, and efflux in human monocytes and macrophages. Am J Physiol. 1986 Jul;251(1 Pt 1):C128–35.

170. Gregor P, Nash SR, Caron MG, Seldin MF, Warren ST. Assignment of the creatine transporter gene (SLC6A8) to human chromosome Xq28 telomeric to G6PD. Genomics. 1995 Jan 1;25(1):332–3.

171. Sora I, Richman J, Santoro G, Wei H, Wang Y, Vanderah T, et al. The cloning

and expression of a human creatine transporter. Biochem Biophys Res Commun. 1994 Oct 14;204(1):419–27.

172. Bröer S, Gether U. The solute carrier 6 family of transporters. Br J Pharmacol. 2012 Sep;167(2):256–78.

173. Chen Y, Kennedy DJ, Ramakrishnan DP, Yang M, Huang W, Li Z, et al. Oxidized LDL-bound CD36 recruits an Na^+/K^+-ATPase-Lyn complex in macrophages that promotes atherosclerosis. Sci Signal. 2015 Sep 8;8(393):ra91.

174. Bozulic LD, Dean WL, Delamere NA. The influence of SRC-family tyrosine kinases on Na,K-ATPase activity in lens epithelium. Investigative Ophthalmology & Visual Science. 2005 Feb;46(2):618–22.

175. Wang XQ, Yu SP. Novel regulation of Na, K-ATPase by Src tyrosine kinases in cortical neurons. J Neurochem. 2005 Jun;93(6):1515–23.

176. Féraille E, Carranza ML, Gonin S, Béguin P, Pedemonte C, Rousselot M, et al. Insulin-induced stimulation of Na+,K(+)-ATPase activity in kidney proximal tubule cells depends on phosphorylation of the alpha-subunit at Tyr-10. Mol Biol Cell. 1999 Sep;10(9):2847–59.

177. Oudman I, Clark JF, Brewster LM. The effect of the creatine analogue beta-guanidinopropionic acid on energy metabolism: a systematic review. PLoS ONE. 2013;8(1):e52879.

178. Beloueche-Babari M, Box C, Arunan V, Parkes HG, Valenti M, de Haven Brandon A, et al. Acquired resistance to EGFR tyrosine kinase inhibitors alters the metabolism of human head and neck squamous carcinoma cells and xenograft tumours. Br J Cancer. 2015 Mar 31;112(7):1206–14.

179. Jain M, Nilsson R, Sharma S, Madhusudhan N, Kitami T, Souza AL, et al. Metabolite profiling identifies a key role for glycine in rapid cancer cell proliferation. Science. 2012 May 25;336(6084):1040–4.

180. Zhang WC, Shyh-Chang N, Yang H, Rai A, Umashankar S, Ma S, et al. Glycine decarboxylase activity drives non-small cell lung cancer tumor-initiating cells and tumorigenesis. Cell. 2012 Jan 20;148(1-2):259–72.

181. More TH, RoyChoudhury S, Christie J, Taunk K, Mane A, Santra MK, et al. Metabolomic alterations in invasive ductal carcinoma of breast: A comprehensive metabolomic study using tissue and serum samples. Oncotarget. 2018 Jan 5;9(2):2678–96.

182. Chan KWY, Jiang L, Cheng M, Wijnen JP, Liu G, Huang P, et al. CEST-MRI detects metabolite levels altered by breast cancer cell aggressiveness and chemotherapy response. NMR Biomed. 2016 Jun;29(6):806–16.

183. Yan Y-B. Creatine kinase in cell cycle regulation and cancer. Amino Acids. 2016 Aug;48(8):1775–84.

184. Bradner JE. A pulse at the heart of targeted therapy. Nature chemical biology. 2009 Mar;:144–5.

185. Jørgensen HG, Allan EK, Mountford JC, Richmond L, Harrison S, Elliott MA, et al. Enhanced CML stem cell elimination in vitro by bryostatin priming with imatinib mesylate. Experimental Hematology. 2005 Oct;33(10):1140–6.

186. Zhou Y, Tozzi F, Chen J, Fan F, Xia L, Wang J, et al. Intracellular ATP levels are a pivotal determinant of chemoresistance in colon cancer cells. Cancer Res. 2012 Jan 1;72(1):304–14.

187. Donnell AF, Michoud C, Rupert KC, Han X, Aguilar D, Frank KB, et al. Benzazepinones and benzoxazepinones as antagonists of inhibitor of apoptosis proteins (IAPs) selective for the second baculovirus IAP repeat (BIR2) domain. J Med Chem. 2013 Oct 24;56(20):7772–87.